Bioprocessing of oncolytic group B adenovirus for scalable production

Lisa May Cooper

Wolfson College

University of Oxford

A thesis submitted for the degree of Doctor of Philosophy

to the Department of Oncology, University of Oxford

Trinity Term 2014

Supervisors: Professor Leonard Seymour and Dr Kerry Fisher

Declaration of Authentication

All the work presented in this thesis was performed by me and in no way forms part of any other thesis in this or any other university. Where contributions have been made by others, this is acknowledged. The work was performed under the supervision of Professor Leonard Seymour, Department of Oncology, Division of Medical Sciences, University of Oxford, and Dr Kerry Fisher, PsiOxus Therapeutics, Milton Park, Oxford.

Lisa May Cooper

October 2014

Dedication

This thesis is dedicated to my Grandparents.

Acknowledgements

I would like to thank my supervisors, Professor Leonard Seymour and Dr Kerry Fisher, for their scientific insight, discussion and guidance throughout this project. I am also grateful to past and present members of the Seymour Lab who have been a pleasure to work with. In particular, I would like to thank Dr Clemens Thoma and Dr Alison Tedcastle, who have provided thoughtful comments and technical guidance throughout this project.

I am extremely grateful to PsiOxus Therapeutics for enabling this project and for providing ColoAd1. Particular thanks go to Dr Jeetendra Bhatia, Ashvin Patel and Dr Simon Alvis for their input at various stages throughout this project. Thanks also to Dr Alex Ceroni and Dr Daniel Ebner at the Target Discovery Institute, University of Oxford, for technical assistance and expertise in performing the high throughput screen, along with many thanks to Dr Francesca Buffa and Dr Sheng Yu for their help with the statistical analysis of the screen data. I also would like to thank past and present members of the Clinical Biomanufacturing Facility at the University of Oxford, particularly Dr Alison Crook, for inspiring me to take on this project. I am also grateful to Dr Sarah Moyle, Dr Eleanor Berrie and Emma Bolam for gifting suspension HEK293 cells used in this project and to Dr Nicky Green for scientific discussion from the very start of this project.

Finally, I would like to thank my parents, my brothers, Leanne and Mila for their unwavering love and support, and huge thanks go to my closest friends who have provided many good times in and around The Shire!

Bioprocessing of oncolytic group B adenovirus for scalable production

Lisa Cooper, Wolfson College, University of Oxford.

A thesis submitted for the degree of Doctor of Philosophy to the Department of Oncology, University of Oxford. Trinity Term 2014.

Abstract

The central aim of this thesis was to develop strategies to improve the manufacture of the group B chimeric oncolytic adenovirus, ColoAd1, which rapidly kills and lyses host cells. In attempting to improve the cellular yield of ColoAd1, this thesis therefore sought to identify host infection-related factors that limited ColoAd1 production.

In the widely-used manufacturing cell line, HEK293, ColoAd1 replication depleted intracellular ATP earlier than Ad11p and activated the intracellular energy sensor, AMPK. This might have reflected earlier ATP depletion, or possibly the absence of the E4orf4 protein from ColoAd1 compared to Ad11p. Despite this difference in AMPK activation, both viruses appeared able to maintain mTORC1 activity, which may be essential particularly for protein synthesis in the early stages of virus infection. For production purposes, preventing intracellular ATP depletion was seen as an attractive mechanism of maintaining ColoAd1 infected host cell viability and was hypothesised to lead to increased virus yield. A range of strategies were explored to enhance depleting ATP levels. Even though none of these were dramatically successful, they indicated that perhaps the anabolic building blocks required for viral replication were more important than cellular energy levels. Finally, a screening methodology based on siRNA knockdown was used to identify kinases that affected ColoAd1 replication. Many hits were identified, and several candidate kinases indicated a role for intracellular calcium signalling limiting virus particle production.

Overall, data presented in this thesis supports the manufacture of ColoAd1 in HEK293 cells and suggest that enhancing glycolysis may increase ColoAd1 yield. It also provides mechanistic insights into the replication of ColoAd1 and Ad11p that may inform the improved design of group B oncolytic adenoviruses.

Contents

Abbreviations

/	per
β-gal	β-galactosidase
µ	micro
4EBP1	eIF4E-binding protein 1
5' and 3'	5 prime and 3 prime ends of an RNA or DNA molecule
5FC	5Fluorocytosine
5FU	5'fluorouracil
ACC	Acetyl CoA Carboxylase
Ad2	adenovirus serotype
Ago	Argonaute
Akt	protein kinase B
AMPK	Adenosine 5’ Monophosphate-Activated Protein Kinase
ANOVA	analysis of variance
ADP	adenosine diphosphate
AMP	adenosine monophosphate
ATP	Adenosine Triphosphate
ATCC	American type culture collection
BCA	Bicinchoninic Acid
bp	Base Pairs
BSA	Bovine Serum Albumin

CAMKK2	Calcium Calmodulin Kinase Kinase II
CAR	Coxsackie and Adenovirus Receptor
CD	Cytosine Deaminase
CEA	Carcinoembryonic Antigen
CFSE	Carboxyfluorescein Diacetate, Succinimidyl Ester
CMV	Cytomegalovirus
CPE	Cytopathic Effect
C_T	Threshold cycle number
DAB	Diaminobenzidine
DAF	Decay Accelerating Factor
DAPK	Death Associated Protein Kinase
DCA	Dichloroacetate
DMEM	Dulbecco's Modified Eagle Medium
DMSO	Dimethyl Sulphoxide
DNA	Deoxyribonucleic Acid
dsDNA	Double stranded DNA
DSG	Desmoglein
dsRNA	double stranded RNA
siRNA	small interfering RNA
shRNA	short hairpin RNA
ssRNA	single stranded RNA

EBV	Epstein-Barr virus
ECM	extracellular matrix
EMA	European Medicines Agency
eIF	eukaryotic initiation factor
FBS	foetal bovine serum
FCS	foetal calf serum
FDA	Food and Drug Administration
FDG-PET	Fluorodeoxyglucose Positron Emission Tomograph
GM-CSF	granulocyte macrophage colony stimulating factor
GMP	good manufacturing practice
GSH	Glutathione
HAd	Human adenovirus
HEK293	Human embryonic kidney cells
h	hours
HCV	hepatitis C virus
HK	HexoKinase
HPV	human papilloma virus
HPSG	heparin sulphate glycosaminoglycans
HPV	human papilloma virus
HSV-1	human herpes simplex virus type 1
HSV-TK	herpes simplex virus thymidine kinase

hTERT	human telomerase reverse transcriptase gene
IC_{50}	virus dose required to kill 50% of cells
ICAM	Intracellular Adhesion Molecule
IFN	interferon
IL	interleukin
IT	intratumoural
ITR	Inverted Terminal Repeat
M	Metroformin
MAPK	mitogen activated protein kinase
MCAM	melanoma cell adhesion molecule
MCB	master cell bank
MHC	Major Histocompatibility Marker
MHRA	Medicines and Healthcare Products Regulatory Agency
MLP	Major Late Promoter
MOI	Multplicity of Infection
mRNA	messenger RNA
mTOR	Mammalian Target of Rapamycin
NAC	N-acetyl L-cysteine
NACA	N-acetyl L-cysteine Amide
NDV	Newcastle disease virus
NECL	Nectin-Like Molecule

Oct	cationic membrane transporters
orf	open reading frame
PCR	polymerase chain reaction
PFU	plaque forming unit
PKR	protein kinase R
PP	protein phosphatase
PSA	prostate specific antigen
pTP	pre-Terminal Protein
QC	quality control
QPCR	quantitative PCR
RISC	RNA induced silencing complex
RNA	Ribonucleic acid
RNAi	RNA interference
ROS	Reactive Oxygen Species
pRB	Retinoblastoma Protein
RSV	Rous sarcoma virus
S6K	S6 ribosomal protein kinase
SV40	Simian Virus 40
TBST	Tris-Buffered Saline and Tween
TCID50	tissue culture infective dose 50
TGFβ	transforming growth factor beta

TK	thymidine kinase
TNF	tumour necrosis factor
TSC	Tuberous Sclerosis Complex
TVEC	Talimogene laherparepvec
UTR	untranslated region
VA	Adenovirus non-coding virus associated RNA
VCAM	Vascular Cell Adhesion Molecule
VEGF	Vascular Endothelial Growth Factor
vp	virus particle
VSV	vesicular stomatitis virus
WCB	working cell bank

1 Introduction

Cancer remains an unruly disease, often resistant to multiple attempts to treat or control. Despite recent advances in diagnosis, early intervention and targeted therapies, cancer remains the most common cause of death and morbidity in the UK with cancer incidence also likely to rise in the future [1]. Some cancers are amenable to curative surgery when diagnosed early and locally confined but for metastatic carcinomas, treatment options currently offer time and quality of life improvements rather than complete cures. In contrast to most treatment modalities for metastatic disease, immunotherapy holds the prospect of a complete and durable response. Until relatively recently, this has been more a hope and hypothesis than reality. Initially, only a relatively small number of individuals in specific indications showed responses to immunotherapies such as interleukin-2 (IL-2), for metastatic melanoma or kidney cancer [2]. Now, drugs targeting immune checkpoints are starting to bring immunotherapy closer to mainstream cancer therapy with substantial numbers of patients responding to treatment [3].

Against this backdrop of emerging anti-cancer drugs, oncolytic viruses are receiving considerable attention. These tumour selective viruses are, in principle, capable of bringing multiple mechanisms of action to bear on the tumour by inducing direct cell killing and immune stimulation. Many oncolytic viruses have shown remarkable tumour selectivity and potency, killing a wide range of tumour cells including those that are resistant to conventional drugs or that have cancer stem cell-like phenotypes. Like all new classes of drug candidates, there are significant challenges to bring them to market. As viruses are relatively complex biologicals, manufacturing sufficient quantities of consistent clinical grade material deserves considerable planning and attention. This thesis focuses on one

such oncolytic virus, ColoAd1 (also known as Enadenotucireve), which is currently in phase I clinical trials. The key parameters of viral replication and production are studied in chapter 3 before exploring rate limiting pathways in subsequent chapters. In performing these studies, new information about the virus and its mechanism of action is gained, along with tangible outputs for future manufacturing scale up development. To set the context for this project, the introduction covers the background to cancer and the rationale for intervention with an oncolytic virus before describing the potential limitations to manufacturing productivity that this thesis aims to identify and solve.

1.1 Cancer therapies

In developed countries, cancer is a leading cause of death. In fact, in the United States one in four deaths are caused by cancer [4]. For primary, localised tumours, surgery remains the most effective treatment option and is frequently followed by locoregional radiotherapy and/or systemic chemotherapy. However, once tumours have metastasised, effective treatment options become more limited and patient survival is poor. Although screening programmes have been implemented to enable the early detection of tumours and treatment before metastasis, alternative effective therapies for metastatic disease are still required.

Current therapy for metastatic disease includes radiation therapy, which can cure around 40% of patients [5]. However, radiotherapy does not always irradiate the entire tumour mass so it is often combined with surgery, and/or chemotherapy. Cytotoxic chemotherapeutic agents have different mechanisms of action and can be broadly grouped into DNA damaging agents, antimetabolites that inhibit DNA synthesis and microtubule inhibitors. Most of these chemotherapeutics are non-specifically cytotoxic to proliferating

cells, which not only causes significant side effects in non-cancerous rapidly proliferating tissues, but also limits their therapeutic index. For this reason, treatment regimens are often designed to administer cytotoxic chemotherapeutics at the maximum tolerated dose with treatment-free periods that allow normal cells to recover. However, this method is thought to contribute to drug resistance of tumours as malignant cells that are resistant to treatment survive and thrive during treatment free periods [6]. Therefore, therapeutics with selective toxicity in cancer cells, and not normal cells, are sought. However, the development of such 'targeted' drugs requires a detailed understanding of the inherent differences between cancer cells and normal cells.

1.2 Viruses and cancer

Much of our fundamental knowledge of the transformation process has co-evolved with the study of viruses. Viruses were first described as "filterable agents" and have since been defined as DNA- or RNA-containing particles that require a host cell for the replication and expression of their genetic material. Now, the Baltimore classification groups animal viruses into seven categories depending on genome composition and replication mechanism [7]. Early work with retroviruses and DNA viruses that caused cancer in animals, lead to the discovery of oncogenes and tumour suppressor genes. Since then investigations into the fundamental molecular biology of cancer have identified many oncogenes and tumour suppressor genes in humans [8]. Combined with other studies of the transformation process, certain hallmarks of cancer have been identified such as the ability of transformed cells to sustain unlimited proliferation in the absence of growth factor signalling, without responding to inhibitory signals, and evading of apoptosis, as well as promoting angiogenesis and tissue invasion [9, 10].

The first oncogene was found in the Rous sarcoma virus (RSV), a retrovirus that causes sarcomas in chickens [11]. When sequences similar to the oncogene of RSV were identified in DNA of uninfected cells [12], the concept of a cellular proto-oncogene in normal cells that can give rise to an oncogene in tumour cells was established. The RSV oncogene became known as the *v-src* gene and its protein product (v-Src) was the first protein to show tyrosine kinase activity [13]. The *src* gene was later identified in humans [14] and, since, many human cancers, such as those of the colon, breast and pancreas, were found to have enhanced c-Src protein activity [15]. Subsequently, other oncogenic animal viruses and associated oncogenes were discovered. The *myc* oncogene was identified in the avian myelocytoma virus [16] and the *ras* oncogene was found in the rat sarcoma virus [17].

The first tumour suppressor gene identified was *TP53*, and it was found by its association with the Simian virus 40 (SV40) large T-antigen [18]. *TP53* was subsequently found to play an important role in maintaining genomic stability by inducing cell cycle arrest or apoptosis in response to DNA damage [19]. To achieve cellular transformation, SV40, adenovirus and human papilloma virus (HPV) are examples of viruses that express proteins that bind and inactivate p53 [20, 21]. Inactivation of another key tumour suppressor protein, the retinoblastoma protein (pRb), is also achieved by DNA viruses, such as SV40, adenovirus and papilloma viruses [22-24]. Importantly, the first human oncogenic virus, Epstein-Barr virus (EBV), was discovered in 1964 [25]. Since then, it has been estimated that approximately 15% of cancers worldwide are caused by oncogenic viruses [26]. However, most of these cases are confined to cancers of the cervix and liver [26] where specific causative oncogenic viruses are well described [27, 28].

Most viruses do not cause cancer; instead, they transiently transform host cells in order to acquire resources for replication and particle assembly. For example, they stimulate cell cycle entry to access host cell machinery required for viral replication or they inhibit apoptotic pathways that prevent cellular defences from attenuating virus replication. In some ways, the requirements of viruses and cancer cells are similar. In terms of the metabolic requirements of viruses and cancer cells, both require nucleotides, proteins and lipids for replication and cell division respectively. In parallel, viruses and tumour cells have similarities in immune evasion. Viruses have evolved to avoid, or delay, immune clearance. This is achieved, for example, by downregulating MHC1 from the cell surface. Similarly, tumour cells evolve to avoid immune clearance by a process of immunoediting [29]. Tumours also secrete soluble factors that supress or attenuate immune responses, such as transforming growth factor-β (TGF-β), interleuking-10 (IL-10) and vascular endothelial growth factor (VEGF). These soluble factors promote an immunosuppressive environment within the tumour [30] and it is in this immunosuppressive environment that oncolytic viruses can replicate and thrive [31].

Overall, with transformation and virus processes closely linked, it is unsurprising that cancer cells are highly productive environments for viruses to propagate. Therefore, it is appealing to consider that the increased permissiveness of cancer cells to viruses could in some ways be exploited therapeutically.

1.2.1 Oncolytic virotherapy

The field of oncolytic virotherapy developed from early anecdotal evidence of tumour regression coinciding with viral infections, which were mostly reported for leukaemias and lymphomas [32]. In a number of historically significant clinical trials, wild-type viruses were administered to patients with different types of cancers, including haematological malignancies and solid tumours, and regression was observed in many cases [33]. In 1956, Smith et al. reported that they had administered wild type adenovirus to thirty patients with cervical cancer, and 65% of inoculations produced evidence of tumour necrosis that did not affect normal tissue [34]. Most studies at that time administered a single type of wild-type virus to multiple patients. However, in one controlled study, a single patient with acute myeloid leukemia was treated with multiple types of wild-type viruses and a reduction in the number of peripheral myeloblasts occurred after administration of each virus [35]. Taken together, these studies suggested that the administration of wild-type viruses was safe and effective, which was a promising start for the field.

1.2.2 Use of wild type viruses or unmodified vaccine strains to treat cancer

In keeping with the hypothesis that tumour cells are permissive hosts, several viruses that do not replicate well in normal cells have been shown to be highly active in tumour cells. At one level, the increased permissiveness has been associated with the upregulation in cell surface receptors. Different viruses infect via different receptors that are differentially expressed on cancer cells and normal cells. For example, the Edmonston strain of measles virus naturally infects via the cell surface receptor CD46 [36], which is upregulated on some tumours as a mechanism of protection against complement-mediated cell death [37]. Furthermore, CD46 receptor expression has been shown to correlate with virus gene expression, syncytia formation and oncolysis by a genetically modified measles virus [38].

Similar examples exist for poliovirus, which infects via nectin-like molecule 5 (NECL-5), a receptor that is upregulated on glial, colorectal, breast, lung and hepatocellular carcinomas [39]. Coxsackievirus A21 naturally infects via intracellular adhesion molecule 1 (ICAM-1) and/or decay-accelerating factor (DAF), receptors which are over expressed on malignant melanoma and breast cancer cells [40]. These findings demonstrate that the cellular expression of a viral uptake receptor is required to permit viral entry into the target cell and altered expression patterns on malignant cells can determine some level of tumour cell selectivity. However, the presence of receptors alone does not guarantee that productive replication will follow.

The primary mechanism of increased tumour cell permissiveness for oncolytic viruses compared to normal cells is the mutation of signalling pathways responsible for the detection of viral infection and DNA damage. In circumventing these pathways, viruses are able to replicate unnoticed. Vesicular stomatitis virus (VSV) and, to a certain extent, Newcastle disease virus (NDV) have natural selectivity for tumour cells defective in interferon signalling [41]. NDV also has natural selectivity for tumour cells that are defective for apoptosis [42, 43].

In addition, intracellular factors can establish productive replication in cancer cells. Reovirus and herpes simplex virus 1 (HSV-1) are more permissive for tumour cells that have an activated Ras signalling pathway [44, 45]. Myxoma virus has natural selectivity for cells with active Akt signalling [46], which is a feature of many human tumours as reviewed in [47]. This highlights the inherently increased susceptibility of some malignant

cells for virus replication and the ability of some viruses to exploit cancer specific intracellular mutations.

1.2.3 Viruses genetically engineered to enhance selectivity for cancer cells

Initially, viruses were engineered to confer tumour selectivity by attenuating replication in normal cells. This aim was achieved by deleting viral genes required for efficient replication in normal cells. For example, ONYX-015 was originally designed to selectively replicate in p53-defective tumour cells. This was possible as adenovirus normally expresses the E1B 55K protein, that binds and inhibits p53 to prevent apoptosis in virally infected cells. Deleting the gene for E1B 55K was hypothesised to restrict ONYX-015 replication to cells expressing mutant p53 [48]. The *TP53* gene is frequently mutated in human tumours, and approximately 75% of these mutations are missense mutations that cause a loss of wild type p53 protein function [49]. Indeed, replication of ONYX-015 was demonstrated in a range of tumour cell lines expressing defective p53, in contrast to normal cells, in which a lack of replication of ONYX-015 compared to wild type Ad5 was demonstrated [50]. However, it later became apparent that replication of ONYX-015 in tumour cells was not dependent on p53 status [51], instead, it was dependent on the export of late adenovirus mRNA, which was required for infectious particle production [52]. In normal cells, ONYX-015 failed to replicate due to the loss of E1B 55K function in late adenovirus mRNA export, whereas, tumour cells compensated for the loss allowing infectious virus particle production. Regardless of the mechanism for ONYX-015 selectivity, this oncolytic agent progressed through clinical trials (section 1.2.6); in which selective replication in tumour cells was identified with attenuated replication in normal

cells and no maximally tolerated dose was achieved [53]. These findings proved the concept that attenuating viral replication in normal cells can increase the therapeutic index.

In a similar way, the replication of HSV-1 has been attenuated in normal cells by deleting the viral *γ34.5* gene that encodes the ICP34.5 protein. ICP34.5 normally inhibits the anti-viral response of host cells by binding protein phosphatase 1 (PP1) to facilitate dephosphorylation of the eukaryotic initiation factor 2 alpha (eIF2α). Protein kinase R (PKR) is one of four kinases capable of phosphorylating eIF2α and is activated by dimerization and autophosphorylation in response to binding intracellular double stranded RNA (dsRNA). Phosphorylation of eIF2α inactivates translation initiation, which inhibits protein synthesis and prevents viral replication. Therefore, in virally infected normal cells, with intact PKR anti-viral signalling pathways, replication is attenuated when HSV-1 lacks the ICP34.5 protein.

An alternative approach to ensuring selective replication of oncolytic viruses in tumour cells, and not normal cells, uses tissue or tumour specific promoters that replace early viral promoters required to initiate viral replication. This goal has been achieved most successfully using adenovirus [54]. Indeed, replication of the oncolytic adenovirus CG7060 was controlled by the prostate-specific antigen (PSA) specific promoter-enhancer element to permit replication in prostate tissue where PSA is highly expressed [55, 56]. Furthermore, replication of oncolytic adenovirus CG7870 was controlled by both the prostate specific rat probasin promoter and the PSA promoter-enhancer, instead of being controlled by the adenovirus E1A and E1B gene promoters respectively [57, 58]. Other oncolytic viruses, such as Telmoelysin, use tumour specific promoters. Telomelysin is a

replication competent adenovirus that contains the human telomerase reverse transcriptase gene (*hTERT*) promoter to drive transcription of viral *E1A* and *E1B* genes. *hTERT* normally encodes the catalytic subunit of telomerase. Normal differentiated cells do not express telomerase, in contrast to many cancer cells [59]. Since *hTERT* expression correlates with telomerase activity [60], the selective replication of Telomelysin is dependent on telomerase [61].

The attenuation of viral replication in normal cells and selective replication of oncolytic viruses in tumour cells is likely to have contributed to the excellent safety profile that genetically engineered viruses have displayed in the clinics (section 1.2.6). However, the lack of anti-tumour efficacy found with some of these selective oncolytic agents in clinical trials has highlighted the need for improvements. To this end, some oncolytic viruses have been genetically engineered to contain transgenes that express proteins that are either inherently cytotoxic, or that induce cytotoxicity by pro-drug therapy. Other transgenes expressed from oncoloytic viruses induce immune mediated cytotoxicity.

1.2.4 Viruses genetically engineered to express therapeutic transgenes to enhance anti-tumour efficacy

Viral expression of proteins that render cells susceptible to death induced by pro-drugs, otherwise known as suicide therapy, can be considered a form of gene therapy that overlaps with the field of oncolytic virotherapy. There are many suicide gene therapy systems available (reviewed in [62]). The most extensively studied systems are expression of the HSV thymidine kinase (TK), which makes the cell susceptible to ganciclovir, and expression of cytosine deaminase (CD), which renders the cell susceptible to 5-fluorocytosine (5-FC). Both systems have been introduced into oncolytic agents in an attempt to improve anti-tumour efficacy. This approach is not incompatible with any of the viruses discussed above. However, suicide gene therapy has been most successfully achieved using adenovirus, probably because the adenovirus genome is relatively simple to manipulate to confer strong transgene expression from infected cells.

HSV TK has been expressed from the oncolytic adenovirus Ad5-SSTR/TK-RGD. TK converts non-toxic ganciclovir to ganciclovir monophosphate, which is then converted to a triphosphate form by cellular kinases. Cell death is induced by the triphosphate form of ganciclovir by inhibiting DNA replication. A phase I clinical trial studied Ad5-SSTR/TK-RGD, administered by intraperitoneal injection, for the treatment of ovarian and endometrial cancer. The trial showed that the treatment was safe and somewhat effective, with disease in one patient resolving, and stable disease experienced by other patients, although progressive disease still developed in half of the patients [63].

Further, both TK and CD have also been expressed from the oncolytic adenovirus Ad5-CD/TK*rep*. Phase I clinical trials studied A5-CD/TK*rep* alone and in combination with radiation for the treatment of prostate cancer, and showed that transgene expression could be maintained for up to 3 weeks with stable disease achieved after intra-tumoural (IT) administration [64, 65].

Suicide oncolytic therapy aims to enhance anti-tumour efficacy by augmenting cell death induced by viral replication directly in tumour cells. An alternative strategy is to arm viruses with immunostimulatory agents that recruit the immune system to destroy the tumour cells. Many transgenes encoding immunostimulatory molecules have been inserted into oncolytic viruses (reviewed in [66]). To date, granulocyte-macrophage colony-stimulating factor (GM-CSF) has been the most successful immunostimulatory molecule inserted into oncolytic viruses. Talimogene laherparepvec (TVEC, formerly OncoVEX) is an oncolytic virus based on HSV-1, which was made tumour selective by deleting the γ34.5 and ICP47 viral genes required for replication in normal cells. These deletions allowed the GM-CSF transgene to be inserted and GM-CSF expression enhanced its anti-tumour properties [67]. Importantly, in phase II clinical trials, TVEC showed tumour destruction at sites distant from the site of IT injection, indicating immune-mediated systemic effects [68].

1.2.5 Bioselection of oncolytic viruses

The problem with the rationally designed strategies described above was that virus replication and potency can be inadvertently attenuated in cancer cells, although to a lesser degree than in normal cells. Therefore, the final strategy for creating potent oncolytic

viruses, involves a method of bioselection. This strategy meets the same objectives as achieved by rational design but allows viruses to adapt to their environment, as they have been doing for many hundreds of years. Bioselection sets up a process whereby the viruses, containing the genetic mutations that produce a required phenotype, will be selected for. In general, different methods can be used to promote genetic mutation and the selection method depends on the phenotype required. For example, ColoAd1 was created by 'directed evolution' [69]. Specifically, the colon cancer cell line HT29 was infected with a set of adenovirus serotypes, from different groups, to encourage genetic recombination and this produced a large library of recombinants. ColoAd1 was then selected for enhanced replication from this library by repeated passage on HT29 cells. In a different approach, a single serotype of adenovirus was subjected to chemical mutatagenesis before selecting mutant viruses capable of replication in cancer cells, again by repeated passage on HT29 cells [70]. Alternatively, mutant viral DNA polymerase has been used to encourage genetic mutation before selecting adenoviruses with improved cytolytic activity [71]. In each of these cases, the method of promoting genetic mutation was different but the concept of selection based on the desired phenotype was similar.

1.2.6 Oncolytic viruses in clinical trials

Many of the oncolytic viruses already discussed have progressed into different stages of clinical trials. Table 1-1 summarises the different types of viruses used as oncolytics in clinical trials at the moment. A comprehensive review of ongoing clinical trials with oncolytic viruses has been written by Russell et al [72]. More recently, Amgen have reported phase III clinical trial results that compared TVEC to GMCSF alone for the treatment of malignant melanoma. TVEC reached its clinical end point, in that it was more effective than GM-CSF alone [73]. This is a huge boost for the field of oncolytic

virotherapy and builds on the success of H101, an oncolytic adenovirus approved in China for head and neck carcinoma.

H101 is a virus similar to ONYX-015. The genetic modifications of ONYX-015 have already been discussed (section 1.2.3). In humans, ONYX-015 administered as a single agent for the treatment of head and neck cancer, was generally well tolerated, with no maximally tolerated dose identified by IT administration, and tumour-selective viral replication was confirmed [74]. However, the anti-tumoral activity of ONYX-015 as a single agent proved limited with significant tumour regression (>50%) observed in only ~14% of head and neck cancer patients [75, 76]. ONYX-015 was more effective in combination with standard chemotherapy. Tumour regression (>50%) was observed in ~63% of patients and complete responses observed in 27% of patients with head and neck cancer [77]. Despite these results, the development of ONYX-015 was halted and ONYX-015 superseded by H101, an E1B-55K deleted Ad5 with similarities to ONYX-015 but containing an additional deletion in the E3 region. H101 later gained approval from Chinese State Food and Drug Administration for use in combination with chemotherapy for the treatment of late stage head and neck cancer, after a phase III clinical trial demonstrated a 37% improvement in tumour regression with H101 in combination with cisplatin and 5FU compared to cisplatin and 5FU alone [78]. H101 was the first oncolytic agent to be approved.

Virus	Genetic target in cancer	Genetic modification(s)	Transgene
Non-engineered oncolytic viruses			
NDV	Unknown	N/A	N/A
Reovirus (Reolysin)	Defects in PKR/IFN pathways	N/A	N/A
Mumps	Unknown	N/A	N/A
West Nile	Unknown	N/A	N/A
Adenovirus	Unknown	N/A	N/A
Vaccina	Unknown	N/A	N/A
Engineered non-armed oncolytic viruses			
Adenovirus (H101)	Defects in p53 pathway and/or late RNA transport	E1B-55k (-), E3 (-)	N/A
Adenovirus (ONYX-015)	Defects in p53 pathway and/or late RNA transport	E1B-55k (-), E3B (-)	N/A
Adenovirus (Ad5-hTERT-E1A)	hTERT promoter	E1A (-)	N/A
Adenovirus (CG7060)	Prostate tissue-specific promoter	PSE1A, E3B (-)	N/A
Adenovirus (CG7870)	Prostate tissue-specific promoter	PSE1A, PSE1B (-)	N/A
HSV (1716)	Defects in PKR/IFN pathways	ICP34.5 (-)	N/A
HSV (G207)	Defects in PKR/IFN pathways	ICP34.5 (-) ICP (-)	N/A
Engineered armed oncolytic viruses			
Adenovirus (Ad5-D24-GMCFS)	Integrin re-targeted	E1A (-)	GMCFS for immune stimulation
Adenovirus (Ad5/3-D24-GMCSF)	Integrin re-targeted	Ad3 fibre, E1A (-)	GMCFS for immune stimulation
Adenovirus (CGTG-401)	Active telomerase	hTERT promoter	CD40L for immune stimulation
Adenovirus (Ad5-CD/TKrep)	Defects in p53 pathway and/or late RNA transport	E1B-55k (-), E3B (-), CD/TK	CD/TK for prodrug therapy
Vaccinia (JX-594)	TK active in cancer cell	TK (-)	GMCFS for immune stimulation
HSV (TVEC)	Defects in PKR/IFN pathway	γ-34.5 (-) ICP47 (-)	GMCFS for immune stimulation
MV-CEA	CD46 receptor binding	N/A (vaccine MV strain)	CEA for monitoring
Bioselected oncolytic viruses			
Adenovirus (ColoAd1)	CD46 receptor binding	Chimeric E2B, E3 (-), E4orf4 (-)	N/A

Table 1-1: Examples of oncolytic viruses that have been tested or are currently being tested in clinical trials. Table modified from [72] and [79].

1.2.7 Delivery of oncolytic viruses

The success of oncolytic virotherapy in humans has been hampered by difficulties in delivering enough of the therapeutic dose to tumours. Most of the viruses discussed in section 1.2.6 have been delivered by IT administration. However, successful treatment of metastatic lesions will most likely to be achieved by intravenous administration. In order to target metastases, intravenous delivery of some oncolytic viruses has been attempted. JX594, an oncolytic vaccinia virus has been intravenously delivered and, although extravasation of virus from the bloodstream to tumours has proved difficult to achieve in humans, it did occur in a dose dependent manner with JX594, particularly above a dose of 10^9 infectious units [80]. In addition, any virus reaching the tumour also encounters tissue stroma and extracellular matrices that can impede viral spread. Therefore, some oncolytic viruses have been armed with transgenes that express enzymes to degrade the extracellular matrix (ECM). For example, oncolytic adenovirus ICOVIR17 has been modified to express hyaluronidase, an enzyme that degrades ECM, and this modification enhanced its anti-tumour efficacy *in vivo* [81]. Taken, together if intravenous administration can successfully deliver oncolytic viruses to metastases then large quantities of virus would be required.

Pre-existing antibodies that neutralise viruses in the bloodstream impede the delivery of oncolytic viruses to metastatic lesions. This has been most well documented for Ad5. A large proportion of populations from many areas of the world have been exposed to, and have neutralising antibodies against, Ad5 [82]. However, alternative subtypes of adenovirus, especially group B adenoviruses, are able to circumvent pre-existing immunity to Ad5 [83]. This has provided an opportunity for intravenous delivery of oncolytic adenoviruses based on the group B subtype. ColoAd1 is a chimeric conditionally

replicating group B oncolytic adenovirus that was generated by the method of bioselection (section 1.2.5) and is currently under investigation in a phase I clinical trial for intravenous delivery to treat metastatic epithelial based carcinomas.

1.3 Adenovirus

As discussed, a wide range of viruses have been used for oncolytic virotherapy (sections 1.2.1-1.2.6) and it is likely that virus selection and delivery appropriate for the targeted cancer will be important. Adenovirus is arguably the most versatile oncolytic virus and is certainly the most widely used oncolytic virus in the clinics (Table 1-1). In addition, a large amount of knowledge on adenovirus infection and replication has accumulated over the past 50 years, which can be used to improve the anti-tumour efficacy of these oncolytic agents.

Human adenovirus (HAd) was first isolated from the adenoids in 1953 [84]. Since then more than 50 subtypes of HAd have been identified and classified into 6 subgroups (A-F) based on a combination of properties. At first, HAds were classified into serotypes by their ability to agglutinate erythrocytes [85]. However, different serotypes were also capable of forming tumours in hamsters and rats so this contributed to the classification, with group A adenoviruses being most oncogenic and groups B - D being weakly or non-oncogenic [86]. Later, it was found that genome homology within different serotypes could be used to classify adenoviruses [87] and this is the main basis for classification today. Historically, group C HAds have been most widely studied, especially types 2 and 5, so most is known about their structure and function.

1.3.1 Adenovirus structure

Adenoviruses are non-enveloped particles, 70-90 nm in diameter, with an inherently ordered structure. An adenovirus particle consists of an icosahedral capsid, composed of 240 homotrimeric hexon proteins that form 20 faces and 30 edges, with each of the 12 vertices composed of a penton capsomere, containing a covalently linked complex of homopentameric penton base and homotrimeric fibre protein (Figure 1-1). Other minor proteins associated with the capsid are proteins IIIa, VI, VIII and IX that function to maintain the rigid capsid structure. Inside the capsid are 6 core proteins that, with the exception of protease, maintain association of the double stranded viral DNA with the protein capsid. The structure and function of the minor adenovirus proteins has been reviewed in [88]. Although the minor proteins are small in size and number, they help to maintain the stable structure of a functional particle. This is especially true of protein IX, which, although dispensable for productive viral replication, seems to ensure that the particle is heat stable [89].

The majority of the adenovirus capsid is composed of hexon protein and the size of each hexon monomer varies between serotypes. Ad2 hexon protein monomer is the largest of all serotypes and Ad5 hexon is smaller than Ad2 hexon but larger than Ad11 hexon [90]. As hexon is the largest and most abundant capsid protein exposed on the external surface of the particle, it is no surprise that this protein is responsible for mediating the host adaptive immune response, as exemplified by different adenovirus serotypes having different hypervariable region hexon loops exposed on their external surface that are targets of serotype-specific antibody neutralisation [90]. However, hexon is not the only protein that contains epitopes for antibody neutralisation.

Fibre is an important functional protein exposed on the external surface of adenovirus. Each fibre protein can be divided into a tail, shaft and knob region. The tail of each fibre contains an N-terminal region that is highly conserved between serotypes and mediates non-covalent binding to a hydrophobic pocket formed between penton base monomers [91]. The shaft of the fibre consists of a variable number of repeating sequences that form anti-parallel strands connected by a β -turn. Importantly, the number of repeats determines fibre length, which can vary between serotype. For example, electron microscopy has determined that HAd serotype 3 has very short fibres with only 5.5 pseudo repeats, whereas HAd12 has long fibres with 22.5 pseudo repeats [92]. Figure 1-1 depicts the fibre length of Ad5 (group C) and Ad11 (group B) adenoviruses that are relevant to this thesis. Insertion of amino acids at specific positions in the β-turns can disrupt the fibre shaft rigidity and create hinge regions that allow flexibility for receptor binding [93]. At the C-terminal end of the fibre shaft is the globular knob region, which is formed by eight β-barrels that form 3 subunits with a number of variable loops that determine receptor binding [94].

In total, there are about 2,700 polypeptides in a single adenovirus particle, contributing to a molecular weight of about 1.5 x 10^8 Da [88, 95], highlighting the complexity of an adenovirus particle. However, this complexity is reduced by the ordered structure, which permits it to function in the host cell that it replicates in.

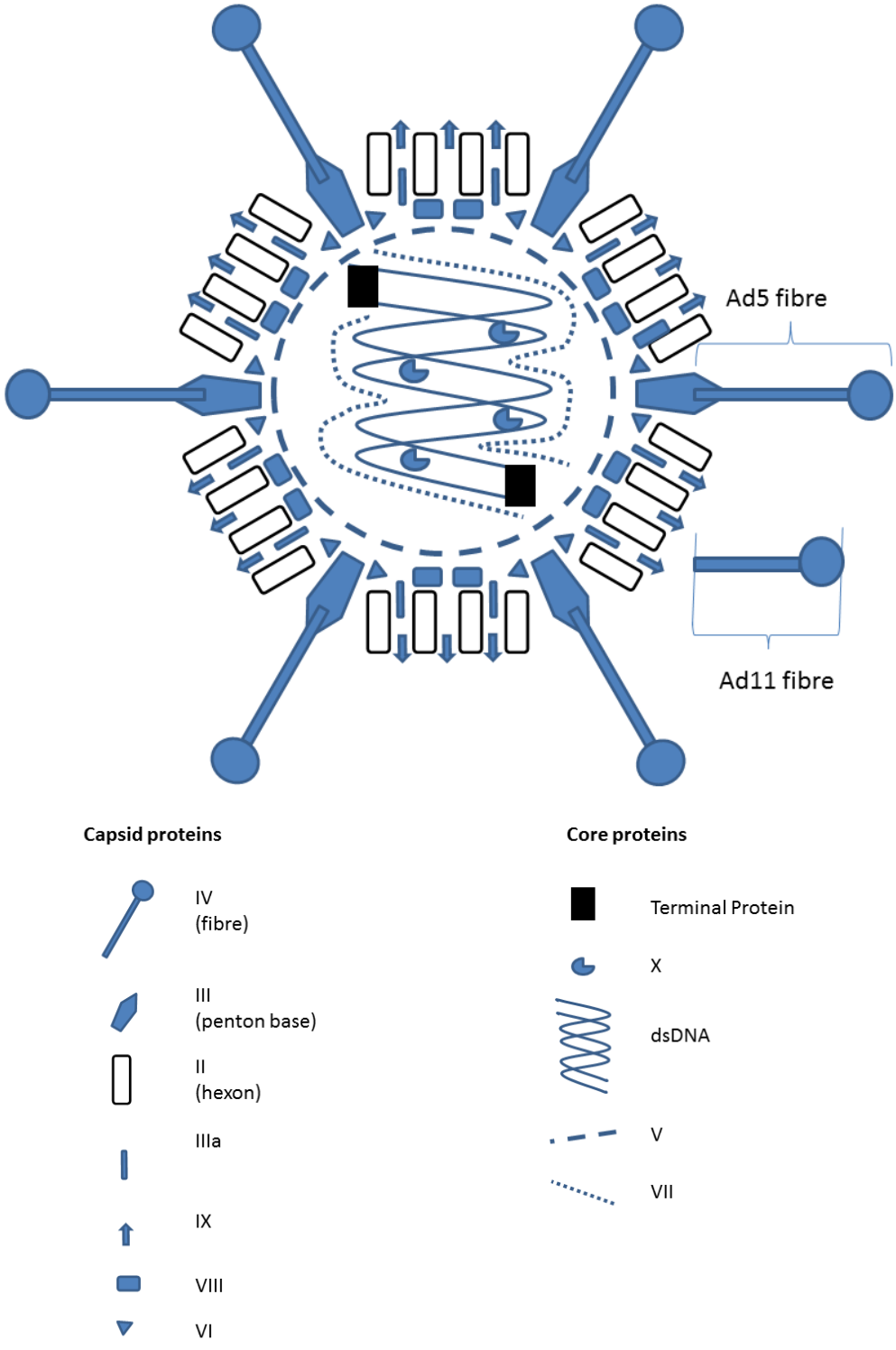

Figure 1-1: Adenovirus particle structure

The structure of Ad2 and Ad5 has been determined by electron microscopy and X-ray crystallography. Depicted are the structural components that constitute an imaginary cross-section of the capsid and core (not to scale). The length of the Ad5 fibre protein is depicted relative to the length of Ad11 (not to scale). Diagram adapted from [91, 95].

1.3.2 Adenovirus replication cycle

The adenovirus lifecycle can be separated into distinct stages of attachment, internalisation, endosomal escape, nuclear trafficking, replication, packaging and release (Figure 1-2). This has been most well characterised for Ad2 and Ad5.

Cellular Attachment

First, adenovirus attaches to the cell surface by binding to cell surface receptors via the fibre knob. The majority of HAds, from groups A, C, D, E and F, bind the Coxsackie and adenovirus receptor (CAR) [96, 97] mediated by a highly conserved binding site on HAd fibre knob. However, *in vitro* different HAd subtypes have different affinities for CAR. For example, Ad2 has an 8-fold higher binding affinity for CAR than Ad12 [98]. By contrast, receptor binding *in vivo* depends on access to the receptor. CAR is highly expressed during embryonic development but expression decreases after birth. In adults, mRNA encoding CAR can still be detected at high levels in some tissues such as the heart, brain, pancreas, testes and prostate [96]. Further, in epithelial tissues, CAR is normally located within tight junctions on the basolateral surface of polarised cells, which restricts HAd binding from the apical surface [99, 100]. This means that CAR expression is not always predictive of HAd infection efficiency *in vivo*. In addition, CAR expression actually decreases in some carcinomas such as bladder cancer [101]. In contrast, group B adenoviruses use CD46 as the primary cellular receptor for infection [102], as well as desmoglein-2 (DSG-2) [103], and CD46 expression is upregulated in many carcinomas [37]. This suggests that, group B adenoviruses could be inherently more cancer selective than group C adenoviruses.

Internalisation and endosome escape

Once attached to the cell surface via CAR, the penton base interacts with $\alpha_V\beta_3$ and $\alpha_V\beta_5$ intergrins via its exposed RGD sequences [104]. This triggers internalisation. Evidence for adenovirus internalisation via clathrin-coated vesicles was first observed by electron microscopy [105]. Consistent with this, adenovirus internalisation was inhibited in cell lines that expressed mutant dynamin, which is required for clathrin-mediated endocytosis [106] After endosome separation from the plasma membrane, the endosomal H+ATPase maintains a pH of 6.0 and this pH disrupts the structure of the adenovirus capsid to expose the penton base that acts, along with adenovirus L3/p23 protease, protein VI and fibre proteins, to lyse the lipid bilayer of the endosome [107]. After endosomal escape, adenovirus capsids associate with dynein to transport the partially dismantled capsid to the minus end of microtubules, which are usually next to the nucleus [108].

However, not all adenovirus subtypes seem to use clathrin-mediated endocytosis for internalisation and nuclear trafficking. Most notable differences exist between group C adenoviruses, which rapidly escape the endosome and traffic to the nuclear envelope within minutes of attachment, and group B adenoviruses, which seem to accumulate in lysosomes and traffic to peri-nuclear localisations before escape and rapid transport to the nuclear pore complex [109]. The delay in nuclear trafficking is thought to be due to the lower pH required for group B adenoviruses to escape the endosome compared to group C. For example, the group B adenovirus, Ad7, remains in late endosomes until it encounters an appropriate pH required for endosome escape and this is thought to be mediated by the fibre sequences of Ad7 [110].

Nuclear import, genome transcription, translation and replication

Adenoviral protein VII targets the adenovirus capsid to the cytoplasmic side of the nuclear pore complex for transport of viral DNA into the nucleus [111]. Once inside the nucleus, E1A is the first gene to be expressed due to its constitutively active promoter, which drives transcription of a single pre-mRNA that is alternatively spliced to produce the 12S and 13S protein products that both contain 2 highly conserved regions responsible for binding the tumour suppressor protein pRb, which releases E2F to enable transcription of E2F-dependent genes [24]. The E1A gene is responsible for activating all other early HAd genes. E1A also activates cellular genes, such as genes encoding *myc* by interaction with p400 [112].

Genomes of different HAd subtypes have the same general structure. The inverted terminal repeats (ITRs) at each end of the adenovirus genome act as primers to initiate DNA replication. The pre-terminal protein binds to a consensus sequence in the ITRs and recruits viral DNA polymerase to allow DNA replication to progress by a strand displacement mechanism [113].

Late gene expression and particle release

Late proteins are transcribed from the major late promoter (MLP) and produce structural proteins required for adenoviral packaging. Late viral mRNAs are preferentially translated over host cell proteins by a mechanism of ribosome shunting [114]. The late structural proteins are then transported back into the nucleus where adenoviral DNA is packaged into capsids. Packaged adenovirus particles accumulate before release by a lytic process that is

thought to involve adenovirus death protein (ADP) [115], although not all adenoviruses express this protein so the release process is relatively uncharacterised for some subtypes.

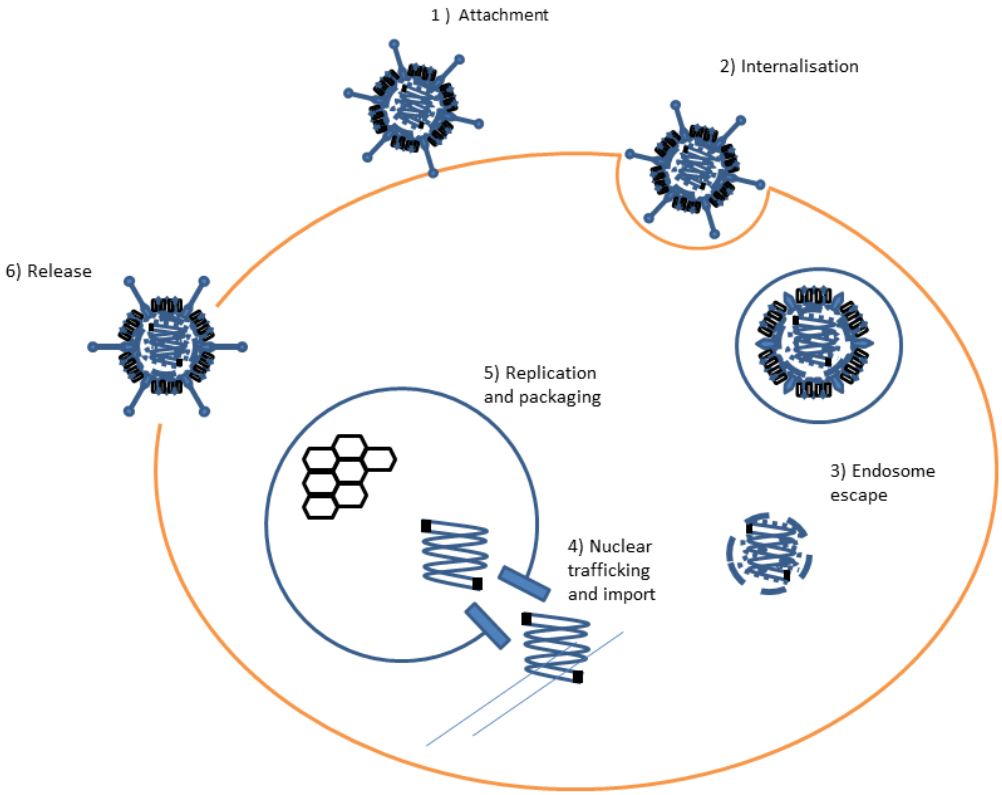

Figure 1-2: Adenovirus lifecycle

Adenovirus infection begins with attachment to cellular receptors (1), followed by internalisation (2) with subsequent escape from the (3) and trafficking of the partially dismantled capsid along microtubules to the microtubule organising centre (MOC) located next to the nucleus (4). Adenoviral DNA is transported into the nucleus via the nuclear pore complex where early viral genes are transcribed and after expression of the early viral genes, DNA replication occurs before the late viral proteins are expressed and imported into the nucleus where particles are packaged (5) and released (6). Adapted from [109].

1.3.3 ColoAd1 structure and properties

Initial experiments *in vitro* demonstrated that ColoAd1 was significantly more potent than Ad5 at killing many human carcinoma cell lines, with limited cytotoxicity in normal human epithelial and endothelial cells [69]. The physical properties of ColoAd1 were characterised by HPLC, which showed that the outer capsid was mainly derived from Ad11p [69]. Genome sequence analysis confirmed that ColoAd1 was mainly Ad11p with a nearly complete deletion of the E3 region, a smaller E4 region deletion and a chimeric Ad3/Ad11p E2B region (Table 1-2). ColoAd1 also had greater cytotoxicity than Ad11p and Ad3 on human cancer cell lines, suggesting that, although ColoAd1 has the same surface charge as Ad11p, the genetic differences suffice to provide enhanced oncolytic potency [69].

ColoAd1 is a chimeric conditionally replicating group B oncolytic adenovirus that was generated by a method of bioselection [69]. The genetic differences between Ad11p and commonly studied Ad5 have been reviewed in [116] and are summarised in Table 1-2. ColoAd1 differs from Ad11p by frequent substitutions of Ad3 sequences in the E2B region, which encodes the pre-terminal protein (pTP) and DNA polymerase. This chimeric E2B region has been hypothesised to enhance pTP and viral DNA polymerase binding to the consensus sequence in the inverted terminal repeats (ITRs) of ColoAd1, which were also found to be identical to Ad3 ITRs [69].

The *E4orf4* mutation of ColoAd1 is hypothesised to attenuate replication in normal cells. Most E4orf4 functions have been determined with Ad5; however there is only 44.3% amino acid similarity between Ad5 and Ad11 [116]. Hence, it is possible that different

E4orf4 functions exist between Ad5 and Ad11p, which are absent from ColoAd1. The 24 base pair deletion in the E4 region of ColoAd1 is within the E4orf4 reading frame. The E4orf4 protein product normally localises to the nucleus, in part due to a highly basic sequence, and is known to interact with the regulatory subunit of protein phosphatase 2A (PP2A) [117]. E4orf4 partly regulates the switch between the transcription of early and late adenoviral genes. E4orf4 inhibits E1A induced transcription by dephosphorylating transcription factors involved in E1A induced transactivation of early genes, including JunB and c-Fos components of AP-1 [118]. The inhibition of E1A transcription is in turn partly responsible for the down regulation of E2 and E4 gene transcription [119]. The E4orf4/PP2A complex also dephosphorylates SR proteins that are responsible for alternative splicing of late adenoviral mRNAs [120]. E4orf4 may also activate the mTOR pathway [121]. E4orf4 has also been shown to regulate adenoviral DNA replication [119, 122].

The *E3* deletions in ColoAd1 are likely to modulate the host immune response to infection. The *E3* gene encodes proteins that are not essential for adenovirus replication. For example, Ad5 encodes the E3 19K protein that inhibits MHC1 transport from the ER to the plasma membrane, which prevents MHC1 antigen presentation to cytotoxic T-lymphocytes [123]. The Ad5 14.7K E3 protein inhibits TNFα-induced apoptosis. The Ad5 11.6K E3 protein, or ADP, is the only E3 protein that is not expressed by the E3 promoter and is expressed during the late phase of infection where it acts to induce cell death for release of packaged particles [115].

Genome	Ad5	Ad11	ColoAd1
Length	35935 bp	34794 bp	32325 bp
GC content	55.19%	48.87%	49.63%
Early region – E1			
E1A	Present	Present	Present
E1B	Present	Present	Present
Early region – E2			
E2A	Present	Present	Present
E2B	Present	Present	Ad3 substitutions
Early region – E3			
20.3K	Absent	Present	Absent
20.6K	Absent	Present	Absent
11.6K (ADP)	Present	Absent	Absent
16.1K	Absent	Present	Absent
10.3	Absent	Present	Absent
15.2	Absent	Present	Absent
18.5K	Absent	Present	Fused with 15.3K
15.3K	Absent	Present	Fused with 18.5K
Early region – E4			
Orf4	Present	Present	Partial deletion
Late region	L1-L5	L1-L6	L1-L6
L5 fibre	Long	Short	Short
Other			
Primary receptor	CAR	CD46	CD46
Serum prevalence	High (>50%)	Low (<10%)	Same as Ad11
VA RNA	2	1 (66% homology to Ad5 VA RNA II)	Same as Ad11
ITR	Present	Present	Present

Table 1-2: Genetic differences between commonly used Ad5 to Ad11p and ColoAd1

Details of the key genetic differences between Ad5, Ad11p and ColoAd1 as adapted from [116] and [69].

1.4 Adenovirus production

The manufacture of medicinal products intended for human use is strictly regulated to ensure patient safety. Products, such as oncolytic adenoviruses, intended for human use would be manufactured at facilities that adhere to Good Manufacturing Practice (GMP) and that are authorised and licenced by agencies, such as the Medicines and Healthcare Products Regulatory Agency (MHRA) in the United Kingdom or the Food and Drug Administration (FDA) in the United States of America, to ensure compliance to regional guidelines and directives for GMP. Some of the documentation and records that are required to meet GMP have been reviewed in [124]. More specifically, some of the challenges involved in manufacturing adenoviruses for use in clinical trials have been reviewed in [125]. Processes used for the manufacture of adenoviruses have also been published and can generally be divided into an "upstream" cell culture phase and a "downstream" purification phase (Figure 1-3).

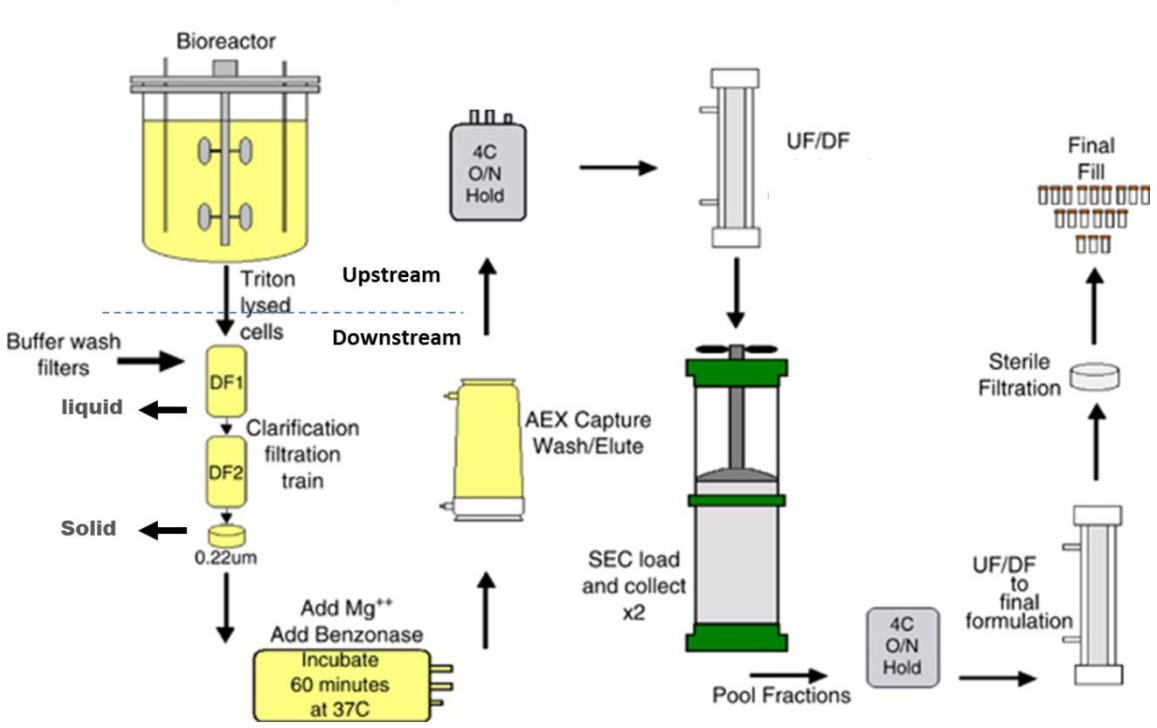

Figure 1-3: Process widely used for the manufacture of clinical grade adenovirus

Depicted is a process used to manufacture adenovirus. Cells are cultured in a bioreactor for optimal growth before infection. After infection, the culture is harvested before the cell lysate is clarified by filtration, treated with benzonase to degrade contaminating DNA, and purified by a series of chromatography steps before buffer exchange into the final formulation buffer and filling into vials for clinical use. Ultrafiltration (UF), Diafiltration (DF), Anion Exchange Chromatograph (AEX), Size Exclusion Chromatography (SEC), Overnight (ON). Adapted by permission from Macmillan Publishers Ltd: Nature Oncogene, copyright 2005 [126].

Cell line selection for the manufacture of an oncolytic adenovirus should first consider any genetic alterations of the recombinant adenovirus from wild type. For example, replication deficient oncolytic adenovirus designed for suicide gene therapy (as discussed in section 1.2.4) may contain E1 gene deletions that would require *trans* complementation of the E1 gene from a cell line such as HEK293, 911 or PerC6 for viral particle production [127]. In such cases, it is possible that replication deficient Ad5 could revert to a replication competent adenovirus (RCA) by recombination between regions of homology in the E1 region of host cell and the adenovirus genome. In order to reduce the possibility of

recombination, some cell lines such as PerC6 contain minimal DNA sequences required for replication of E1 deficient Ad5 [127]. Nevertheless, production of RCA in batches of replication deficient oncolytic adenovirus would be rigorously tested for by infecting a non-*trans* complementing cell line, such as A549, and monitoring the infected cells for any indication of viral replication by observing cytopathic effect (CPE) [125].

In contrast, replication competent oncolytic adenoviruses, such as ColoAd1, contain the wild-type E1 gene and would not require *trans* complementation of E1 from a host cell line for viral particle production. In some ways replication competent adenoviruses have a wider variety of cell lines that they are able to replicate in as their genomes contain all of the genes required for replication. In this case, cell line selection may simply be based on the availability of cell lines with master cell banks (MCB) and working cell banks (WCB) that meet GMP. Alternatively, if suitable GMP compliant cell lines are not available then GMP cell banking may be required. However, this would be a potentially costly, lengthy process that would require extensive characterisation of the cell line and thorough Quality Control (QC) testing of the MCB and WCB to meet GMP.

Cell line selection for the manufacture of ColoAd1 took these factors into account and the HEK293 cell line was selected. This cell line contains a continuous fragment of Ad5 DNA, containing both E1A and E1B Ad5 genes, integrated into chromosome 19 of HEK cells [128]. These genes are not required for the replication of ColoAd1 as the ColoAd1 genome contains the E1 gene derived from Ad11p and this is approximately 50% homologous to the E1 gene from Ad5, so the risk of recombination was considered to be minimal. In addition, the HEK293 cell line has advantages of being well characterised, widely used in

many GMP compliant processes and readily available from GMP compliant facilities. HEK293 cells also grow adherently and can be adapted to grow in suspension cell culture, thus providing the opportunity to scale-up the process for large scale manufacture.

In some ways cell line selection significantly impacts the upstream process used for the manufacture of oncolytic adenovirus. Upstream processing largely depends upon how the cell line grows, either anchorage dependently (adherent) or in anchorage independently (suspension). For adherent cell culture, multi-layered tissue culture flasks offer a larger surface area for cell growth than traditional tissue culture flasks and they have generally superseded Roller Bottle technology [129]. For example, HYPERflasks from Corning have a surface area of 1720cm^2, which is 10-fold higher than the largest tissue culture flask available for the equivalent flask volume. However, each HYPERflask requires 560mL of media, which is much more than media volume required for the equivalent number of 175cm^2 tissue culture flasks. This large volume increase per unit surface area is a significant disadvantage at scale where large volumes are difficult to handle in a single processing step, even with the use of Cell Culture Automation Platforms. Micro carrier cultures are also a popular scalable alternative to Roller Bottles, especially for virus production, as cell density can be increased by increasing the number of micro carrier beads per unit of volume [130]. However, more recently, novel bioreactors that specialise in high density adherent cell culture have become commercially available. For example, the iCELLis bioreactor has a compact fixed bed that provides a 500m^2 surface area in a 25L volume, which is equivalent to 3000 Roller Bottles [131].

The main disadvantage of large scale adherent cell culture is the requirement for medium supplementation with foetal bovine serum (FBS), which must be free from adventitious agents to meet GMP. The European Medicines Agency (EMA) has issued guidelines on the use of bovine serum in the manufacture of human biological medicinal products (EMA/CHP/BWP/457920/2012 rev 1). A practical consequence of these guidelines is that FBS is sourced from regions of the world that pose less risk of contamination from adventitious agents such as viruses and prions. In addition, FBS is often sourced in large quantities to avoid problems with batch to batch variation and to avoid extensive GMP testing of multiple smaller batches of FBS. Overall, this makes medium supplementation with GMP compliant FBS expensive for large scale adherent cell culture and is particularly challenging for the scale up of processes used to manufacture mesenchymal stromal cells for clinical studies [132].

One advantage of suspension cell culture is that medium can be chemically defined and serum free. In addition, suspension cell culture is arguably more scalable than adherent cell culture as cell density can be increased per unit volume without limitations of surface area available for cell growth and proliferation. Processes used to culture suspension cells are often scaled up from orbital shaking Erlenmeyer flasks that have a working culture volume of up to 3L per flask, to stirred tank bioreactors that have a working culture volume of up to 20,000L and offer additional control of agitation, aeration, pH, and temperature [133]. However, Wave bioreactors have also emerged as an intermediate scale alternative to stirred tank bioreactors with the main difference being the method used to mix and aerate the culture [134]. Improvements in bioreactor design and control have also generally improved the performance of cells cultured in suspension [135].

As highlighted, a scalable process has unit operations that allow capacity to increase without increasing volume or that increases the capacity of a single processing step without affecting product quality or yield. Ultimately, the scale of manufacture depends upon the amount of clinical product that is required and this depends upon the number of patients involved and the dose administered to each patient. The Phase I clinical trial of ColoAd1 involves a dose escalation study, requiring up to 10^{13} viral particles/dose to be administered intravenously. In comparison, the replication-selective PSA targeted oncolytic adenovirus, GC7870, was administered intravenously at quantities of up to $6x10^{12}$ vp/dose in a Phase I clinical trial [57]. This means that potentially large quantities of ColoAd1 will be required for clinical trials and perhaps beyond.

The inevitable lytic life cycle of productive adenovirus replication (section 1.3.2) inherently limits manufacture to batch processing. To date, increasing adenovirus yield per batch has been achieved mainly by increasing the cell density at infection. However, a "cell density effect" has been observed where Ad5 yield per cell actually decreases with increasing density of suspension HEK293 cells [136]. This has been hypothesised to be due to nutrient limitations and waste product accumulation [137] and can be overcome by using continuous perfusion of cell culture media in large scale bioreactors [138]. However, since published strategies for enhancing adenovirus yield from HEK293 cells are limited, an increased knowledge of the host cell factors that limit adenovirus yield would begin to address this. This thesis will therefore aim to identify the host cell factors that could be responsible for limiting adenovirus yield. Once these factors are identified it is intended that they would be targets for intervention at any scale of manufacture.

1.5 Hypothesis

The enhanced oncolytic properties of ColoAd were hypothesised to induce early cell lysis that kills host cells prematurely, thus providing several opportunities to investigate methods that may increase virus manufacturing yield. Each chapter describes different approaches to address this overall hypothesis:

- Chapter 3 characterises ColoAd1 replication in HEK293 cells.
- Chapter 4 dissects the cellular response to ColoAd1 infection in HEK293 cells and seeks to define strategies to enhance infected cell viability.
- Chapter 5 attempts to enhance cellular glycolytic pathways to increase ColoAd1 production.
- Chapter 6 uses a high throughput siRNA screen in attempting to define kinases that influence ColoAd1 replication.

2 Materials and Methods

2.1 Cell culture

The cell lines described in Table 2-1 were cultured using the methods described in sections 2.1.3 - 2.1.2 to a maximum passage number of 25.

Cell Line	Description	Origin	Culture Medium	Additions for complete media
HEK293 (adherent)	Human embryonic kidney cells	ATCC	DMEM	2 or 10% FBS 1% pen/strep
HEK293 (suspension)	Suspension adapted human embryonic kidney cells	Gifted from CBF	CD293	4mM L-glutamine
A549	Human caucasian lung carcinoma	ECACC	DMEM	2 or 10% FBS 1% pen/strep
HT29	Human colon adenocarcinoma	ATCC	DMEM	2 or 10% FBS 1% pen/strep
RCC4-EV	Renal cell carcinoma, empty vector	Gifted from CR-UK	DMEM	2 or 10% FBS 1% pen/strep

Table 2-1: Cell line details

2.1.1 Adherent cell culture

Cells were grown in a humidity-controlled incubator at 37°C with 5% CO_2. Cells were split once they reached 80-95% confluence. This was performed using sterile techniques in a class II laminar-flow cabinet. Briefly, the supernatant was removed from the flask and cells washed with PBS before incubation with 1 – 2 mL trypsin-EDTA until all cells had detached from the surface of the flask. Cells were then resuspended media containing 10% FCS and a proportion of these cells added to a new flask containing serum-positive medium.

2.1.2 Suspension cell culture

Suspension HEK293 cells were grown in 125mL non-baffled, disposable, polypropylene, sterile Erlenmeyer flask (Corning) using CD293 media (Life Technologies) supplemented with 4mM L-glutamine (Sigma). Cells were split once they reached a density of 2 x 10^6

cells/mL by removing the cells from the flask, centrifugation at 300xg to pellet cells, and resuspension in pre-warm complete CD293 media, to achieve a cell density not less than 2 x 10^5 cells/mL.

2.1.3 Storage of cell lines

Adherent cell lines were grown to 90-95% confluence in 175cm^2 flasks. Serum-positive medium was removed from the flasks and cells washed with PBS (Life Technologies) before incubation with 2 mL trypsin-EDTA (Sigma) until all cells had detached from the surface of the flask.Freezing solution, containing 10% sterile dimethyl sulphoxide (DMSO, Sigma-Aldrich), 45% FCS and 45% medium containing 10% FCS, was prepared. The cell pellet was resuspended in this freezing solution and dispensed into 1 mL aliquots in cryovials, before storage at -80°C in a Mr. Frosty container (Nalgene) for at least 12 hours. Before use, adherent cells were thawed in a water bath at 37°C before being quickly resuspended in 9 mL of pre-warmed serum-positive medium and centrifuged at 200g for 10 minutes. After removing the supernatant, the cell pellet was resuspended in 20mL of pre-warm serum positive medium and transferred to a 75cm^3 flask for over-night incubation.

2.1.4 Storage of suspension cell lines

Cells were split and fed the day before freezing. Freezing solution, containing 7.5% sterile dimethyl sulphoxide (DMSO, Sigma-Aldrich), 42.5% complete media and 50% conditioned medium, was prepared. The cell pellet was resuspended in this freezing solution and dispensed into 1 mL aliquots in cryovials, before storage at -80°C in a Mr. Frosty container (Nalgene) for at least 12 hours. Before use, suspension HEK293 cells were thawed in a water bath at 37°C before being re-suspended in 12.5 mL of pre-warmed complete media and transferred to a 125 mL Erlenmeyer flask (Corning).

2.1.5 Cell counting

Cell suspensions from adherent (section 2.1.1) or suspension culture (section 2.1.2) were prepared. Equal volumes of cell suspension and trypan blue (Sigma) were gently mixed together before loading in a haemocytometer (Marienfeld) to count the cells under a light microscope (Eclipse TS100, Nikon). Cells with trypan blue dye incorporated were counted as dead. Cells that were not coloured blue and that were capable of excluding the dye were counted as viable. Total cells were the sum of the dead and viable cells.

2.1.6 Cell plating

Unless otherwise stated, all cells were routinely seeded for 16 hours overnight at 10,000cells/well in a 96 well plate or 350,000cells/well in a 24 well plate.

2.2 Cellular Assays

2.2.1 MTS

MTS [3-(4,5-dimethylthiazol-2-yl)-5-(3-carboxymethoxyphenyl)-2-(4-sulfophenyl)-2H-tetrazolium] is a tetrazolium compound that is reduced to a soluble, blue coloured formazan product in metabolically active cells (Figure 2-1). The amount of formazan produced can then be measured by its absorption at a wavelength 490nm and is directly proportional to the number of metabolically active cells. The CellTiter 96® Aqueous Non-Radioactive Cell Proliferation Assay (Promega) was used to determine cell viability by this method. Cells that required a viability reading, had supernatant removed the well and 100µL PBS added with 20µL MTS reagent. Cells were incubated with MTS reagent for 1-4 hours before absorption at 490nm was determined using a Wallac 1420 Victor^2 multi-label counter (PerkinElmer Life and Analytical Sciences, UK).

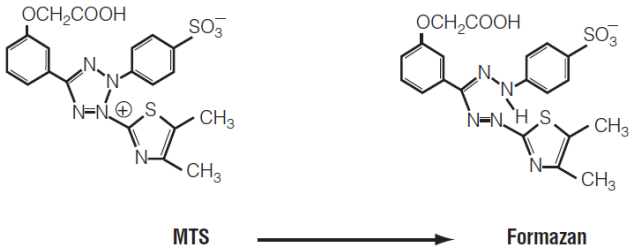

Figure 2-1: Conversion of MTS to Formazan by metabolically active cells

2.2.2 Resazurin

Resazurin is a weakly fluorescent dye that is reduced by viable cells to resorufin, a highly fluorescent compound that emits fluorescence at 590nm (Figure 2-2). The amount of resorufin produced is directly proportional to the number of metabolically active cells. Cells had supernatant removed and 100µL resazurin added at 0.05mg/mL final concentration. Cells were incubated with resazurin reagent for 1 - 2hours before absorption at 490nm was determined using a Wallac 1420 Victor^2 multi-label counter (PerkinElmer Life and Analytical Sciences, UK).

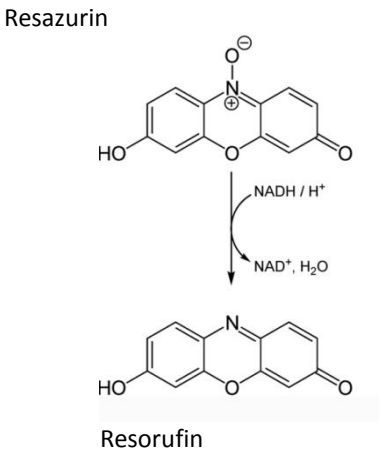

Figure 2-2: Conversion of resazurin to resorufin by metabolically active cells

2.2.3 Intracellular ATP

Intracellular ATP was determined using a luminescent assay system (BioTherma AB 266-111). The principle of the assay is that extracellular ATP is enzymatically degraded before

releasing intracellular ATP. D-luciferin is then converted by luciferase to oxyluciferin in the presence of ATP and oxygen, releasing light that is measured using a luminometer. The amount of light detected is proportional to the amount of intracellular ATP present.

$$\text{ATP + D-luciferin + } O_2 \xrightarrow{\text{Luciferase}} \text{AMP + PPi + oxyluciferin + } CO_2 \text{ + light}$$

To determine the amount of intracellular ATP, supernatant was removed from each well and 20µL PBS added with an equal volume of ATP eliminating reagent, before incubation at room temperature for 10 minutes. Then, 20µL extractant B/S was added before storage at -80°C. Later, 30µL of each pre-prepared sample was added to 80µL of ATP substrate before immediate measurement of the luminescence for 1 second, using a Wallac 1420 Victor^2 multi-label counter (PerkinElmer Life and Analytical Sciences, UK).

2.3 Adenoviruses

The characteristics of the stocks of adenovirus used in this thesis are summarised in Table 2-2. These stocks were prepared as described in section 2.3.1, and characterised using the methods described sections 2.3.2, 2.3.3 and 2.3.4.

Adenovirus	Concentration (vp/mL)	Infectivity (ifu/mL)	Infectivity (TCID50/mL)	Purity (260nm/280nm)
ColoAd1	5.98×10^{11}	1.15×10^{9}	1×10^{10}	1.25
Ad11p	4.79×10^{11}	N/A	1.5×10^{8}	1.32
Ad5	6.49×10^{12}	N/A	N/A	N/A
Ad-β gal	N/A	2×10^{8} – 2×10^{9}	N/A	N/A

Table 2-2: Characteristics of adenoviral stocks used

2.3.1 Adenovirus purification

Viral seed stocks were prepared in HEK293 cells and used as inoculum to create the large stocks described in section 2.3. Viral seed stocks had infectivity determined hexon staining.

HEK293 cells were seeded in a HYPERflask (Corning) in media containing 10% FBS until they reached a confluence of 80-90%. Then the appropriate amount of viral seed stock needed to infect 1 x 10^8 total cells at a multiplicity of infection (MOI) of 10 was diluted in 560mL of media containing 2% FBS. Media in the confluent HYPERflask was replaced with the viral inoculum and stored in a humidified incubator at 37°C in 5% CO_2 until the appearance of cytopathic effect (CPE). Once all of the cells were detached from the surface of the HYPERflask, cells and supernatant were decanted from the HYPERflask and spun at 300xg for 10 minutes. The supernatant was discarded and the cell pellet was suspended in 12mL of cell lysis buffer (10mM Tris, 135mM NaCl, 1mM $MgCl_2$ pH8) before 3 cycles of freeze-thaw, performed by snap freezing in liquid nitrogen and thawing in a waterbath at 37°C. Between the first and second freeze-thaw cycle, benzonase (Novagen) was added to achieve a final concentration of 250U/µL before incubation for 30 minutes at room temperature. The cell lysate was clarified by centrifugation at 300xg for 10 minutes and the supernatant collected noting the volume and discarding the cell debris. Ultraclear ultracentrifugation tubes (Beckman) with 15mL volume were filled with 3mL of 1.25g/L cesium chloride and the under layer filled with 1.35g/L cesium chloride, before adding equal volumes of clarified cell lysate to each tube and the remaining volume filled with PBS. The weight of each tube was measured to ensure that they were equal, before high speed ultracentrifugation using the High Speed Ultracentrifuge (Beckman) at 25,000rpm for 2 hours at 4°C, with the SW40 rotor (Beckman) and the corresponding

swing out buckets (Beckman). The lower, slightly blue coloured, opaque virus band was removed from each tube using a sterile 21G needle (BD Biosciences) and 5mL sterile syringe. Virus bands from multiple tubes were pooled, and the total volume split, before adding equal volumes to two ultraclear ultracentrifugation tubes (Beckman) containing 6mL of 1.35g/L cesium chloride. High speed ultracentrifugation was subsequently performed for 16 hours at 4°C and at 25,000rpm, again using the SW40 rotor (Beckman) and the corresponding swing out buckets (Beckman). The lower, slightly blue coloured, opaque virus band was removed from each tube using a sterile 21G needle and 5mL sterile syringe. Buffer exchange of the virus preparation was then performed using PD10 columns (GE Healthcare) or slide-a-lyzers (ThermoScientific).

2.3.2 Spectrophotometry

Spectrophotometry was used to determine purity and the concentration of viral particles in purified adenovirus stocks. The technique is based on the fact that proteins have an absorbance maximum at 277nm, due to their tryptophan and tyrosine content, and DNA has an absorbance maximum at 260nm. Purified adenovirus stocks were lysed in a final concentration of 0.1% (v/v) SDS and the content of DNA and protein determined by measuring the respective absorbances at 260nm and 280nm, using a UV/vis DU730 spectrophometer (Beckman Coulter) that had been corrected against the 0.1% SDS treated formulation buffer. For purified adenovirus, the ratio of absorbance at 260nm to 280nm should be 1.25 – 1.35. Then viral particle concentration was calculated from the absorbance at 260nm, based on the assumption that at 260nm an absorbance of 1.00Au, with 1cm path length, corresponds to 1.1×10^{12} viral particles/mL [139]. Adenoviral particles are 65 - 85nm in hydrodynamic diameter and aggregation can cause light scattering that influences absorbance measurements. However, light scattering is detectable at 320nm. Therefore, the absorbance at 320nm was also measured to ensure that

the turbidity of the solution did not interfere with the absorbance readings at 260nm and 280nm.

2.3.3 Infectivity assay by TCID50

TCID50 (tissue culture infectious dose causing pathological change in 50% of cultures) was used to determine infectious viral particle concentrations by observing cytopathic effect (CPE). HEK293 cells were seeded in a 96-well flat bottomed plate with 10,000 cells/well, in a volume of 100 µL/well, in medium containing 10% FCS. Plates were incubated overnight at 37°C in 5% CO_2. The following day, medium was removed and replaced with 200uL of virus inoculum, prepared by 10-fold serial dilution of virus stock in medium containing 2% FBS. Each dilution was added to a row of a 96 well plate. Top and bottom dilutions of virus were such that every well in the first row exhibited CPE and none of the wells in the last dilution showed any sign of CPE. Plates were infected in triplicate and incubated at 37°C in 5% CO_2 for 7 days. TCID50 was determined using the Karber method, outlined by the equation:

$$T = 10^{1+D(S-0.5)}$$

Where D = Log_{10} serial dilution factor (1 for a 10 fold dilution series)

S = Sum of the ratios of CPE in each row

Wells were scored positive if any of the cells in that well displayed signs of CPE. An example calculation of TCID50 determination is given below.

100% CPE at dilutions below 10^{-9}, 80% CPE at 10^{-10} and 40% CPE at 10^{-11}

S = (1 + 1+ 1 + 1 + 1 + 1+ 1 + 1 + 1 + 0.8 + 0.4) = 10.2

D = log (10) = 1

Titre (TCID50 / 100µL) = $10^{1 + 1 (10.2 – 0.5)} = 10^{10.7}$

Titre (TCID50 / mL) = $10^{11.7} = 5.0 \times 10^{11}$

2.3.4 Infectivity assay by hexon staining

Infectivity was initially determined using the Adenovirus Functional Titer Immunoassay Kit (Cell Biolabs Inc) and the protocol modified for use with ColoAd1 and Ad11p. For each assay, the Ad-β gal was used from the kit as a positive control that had a known infectivity in the range of 2×10^8 - 2×10^9 ifu/mL.

Briefly, HEK293 cells were seeded in 24-well plates that had been coated with poly-L-lysine (Sigma) at 3.5×10^5 cells/well. Plates were incubated overnight at 37°C with 5% CO_2. Infections were carried out the following day. The virus stock was diluted between 10^3 and 10^6 times in medium containing 10% FCS. Then 100µL of inoculum was added to 1mL of cells/well. After 33 hours medium was removed and the cell monolayer fixed using cold methanol with storage at -20°C for 30 minutes. After removing the methanol and washing with PBS, the plates were incubated with PBS containing 1% bovine serum albumin (BSA) at room temperature for 1 hour with gentle agitation. After removing the blocking buffer, plates were incubated for 1 hour at room temperature with primary antibody (see Table 2-3 for details) that had been diluted in PBS containing 1% BSA. After removing the primary antibody and multiple washes with PBS, plates were incubated for 1 hour at room temperature with secondary antibody (see Table 2-3 for details) that had been diluted in PBS containing 1% BSA. After removing the secondary antibody and performing multiple washes with PBS, staining was performed using 3, 3'-diaminobenzidine (DAB) from ImmPACT DAB Peroxidase (HRP) Substrate (Vector Labs).

Cells that had stained positively for hexon produced a dark brown colour. Positively stained cells were counted in at least 5 separate, random fields of view per well, using a light microscope (Eclipse TS100, Nikon) with 10X objective. Wells containing 5 – 50 positively stained cells per field of view were used to count. The average number of positive cells per well was calculated and viral titre of infectious particles (ifu/mL) determined using the following equation:

$$\frac{(\text{average positive cells / field}) \times (79 \text{ fields / well}) \times (\text{dilution factor})}{0.1\text{mL}}$$

Antibody	Clone	Clonality	Species	Supplier	Dilution
Anti-adenovirus type 3 (ATCC strain VR847)	B025/AD51	Monoclonal	Mouse	Abcam	1:500
Anti-mouse HRP conjugated IgG	N/A	Polyclonal	Rabbit	Abcam	1:1000

Table 2-3: Details of antibodies used for hexon staining assay

2.3.5 IC50 determination

Cells were seeded in a 96-well flat bottomed plate with 10,000 cells/well, in a volume of 100µL/well, with medium containing 10% FCS. Plates were incubated overnight at 37°C with 5% CO2. Infections were carried out the following day in triplicate, using 5-fold serial dilutions of the virus starting at 500 viral particles per cell to 0.032 viral particles per cell. Infected cells were incubated at 37°C for 5 days before using MTS assay (CellTiter 96® Aqueous Non-Radioactive Cell Proliferation Assay, Promega) to determine cell viability according to manufacturer's instructions. Mock-infected cells were used as negative controls and to establish the 100% survival point for each assay.

2.3.6 DNA extraction using Miniprep

Viral DNA was extracted from cell lysate or supernatant samples using the Gen Elute Mammalian Genomic DNA Miniprep Kit (Sigma), according to the manufacturer's instructions. Briefly, samples were thawed, treated with Lysis Solution C and Proteinase K (20mg/mL final concentration), before incubation at 56°C for 1 hour, followed by 70°C for 30 minutes. After adding 200µL ethanol, samples were transferred to DNA binding columns and subsequently centrifuged at 13,000rpm in a Biofuge Pico benchtop centrifuge (Heraues). The liquid eluting from the column was discarded and wash solution added to the column, before centrifugation at 13,000rpm in a Biofuge Pico benchtop centrifuge (Heraues). This wash step was repeated twice before DNA was eluted with an elution buffer containing 10mM tris HCl 0.5mM EDTA pH 8.0.

2.3.7 DNA extraction in plate format

DNA extraction was also performed using SV mammalian DNA extraction kit (Promega) by following manufacturer's instructions, with some alterations. Briefly, proteinase K was diluted in lysis buffer to achieve a final concentration of 20mg/mL, before 75µL was mixed with an equal sample volume. Samples were incubated at 55°C for 30 minutes before sample transfer to the binding plate. After applying a vacuum to the binding plate, the eluting volume was discarded. Then, 1mL of column wash solution was added to each well of the binding plate. Again, the vacuum was applied to the plate and the eluting volume was discarded. This was repeated for a total of three washes. After the final wash, the vacuum was applied to the binding plate for 6 minutes to dry the binding matrix. Finally, sample was eluted from the binding matrix with 250µL of nuclease-free water.

2.3.8 Standard curve preparation for QPCR

Standard curves were treated the same as test samples. Serial 10-fold dilutions of virus stock, with known viral content, were prepared and spiked into the uninfected control samples for each experiment. The typical standard curve ranged from 1 x 10^3 - 1 x 10^8 viral particles. Then standard curves were extracted using same DNA extraction method as the test samples (section 2.3.6 and 2.3.7). Typical standard curves for adherent cell lysate samples are shown in Figure 2-3.

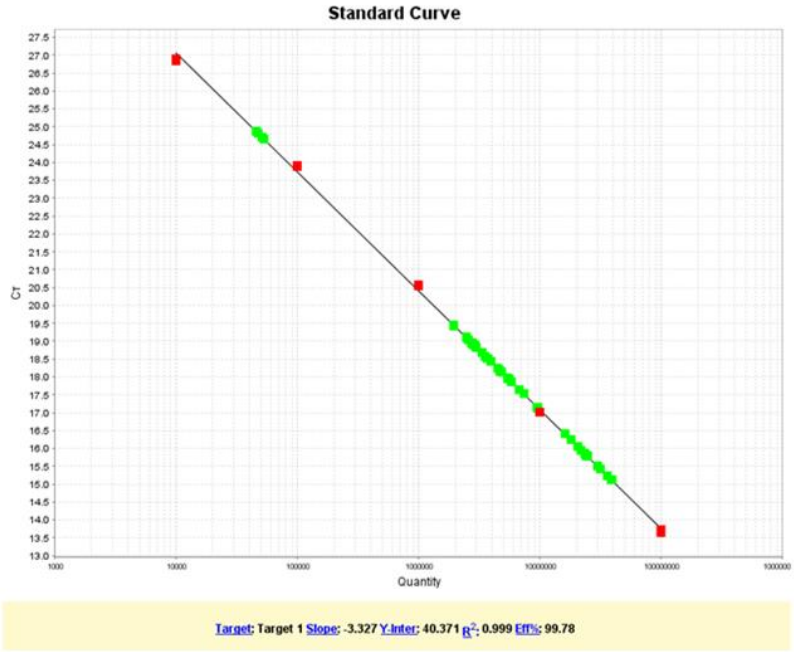

Figure 2-3: Typical standard curves for ColoAd1 detected from HEK293 cell lysate QPCR
Standard curves at 10-fold serial dilutions of ColoAd1 were prepared in a background adherent HEK293 cell lysate, before DNA extraction and QCPR. Typical slope values were -3.32 with a Y-intercept of 40 and 99% efficiency.

The Taqman® detection system was used to determine the amount of ColoAd1 or Ad11p DNA. FAM-TAMRA labelled probe and primers were added to 2X master mix containing Hi-ROX (PCR Biosystems), and made up to 20µL per well with distilled water, to achieve final concentrations of 0.1µM and 0.1 µM respectively. Then, 5µL of each sample was

added per well to a 96 well QPCR plate (Applied Biosystems). QPCR was performed using StepOnePlus™ Real-Time PCR System (Applied Biosystems) with the amplification cycle starting at 50°C for 2 min, before 95°C for 10 min, followed by 40 cycles of 15 sec at 95°C for denaturation and 60°C for 60 sec for annealing and extension. Data was analysed using Applied Biosystems StepOnePlus™ software v2.1, with test samples compared to standards of known viral content based on spectrophotometry analysis.

The details of the primers and probes routinely used in this thesis are as follows.

ColoAd1 / Ad11 Forward primer: TACATGCACATCGCCGGA

ColoAd1 / Ad11 Reverse primer: CGGGCGAACTGCACCA

ColoAd1 / Ad11 Probe: **FAM**-CCGGACTCAGGTACTCCGAAGCATCCT-**TAMRA**

2.3.9 High Throughput QPCR

The QPCR was performed using the same reagents at the same final concentrations as detailed in section 2.3.8. However, the total volume of the final reaction mixture was 5µL, instead of 25µL, and the reaction mixtures were dispensed using the Echo525 liquid handing system (Labcyte) into a 384 well QPCR plate (Roche). In this format, QPCR was performed using the LightCycler® 480 (Roche). Data was analysed using the LightCycler® 480 software.

2.4 FACS

2.4.1 FACS for cellular receptors

Cells were washed with pre-warm PBS before incubation with 5mL of pre-warm Gibco® Cell Dissociation Buffer (Life Technologies) for 5 minutes at 37°C. After cells had detached from the surface of the cell culture flask, an equal volume of DMEM containing 10% FBS was added. Cells were counted and incubated with primary antibody at 4°C for 1 hour (see Table 2-4). Then cells were spun at 300xg for 5 minutes, supernatant removed and washed with PBS. This was repeated twice more, before incubation with secondary antibody (see Table 2-4) at 4°C for 1 hour. Again, cells were pelleted by centrifugation at 300xg for 5 minutes, supernatant removed and washed with PBS. This was repeated twice more, before final re-suspension in PBS. Flow cytometry was performed using a FACS Calibur flow cytometer (BD Biosciences, USA) and analysed using FlowJo software (Tree Star Inc, USA).

For each antibody and cell line combination 10,000 cells were counted. Unstained cells, cells treated with isotype control antibody and cells treated with only the secondary antibody were used to determine the specificity of the primary antibodies. Receptor density on each cell line was semi-quantitated using a method previously reported, the percentage of positive cells (gated for fluorescence above background) was multiplied by the geometric mean of the fluorescence intensity.

Antibody	Clone	Clonality	Species	Supplier	Dilution
Anti-CD46	MEM-258	Monoclonal	Mouse	AbDSerotec	1:100
Anti-DSG-2	3G132	Monoclonal	Mouse	Abcam	1:100
Anti-CAR	RmcB	Monoclonal	Mouse	Millipore	1:100
Anti-α_V integrins	272-17E6	Monoclonal	Mouse	Abcam	1:100
IgG1 isotype control	X40	Monoclonal	Mouse	AbDSerotec	1:100
Anti-mouse FITC-conjugate	N/A	Polyclonal	Rabbit	Abcam	1:100

Table 2-4: Details of antibodies used for FACS

2.4.2 FACS for cell proliferation

Cell proliferation was determined using the CellTrace™ CFSE Cell Proliferation Kit (Invitrogen). CFSE (carboxyfluorescein diacetate, succinimidyl ester) is a colourless, non-fluorescent compound that passively diffuses into cells. Intracellular esterases cleave the acetate groups on CFSE to produce highly fluorescent conjugates that are impermeable to the cell membrane and can be detected by FACS. The fluorescent dye-protein compound also remains stable within the cell and can be inherited by daughter cells after cell division or cell fusion but the amount of fluorescence produced will decrease as the dye-protein complexes are split between daughter cells.

HEK293 cells were seeded overnight in a 24-well plate at 350,000cells/well. The following day, supernatant was removed and 1mL of pre-warm PBS containing CFSE, at a final concentration of 10µM, was added to each well before incubation at 37°C for 15 minutes. Then the CFSE containing PBS was replaced with pre-warmed cell culture medium and incubated at 37°C for 30 minutes to allow CFSE to undergo acetate

hydrolysis. Triplicate wells of HEK293 cells were then either mock infected with media containing 2% FBS or infected with ColoAd1 or Ad11p at 520vp/cell in a total volume of 1mL. After 0 hours, or 48 hours, cells were removed from the well by scraping, pelleted by centrifugation at 300xg and washed 3 times with PBS, before performing a live/dead stain (section 2.4.3) and fixing in 5% formaldehyde solution. Flow cytometry was performed using a FACS Calibur flow cytometer (BD Biosciences, USA) and analysed using FlowJo software (Tree Star Inc, USA).

2.4.3 FACS for live/dead stain

The Zombie NIR^{TM} dye (BioLegend) was used to determine HEK293 cell viability by FACS. The dye is taken up by dead cells with permeable membranes and is excited by a red laser with a fluorescence emission maximum at 746nm. Therefore, Zombie NIR^{TM} dye was diluted into PBS at a dilution of 1:100 and used to resuspend HEK293 cells (section 2.4.2) before incubation with gentle agitation at room temperature, in the dark, for 30 minutes. Cells were pelleted by centrifugation at 300xg for 5 minutes and washed with PBS. This was repeated a further 2 times before fixing in 5% formaldehyde solution. Flow cytometry was performed using a FACS Calibur flow cytometer (BD Biosciences, USA) and analysed using FlowJo software (Tree Star Inc, USA). The proportion of viable and dead cells after infection with ColoAd1 or Ad11p was determined by gating for viable mock infected control cells.

2.5 Protein Assay

The bicinchoninic acid (BCA) assay was used to determine the protein content of cell lysates. The assay uses the temperature dependent ability of peptide bonds to reduce Cu^{2+} ions to Cu^{+} ions in alkali conditions, forming a protein complex that subsequently chelates

BCA. Cysteine, tyrosine and tryptophan residues can also reduce Cu^{2+} ions. The amount of reduction of Cu^{2+} ions is proportional to the amount of protein present in the sample and, as the BCA – Cu^{+} protein complex is a purple-coloured product, the amount of Cu^{2+} reduction can be measured. Then the amount of protein present in a sample can be quantified from samples with known protein concentration.

The Quantipro BCA Assay Kit (Sigma, UK) was used to perform the BCA assay. Briefly, equal volumes (50µL) of cell lysate and reaction mixture (prepared as per manufacturer's instructions) were mixed together. At the same time, a standard curve of BSA ranging from 0.01 – 1mg/mL was prepared and equal volumes of each standard (50µL) and reaction mixture were mixed together. The colour of the samples and the standard curve was developed for 30 minutes at 55°C, before measuring the absorbance at 595nm using a Wallac 1420 Victor^2 multi-label counter (PerkinElmer Life and Analytical Sciences, UK). The correlation between the protein concentration and absorbance of the standard curve was analysed using non-linear regression, and the protein content of the sample determined from the standard curve.

2.6 Western Blot

2.6.1 Sample preparation and running gel

Precast 4-10% gradient Tris-HCl gels (BioRad) were used with the Mini-PROTEAN III electrophoresis system. First, wells of the gel were flushed with running buffer and left to condition at room temperature for 30 minutes. Meanwhile, samples were prepared by diluting in water to achieve 20 – 40µg of protein per sample. Then the same volume of β-mercaptoethanol-containing sample buffer was added to each sample. Samples were then incubated at 95°C for 10 minutes and loaded in to each lane of the precast gel. Some lanes

were loaded with prestained molecular weight protein markers (Precision Plus Protein Dual Colour Standard, BioRad). Gels were run at 200V for 35-40 minutes at room temperature.

2.6.2 Transfer to PVDF

PVDF membrane (BioRad) was pre-conditioned in 100% methanol (VWR) for 5 minutes. Then the membrane, filter paper and fibre pads were pre-soaked in transfer buffer. Fibre pads, followed by filter paper, were placed on both sides of the transfer cassette. Then the gel was placed on the filter paper on one side of the cassette and PVDF membrane placed on the filter paper on other side of the cassette. Closing the cassette created a transfer sandwich that was placed in the mini-gel Western transfer tank (BioRad) with the gel facing the negative electrode. Transfer was performed at 300mA for 1.5 hours at 4°C.

2.6.3 Western blot development

After removing the PVDF membrane from the transfer sandwich, the membrane was washed with TBST (or PBST) and then blocked in 5% skimmed milk (Sigma-Aldrich) at room temperature for at least 30 minutes. The membrane was then incubated with the desired antibody (Table 2-5) at 4°C overnight. After removing the antibody and washing with TBST (or PBST) for 5 minutes, and repeating the wash a further 2 times, the membrane was incubated with the appropriate secondary-HRP conjugated antibody (see Table 2-5) for 1 hour at room temperature. After removing the antibody and washing with TBST (or PBST) for 5 minutes, and repeating the wash a further 2 times, the chemiluminescence of the membrane was developed with Super Signal West Dura Extended Duration Substrate (Thermo Scientific) and detected by exposure on X-ray film (SuperRX, Fujifilm) in a fast speed cassette. An automatic developer (CP1000, Agfa) was used to develop and fix exposed X-ray films.

Antibody	Clone	Clonality	Species	Supplier	Dilution
Anti-AMPKα-Thr172	40H9	Monoclonal	Rabbit	Cell signalling	1:500
Anti-AMPKα	N/A	Polyclonal	Rabbit	Cell signalling	1:1000
pTSC2	N/A	Polyclonal	Rabbit	Cell signalling	1:1000
pRaptor	N/A	Polyclonal	Rabbit	Cell signalling	1:1000
pACC	D7D11	Monoclonal	Rabbit	Cell signalling	1:1000
β-actin	AC-15	Monoclonal	Mouse	Sigma	1:1000
GAPDH	6c5	Monoclonal	Mouse	AbD Serotec	1:1000
Anti-rabbit IgG-HRP	N/A	Polyclonal	Goat	DAKO	1:10,000
Anti-mouse IgG-HRP	N/A	Polyclonal	Rabbit	DAKO	1:10,000

Table 2-5: Details of antibodies used for Western Blot

2.7 Pharmacological interventions

2.7.1 Manipulation of AMPK

Adherent HEK293s were seeded overnight at 500,000 cells/well in a 6-well plate before infection with ColoAd1, which was diluted in media containing 2% FBS to achieve MOI 1 (520vp/cell) in a final volume of 4mL/well. Mock infected cells were treated with media containing 2% FBS at 4mL/well. After 24 hours incubation at 37°C in 5% CO_2, infected and mock infected cells were treated with metformin, compound C or mock treated with media containing 2% FBS. Metformin (Sigma) was used at a final concentration ranging from 0.1mM to 35mM. Compound C (Sigma) was used at final concentrations of 2μM - 64μM.

2.7.2 Manipulation of metabolism

Adherent HEK293s were seeded overnight at 10,000 cells/well before infection with ColoAd1, which was diluted in media containing 2% FBS to achieve MOI 1 (520vp/cell)

in a final volume of 150µL/well. Mock infected cells were treated with media containing 2% FBS at 150µL/well. After 3 hours incubation at 37°C in 5% CO_2, infected and mock infected cells were treated with 3 different concentrations of reagent (Table 2-6), so that the final volume was 200µL/well. The MTS assay was performed 24 and 48 hours after infection to determine the effect of each inhibitor on both uninfected and infected HEK293 cell viability.

	Final concentration (in final volume of 200µL/well)	**Supplier**	**Solvent**
Rapamycin	0.01µM, 0.05µM, 0.1 µM	Sigma	DMSO
ZVAD	5µM, 25µM, 50µM	Tocris	DMSO
Sodium oxamate	0.1mM, 1mM , 10mM	Sigma	Water
Dichloroacetate	0.01mM - 25mM	Sigma	Water
Necrostatin-1	5µM, 50µM, 100µM	DMSO	DMSO
Nicotinamide	1mM, 5mM, 10mM	Sigma	Water
N-acetyl, L-cysteine	1mM, 5mM , 10mM	Sigma	Water

Table 2-6: Details of pharmacological interventions

2.7.3 Calcium chloride

Suspension HEK293 cells at 1 x 10^6vp/cell were infected in 12.5mL of complete CD293 media in 125m Erlenmeyer flask. After 2 hours, CD293 media containing calcium chloride (Sigma) was added to a final volume of 25mL and final concentration of 1mM and 2mM.

2.8 siRNA kinase screen

2.8.1 Optimisation of reverse transfection for siRNA mediated knockdown

Reverse transfection was performed using either Dharmafect-1 (ThermoScientific) or Lipofectamine 2000 (Life Technologies). Transfection reagents were diluted in OptiMEM

(Life Technologies) to achieve final concentrations of 0.025 – 0.3µL per transfection. siRNA was purchased from ThermoScientific and used at 5 – 30nM final concentrations. First, siRNA complexes were formed by incubation with transfection reagents at room temperature for at least 20 minutes, in a volume of 20µL. Then, 80µL of cells, at 8000 cells/well, were added to the siRNA complexes. Cells were allowed to settle with incubation at room temperature for at least 30 minutes, before incubation at 30°C in 5% CO_2 overnight. The following day, media was removed and replaced with media (100 µL/well) containing 2% FBS, 1% penicillin/streptomycin. Then cells were either harvested each day after transfection to determine the amount of siRNA mediated gene knockdown, or incubated for up to three days before infection with ColoAd1. Reverse transfection for each experiment was also performed with the All-stars negative control siRNA (Quiagen) and All-stars Hs death control siRNA (Quiagen).

2.8.2 Infection of siRNA treated HEK293 cells

ColoAd1 inoculum was prepared in media containing 2% FBS, 1% penicillin and 1% streptomycin, to achieve 520viral particles/cell in final volume of 200µL. Three days after reverse transfection, media was removed from the cells and replaced with ColoAd1 innoculum. ColoAd1 infected cells were then incubated at 37°C in 5% CO_2 for 48 hours before storage at -80°C.

2.8.3 Final conditions for siRNA screen

The siRNA library used for the screen was the ON-TARGET*plus*® SMARTpool® human protein kinase library (Dharmacon). siRNA complexes were formed between Lipofectamine 2000 and the siRNA in a volume of 20µL with OptiMEM, to achieve final concentrations of 0.3 µL/well and 30nM, respectively in the final volume of 100µL. Then cells were diluted in media containing 2% FBS without penicillin or streptomycin to

achieve 8000 cells/well. Cells were added to the siRNA complexes in a volume of 80 µL/well, using flexdrop liquid handling system, before incubation at room temperature for 30 minutes, followed by incubation at 37°C in 5% CO_2 overnight. The following day, media was removed and replaced with media (100 µL/well) containing 2% FBS, 1% penicillin and 1% streptomycin, using flexdrop liquid handling system. Then the cells were incubated at 37°C in 5% CO_2 for 48 hours. At this point, the viability of cells was determined using the resazurin assay (section 2.2.2). Then, ColoAd1 infection was performed as described in section 682.8.2 with the flexdrop liquid handling. After 48 hours, plates were stored at -80°C, before DNA extraction (section 2.3.7) and high throughput QPCR (section 2.3.9) to determine ColoAd1 genomes.

2.8.4 siRNA screen analysis

Each QPCR CT value, corresponding to viral particles, was normalised to the average CT value of each plate using a robust version of the Z score. Each cell viability value determined before infection was also normalised to the average cell viability of each plate, using the robust Z score. The robust version of the Z score is given by the following formula:

$$Z' = (x - x\_median) / MAD$$

Where Z' is the robust Z score, x is the reading of each well, x_median is the median of that plate, and MAD for the median absolute deviation of the plate.

Then, a summarised Z score of the ratio (viral particles/cell) of each well was calculated according to the following formula:

$$\Delta Z = \log (Z\_viral\ particles / Z\_cell)$$

The ΔZ scores from duplicate plates were used to perform a Rank Product analysis to identify hits that had a reproducibly high ratio of viral particles/cell.

3 Characterising ColoAd1 replication in HEK293 cells

3.1 Introduction

From a bioprocessing perspective, adenovirus production requires consideration of both viral and cellular parameters affecting manufacturing yield. The HEK293 cell line has historically been used in the manufacture of adenovirus vectors and can easily be adapted to suspension culture. As a replication competent virus, ColoAd1 does not require the complementary expression of early adenovirus transgenes from HEK293 cells and could be manufactured in a range of transformed cells. Nevertheless the availability HEK293 cell banks that meet GMP make them a preferred choice. Most of the bioprocessing experience in HEK293 cells has been in the production of adenovirus type C vectors and little is known about the performance of group B adenoviruses in these cells. ColoAd1 has mutations in three regions of its genome [69] and these may have additional effects on viral replication, especially in HEK293 cells.

In this Chapter preliminary studies were carried out to determine the suitability of HEK293 cells as a production cell line for ColoAd1. As a control for the mutations in ColoAd1, and to provide further insights, the closest wild type virus (Ad11p) was used in these studies.

3.2 Aims

ColoAd1, having been selected for rapid oncolysis, was hypothesised to replicate faster than its parental virus, Ad11p, in HEK293 cells. Further, it was hypothesised that the difference in replication kinetics between ColoAd1 and Ad11p would not be due to a difference in the uptake of the virus but due to inherent differences between the viruses once inside the cell. To address this hypothesis, this chapter aims to:

- Characterise the cellular uptake of ColoAd1 on HEK293 cells.
- Determine the genome replication kinetics of ColoAd1 in HEK293 cells and compare to Ad11p.
- Optimise an infectivity assay that allows for rapid assessment of infectious ColoAd1 particles.
- Assess the release of ColoAd1 particles from HEK293 cells.
- Compare yield of ColoAd1 particles from adherent and suspension HEK293 cells.
- Assess the genetic stability of ColoAd1 to allow for multiple passages of the virus during manufacture.

3.3 Results

3.3.1 Assessment of cell line sensitivity to ColoAd1

The sensitivity of HEK293 cells to ColoAd1, compared to Ad11p and Ad5 wild-type viruses, was determined using the MTS assay. Two other cell types known to be permissive for ColoAd1 were used as comparators. These were the lung carcinomna cell line, A549, and the colorectal carcinoma cell line, HT29. Figure 3-1 shows that the number of ColoAd1 particles required to kill 50% of the cells (IC50) were significantly lower than Ad11p on all cell lines tested ($P<0.0001$). This is consistent with previous reports describing ColoAd1 as a more potent virus [69]. The IC50 of ColoAd1 was significantly ($P<0.0001$) lower than Ad5 on the HT29 and A549 cell lines but interestingly there was no significant difference on HEK293 cells ($P>0.05$). The reason for the discrepancy between ColoAd1 and wild type Ad5 on HEK293 cells is unclear, but it may be due to the presence of Ad5 complementing E1 region in the HEK293 cell line that is not present in A549 or HT29 cell lines.

This data could indicate that HEK293 cells are less sensitive to ColoAd1 induced cell death than HT29 or A549 cells. However, dose response curves of adenoviruses are complicated by the fact that, unlike drugs, adenoviruses are capable of self-amplifying the input dose by replication and release of progeny virus capable of further replication and release. Different viruses may do this at different speeds on different cell lines. Therefore, the differences in IC50 could indicate that ColoAd1 replicates and lyses HEK293 cells slower than in HT29 or A549 cells with resistance to cell death in each cell line remaining the same. To probe this further, each significant stage of the viral replication process was considered to assess where the differences occurred.

A: HT29

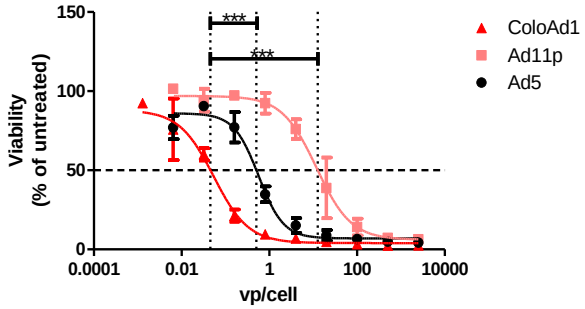

Virus	Cell Line	IC50 (vp/cell)
ColoAd1	HT29	0.045
Ad11p	HT29	12.7
Ad5	HT29	0.507

B: A549

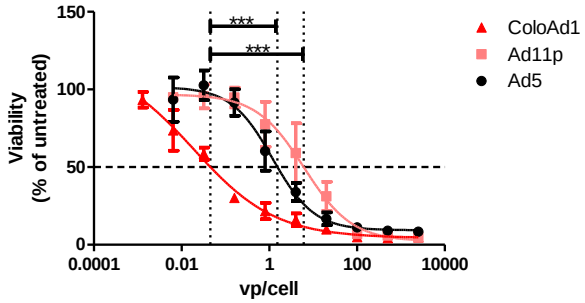

Virus	Cell Line	IC50 (vp/cell)
ColoAd1	A549	0.045
Ad11p	A549	6.07
Ad5	A549	1.53

C: HEK293

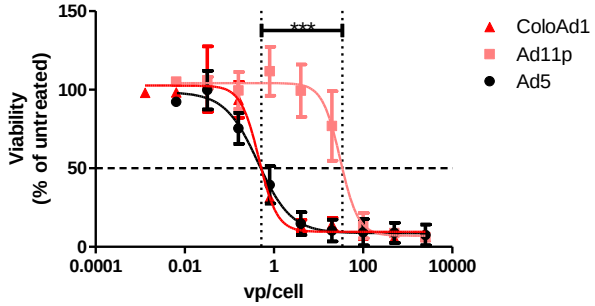

Virus	Cell Line	IC50 (vp/cell)
ColoAd1	HEK293	0.521
Ad11p	HEK293	34.2
Ad5	HEK293	0.507

Figure 3-1: Cell line sensitivity to ColoAd1 as determined by viability assay (MTS)

HT29 (**A**), A549 (**B**) and HEK293 (**C**) cells were seeded overnight in 96 well plates at 10,000 cells/well and then infected with 5-fold serial dilutions of each virus type (Ad5, Ad11p and ColoAd1). Viability (normalised to untreated control cells) was determined 5 days after infection using the MTS assay (see Materials and Methods). Means of 3 independent experiments with standard deviation shown. Four parameter non-linear curve fit is shown with dotted lines indicating IC50 values. One-way ANOVA, using Dunnett's post-test was used to determine the significance of differences in IC50 between ColoAd1 and wild type viruses on each cell line.

3.3.2 Adenovirus receptor expression on HEK293 cells

Adenovirus infection begins with receptor mediated binding to the cell surface. A number of different receptors have been identified that are capable of binding different serotypes of HAds [94]. The primary cellular receptor for Ad5 is the coxsackie virus and adenovirus receptor (CAR) [96], although *in vivo* Ad5 also binds heparin sulphate glycosaminoglycans (HPSG) [140] and blood coagulation factor X [141], with additional reports of less well characterised interactions with α2 domain of major histocompatibility marker 1 (MHC1-α2) [142], vascular cell adhesion molecule 1 (VCAM1) [143] and scavenger receptors [144]. Ad5 is then internalised via the penton base interaction of the RGD motif with α_V-integrins [104]. In contrast, Ad11p uses CD46 [102] and desmoglein 2 (DSG-2) [103], although the degree to which Ad11p preferentially uses each of these receptors remains controversial [145].

Therefore, as Ad5 and Ad11p use different receptors for attachment and internalisation, it is possible that the difference in IC50 on different cell lines and between viruses was due to differential expression of adenovirus receptors. FACS was used to determine the presence of the main adenovirus receptors (CAR, α_V-integrins, CD46 and DSG-2) on each cell line (Figure 3-2) and mean fluorescence intensity used to semi-quantitate the amount of each receptor (Figure 3-3). Conclusions were drawn from this experiment by assuming that the binding efficiency of primary antibody to its target receptor was the same on each cell line, and that the binding efficiency of the secondary antibody to the primary was also the same on each cell line. As a result, it was found that A549 cells expressed high levels of all adenovirus receptors (>95% of cells positive for CD46, CAR, DSG-2 and α_V-integrin). HT29 cells expressed high levels of CD46, CAR and α_V-integrin (>95% of cells positive) but lower levels of DSG-2. HEK293 cells expressed

high levels of all receptors, with no significant difference in expression levels between CD46, DSG-2, CAR or α_V-integrin. Suspension adapted HEK293 cells expressed relatively low DSG-2 and α_V-integrin levels compared to adherent HEK293 cells while CAR and CD46 were comparable. Given that α_V-integrin and DSG-2 are respectively found in tight junctions and desmosomes [146], it is not surprising that HEK293 cells adapted to grow in single cell suspension have reduced DSG-2 and α_V-integrin when compared to epithelial cell lines that grow in adherent monolayers.

These data indicate that receptor expression could not account for the difference in IC50 between cell lines or between viruses as all cell lines expressed high levels of CD46, DSG-2, integrins and CAR. Therefore, the main difference in virus activity must be at the intracellular level.

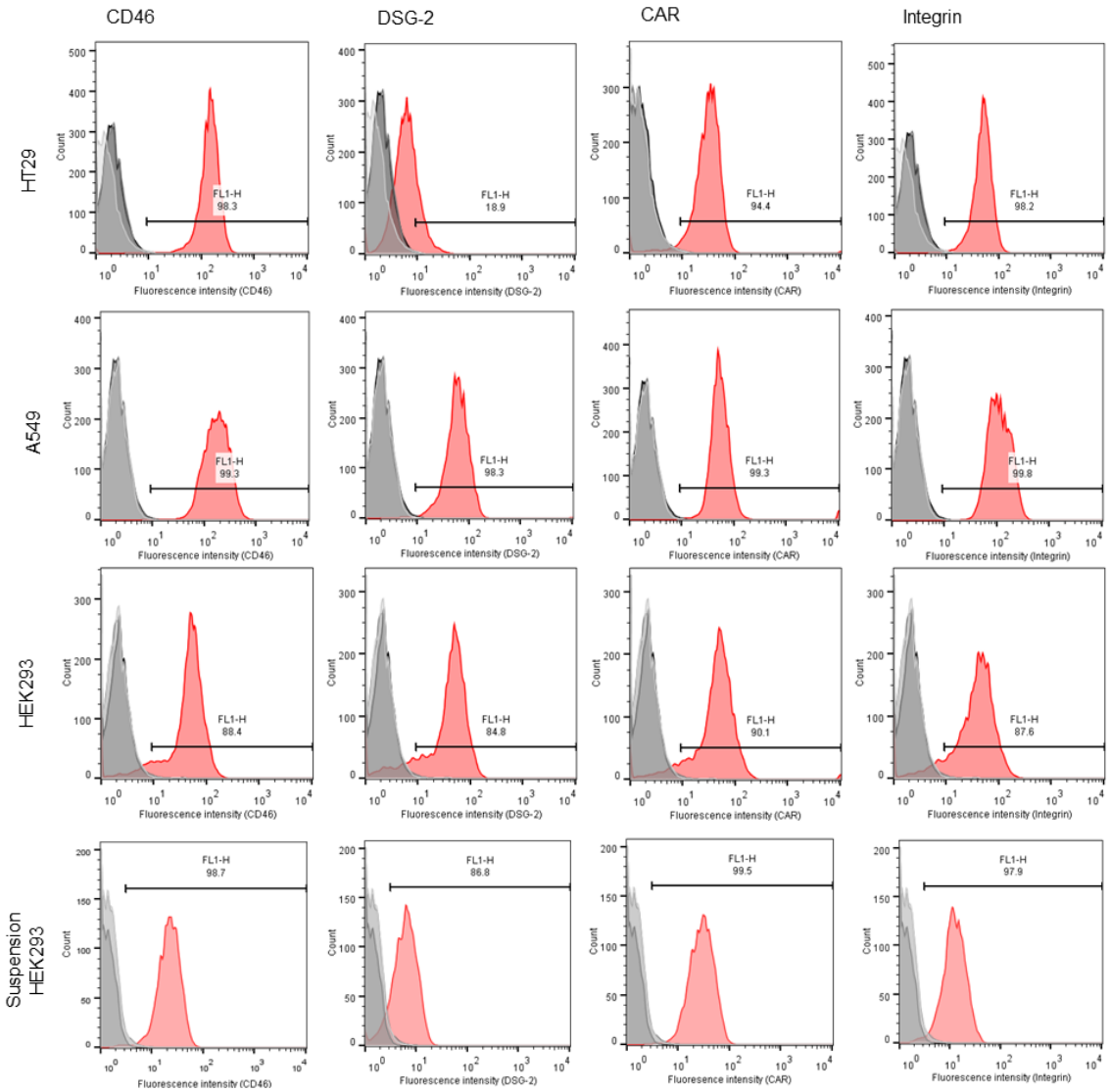

Figure 3-2: Cellular expression of adenovirus receptors on different cell lines

Cell lines HT29, A549, adherent HEK293 and suspension HEK293 were counted and 500,000 cells stained with primary antibody specific for CD46, DSG-2, CAR, α_V-integrin or non-specific isotype. After washing, primary antibody staining was detected using FIT-C labelled polyclonal antibody against mouse IgG. For each stain, 10,000 cells were analysed by FACS and gated in the FL1-H region for fluorescence above background. Histograms, representative of at least 2 independent experiments, show the number of cells (count) against the fluorescence intensity detected in the FL1-H region.

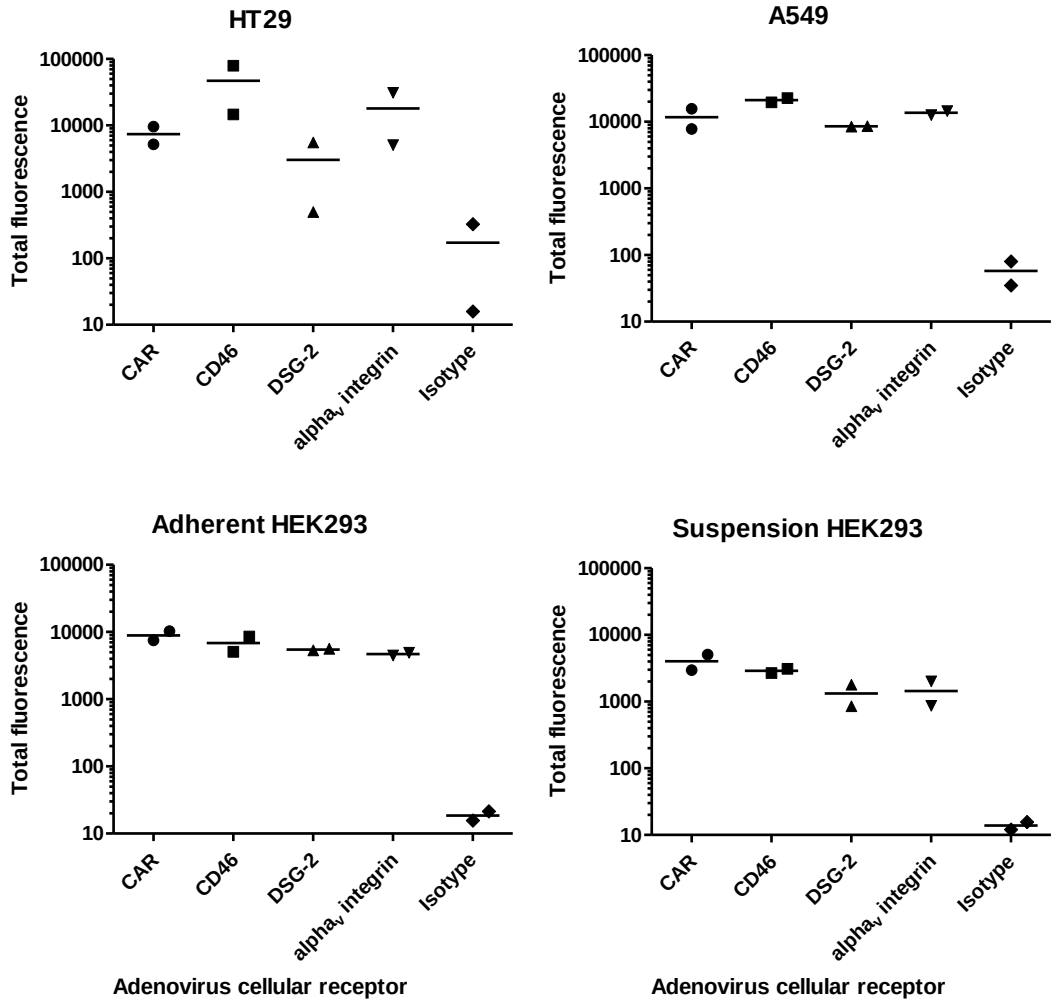

Figure 3-3: Cellular expression levels of adenovirus receptors on different cell lines

Cell lines HT29, A549, adherent HEK293 and suspension HEK293 were counted and 500,000 cells stained with primary antibody specific for CD46, DSG-2, CAR, αV-integrin or non-specific isotype. After washing, primary antibody staining was detected using FIT-C labelled polyclonal antibody against mouse IgG. For each stain, 10,000 cells were analysed by FACS and gated in the FL1-H region for fluorescence above background. In order to semi-quantitate the total amount of receptor expressed on each cell line, the percentage of positive cells in the FL1-H region was multiplied by the mean fluorescence intensity for each adenovirus receptor stain (CD46, DSG-2, CAR, αV-integrin or non-specific isotype). The line represents the mean of 2 independent experiments (shown as different shaped dots) the total fluorescence calculated for each receptor stain on each cell line.

3.3.3 Cellular uptake of ColoAd1 compared to Ad11p on the HEK293 cell line

After recruitment of α_V-integrin to Ad5, clathrin-mediated endocytosis is triggered [105]. However, there is some evidence that group B adenovirus may be internalised by macropinocytosis [147]. Given that there are known differences in uptake receptors and cellular internalisation mechanism between Ad5 and Ad11p, it was decided to focus on elucidating the reason for IC50 differences between ColoAd1 and Ad11p. HEK293 cells were infected with ColoAd1 and Ad11p over a range of particle concentrations and the amount of adenovirus genome bound to the cell after 2 hours determined by QPCR.

There was no significant difference in HEK293 cellular uptake between ColoAd1 and Ad11p at each MOI tested (Figure 3-4). This was not surprising given that the differences between ColoAd1 and Ad11p are within adenoviral genes that do not code for structural proteins. Further, after 2 hours, only approximately 10% of the virus added to cells was detected back (Figure 3-4). For example, MOI of 10 should have achieved 5200vp/cell but only 1000vp/cell was detected back. In fact, at MOI 1, 0.1 and 0.01 the difference between the calculated MOI and the MOI achieved was different by approximately 10-fold. At MOI 10, the difference is 5-fold.

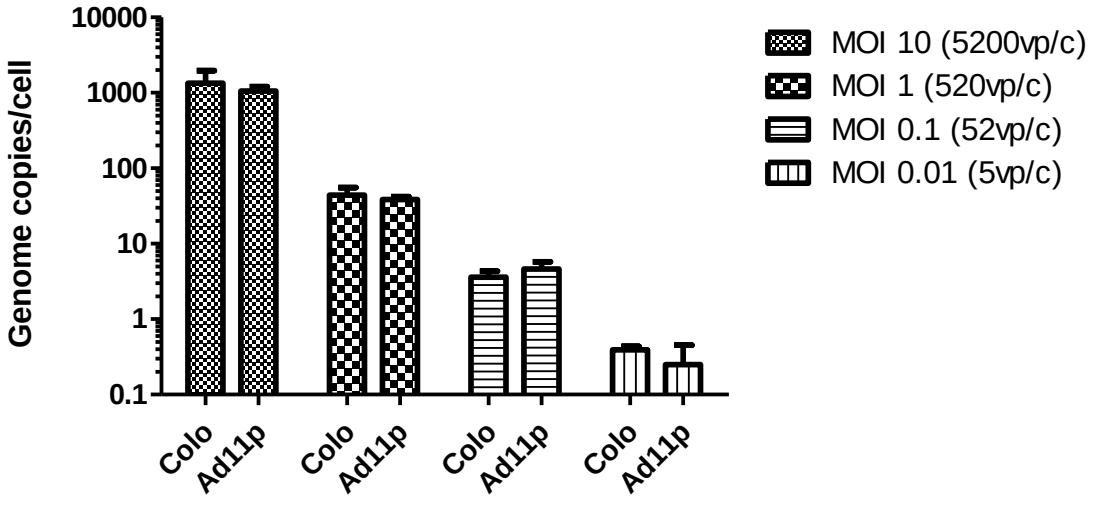

Figure 3-4: Uptake of ColoAd1 on HEK293 cells compared to Ad11p

Adherent HEK293 cells were seeded in 24 well plates at 1,000,000 cells/well, before infection in triplicate with ColoAd1 or Ad11p at MOI 10 (5200vp/cell), MOI 1 (520vp/cell), MOI 0.1 (52vp/cell) or MOI 0.01 (5vp/cell). After 2 hours, the supernatant was removed and cells washed with PBS before cell lysis and DNA extraction to determine genome copy number by QPCR. Genome copies detected are normalised to the number of cells initially seeded. Means of triplicates with standard deviation shown.

3.3.4 ColoAd1 genome replication in HEK293 cells compared to Ad11p

Once internalised, adenoviral particles disassemble in the early endosome and escape before genomes are transported along microtubules, through the nuclear pore complex, in to the nucleus where genome replication begins (section 1.3.2). ColoAd1 has a chimeric E2B region, containing hybrid Ad11p/Ad3 sequences, a mutation which would affect the DNA polymerase [69]. To determine the genome replication kinetics of ColoAd1, HEK293 cells were infected and genome copies associated with the cell and supernatant fractions determined by QPCR. ColoAd1 replicates slightly more genomes earlier than Ad11p (Figure 3-5) and these genomes are released into the supernatant earlier for ColoAd1 than for Ad11p, especially at a lower MOI (Figure 3-6). Therefore, the genetic alteration that ColoAd1 has acquired in the E2B region does not appear to

have a detrimental effect on the replication of its genome, and may even enhance the rate of ColoAd1 genome replication.

A: MOI 1 (520vp/cell)

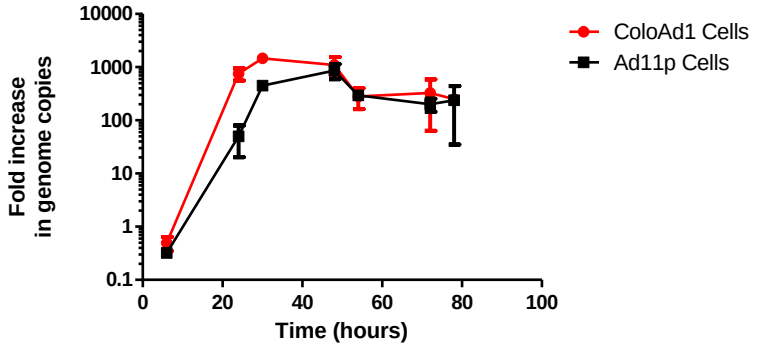

B: MOI 0.1 (52vp/cell)

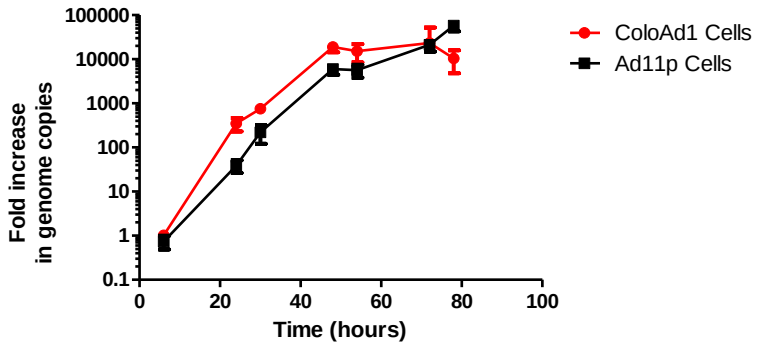

Figure 3-5: ColoAd1 genome replication in HEK293 cells compared to Ad11p

Adherent HEK293 cells were seeded over night at 10,000 cells/well before infection in triplicate with ColoAd1 or Ad11p at MOI 1 (**A**) and MOI 0.1 (**B**). After 6, 24, 30, 48, 54, 72 and 78 hours, cells and supernatant were separated by micro centrifugation and the cell fraction stored at -80°C. Subsequently, the viral genome copies associated with the cell fraction was extracted and quantified by QPCR (see Materials and Methods) before expressing the genomes detected as a fold of increase from the input viral particle dose. Means of triplicates shown with error bars indicating standard deviation.

A: MOI 1 (520vp/cell)

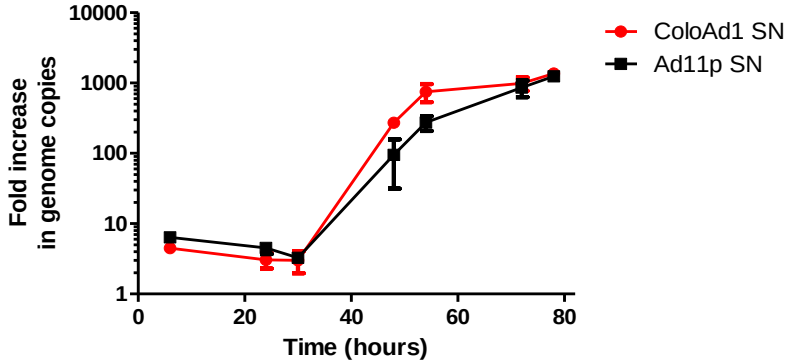

B: MOI 0.1 (52vp/cell)

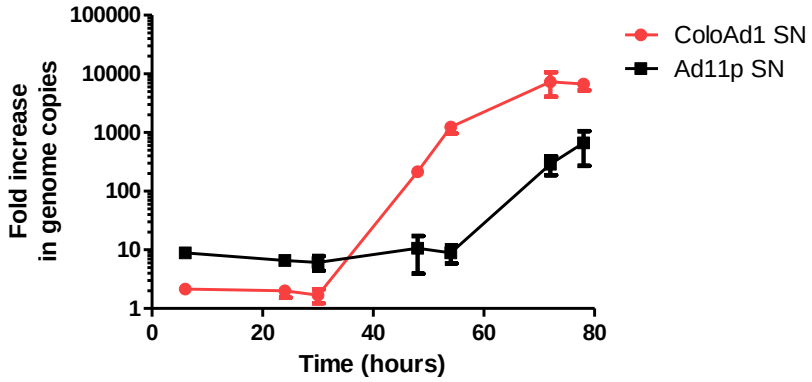

Figure 3-6: ColoAd1 particle release is earlier than Ad11p from HEK293 cells

Adherent HEK293 cells were seeded overnight at 10,000 cells/well before infection in triplicate with ColoAd1 or Ad11p at MOI 1 (**A**) and MOI 0.1 (**B**). After 6, 24, 30, 48, 54, 72 and 78 hours, cells and supernatant were separated by micro centrifugation and the supernatant stored at -80°C. Subsequently, viral genome copies associated with the supernatant were extracted and quantified by QPCR (see Materials and Methods) before expressing the genomes detected as a fold of increase from the input viral particle dose. Means of triplicates shown with error bars indicating standard deviation.

3.3.5 ColoAd1 particle assembly

Adenovirus particle assembly occurs in the nucleus of an infected cell, where hexon protein is transported into the nucleus and assembled with adenoviral DNA [89]. Packaged particles are then released from the cell by a lytic process that is relatively uncharacterised. The formation of infectious packaged particles can be determined using an infectivity assay, of which there are many types. Traditional infectivity assays include plaque assay and TCID50 methods. Plaque assay involves infecting a cell monolayer that is subsequently covered in agarose to prevent spread so that a single infectious particle becomes a plaque, visible after 5-10 days. TCID50 involves infecting single wells over a dilution range and detecting cytopathic effect after about 7 days. However, these assays tend to be lengthy and laborious so they do not lend themselves well in a process development environment where a fast turnaround of multiple samples is required.

Defining an infectivity assay for ColoAd1

The hexon staining infectivity assay described for Ad5 (section 2.3.4) can be completed in 3 days, which potentially allows higher through put of samples for infectivity testing. However, initial experiments indicated that antibodies raised against Ad5 hexon protein did not recognise Ad11p hexon. Therefore, alternative antibodies were sourced. Once the antibodies were optimised, it became evident that at the same fixing time point as Ad5 (48 hours), ColoAd1 showed areas of hexon dense staining that were reminiscent of cell to cell spread and this was seen earlier than Ad5 (Figure 3-7). This suggested that the fixing time recommended for Ad5 would lead to inaccurate determination of ColoAd1 infectivity. Therefore, the fixing time for ColoAd1 infectivity assay was optimised. Figure 3-7 shows that the “spread” phenotype first appeared at 42 hours with ColoAd. However, “spread” occurred after 48 hours with Ad5. Due to time restrictions,

the assay was routinely fixed 33 hours after infection with ColoAd1. Interestingly, this time corresponds with the time where ColoAd1 genomes detected from the supernatant increased (Figure 3-6), suggesting that it might reflect the time when infected cells lyse and spread.

In order to provide an indication of the timings of late protein expression and cell to cell spread of ColoAd1, hexon staining was used during infection and compared the pattern of staining to Ad11p. The "spread" phenotype of hexon staining was observed earlier for ColoAd1 than Ad11p (Figure 3-8). The "spread" phenotype was first observed for Ad11p 72 hours after infection. Again, this timing of "spread" corresponds with the time after release of Ad11p into the supernatant, however, only after infection of Ad11p at the low MOI (Figure 3-6B).

A: ColoAd1

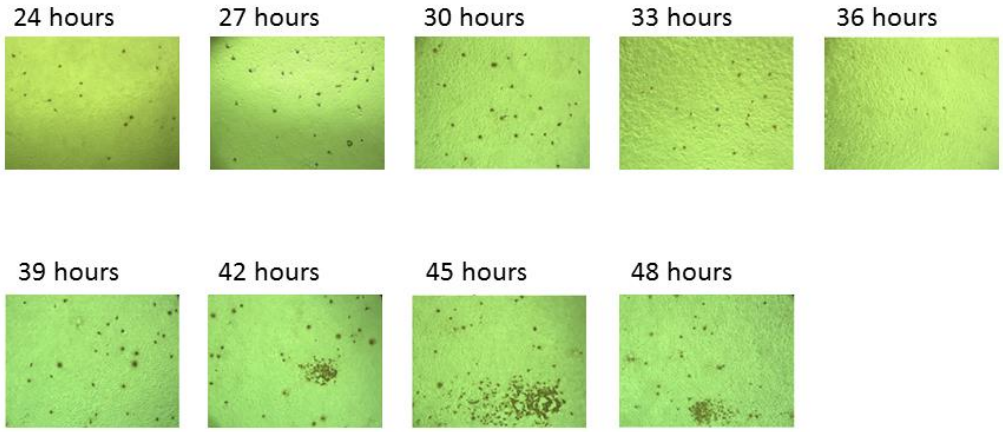

B: Ad5

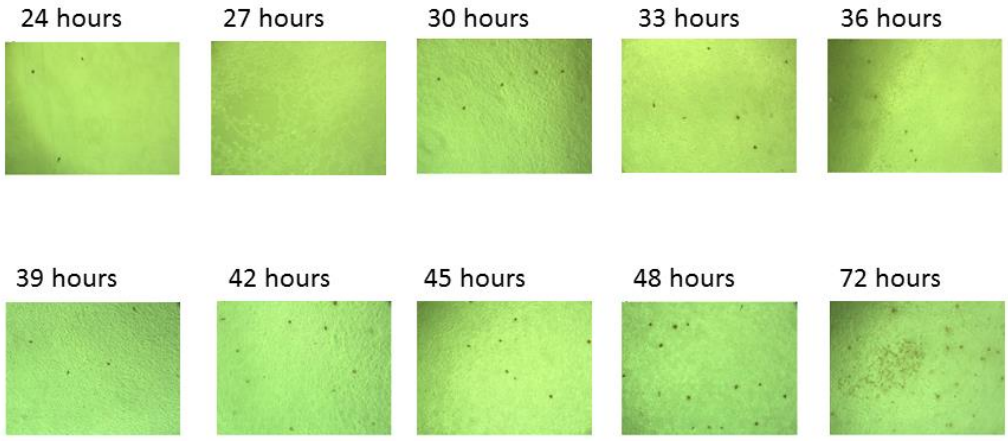

Figure 3-7: Optimising hexon staining as an infectivity assay for ColoAd1 on HEK293 cells

Adherent HEK293 cells were seeded in a 24 well plate at 350,000 cells/well for 2 hours before infection in triplicate with ColoAd1 or Ad5. After 24 hours, cells were fixed and stained for hexon protein at 3 hour intervals. Representative images of hexon staining at each time point are shown at 10x magnification.

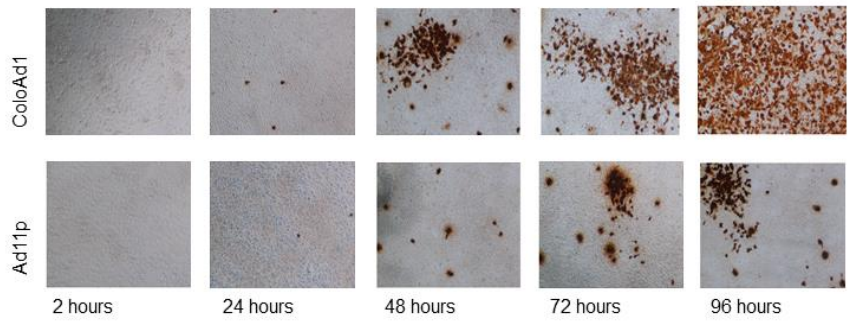

Figure 3-8: Hexon positive HEK293 cells during ColoAd1 and Ad11p infection

Adherent HEK293 cells were seeded in a 24 well plate at 350,000cells/well and infected over a range of dilutions with ColoAd1 or Ad11p. Cells were fixed and stained 2, 24, 48, 72 and 96 hours after infection. Representative images of hexon staining at each time point are shown at 10x magnification.

The disadvantage of performing an infectivity assay using hexon staining was that it only determined initial infection by detectable hexon expression from a single replication cycle. Traditional infectivity assays, such as plaque assays and TCID50, account for the release of virus and subsequent infection of uninfected cells. Therefore, the hexon staining infectivity assay was compared to the TCID50 method and it was found that the hexon staining infectivity assay consistently underestimated the infectivity determined by TCID50 for all types of sample (Figure 3-9). However, due to the short timing of the assay and ease of handling multiple samples in one assay, the hexon staining infectivity assay was used in all other subsequent experiments so subsequent MOIs refers to MOI as determined by hexon staining assay with units of ifu/mL.

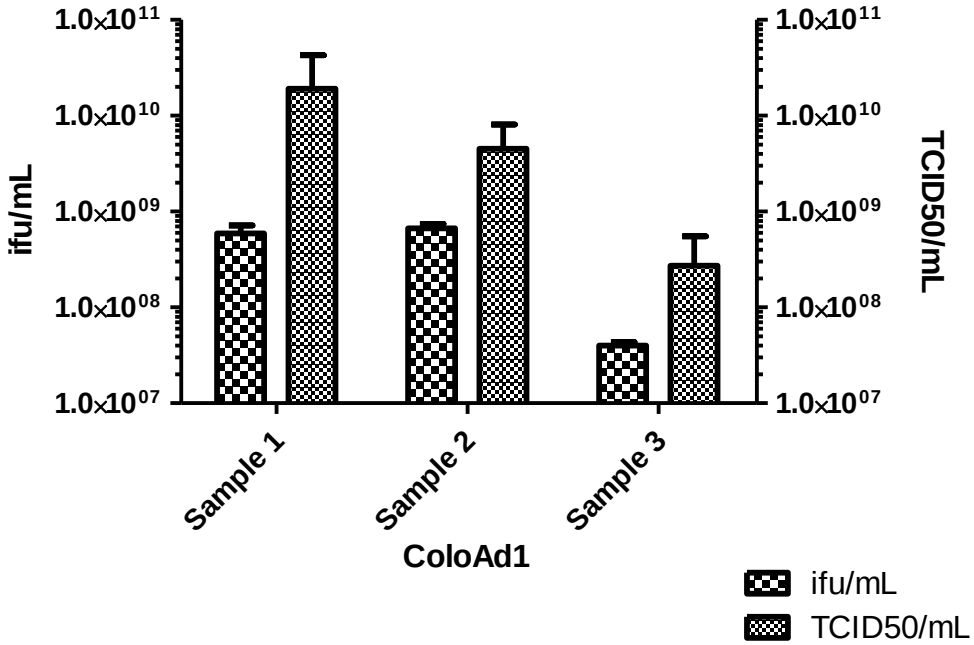

Figure 3-9: Comparison of ColoAd1 hexon staining infectivity assay with TCID50

Adherent HEK293 cells were seeded overnight in 24 and 96 well plates (at 350,000cells/well and 10,000cells/well, respectively). The next day, 3 different samples of ColoAd1 were diluted to infect both the hexon staining assay (24 well plate) and the TCID50 assay (96 well plate) in triplicate. Assay protocols were followed thereafter to quantitate infectious particles (ifu/mL) by hexon staining or TCID50/mL, resepectively. Sample 1 was purified ColoAd1, sample 2 was a cell lysate containing ColoAd1 and sample 3 was cell culture supernatant containing ColoAd1. Mean of triplicates with standard deviation shown.

3.3.6 Use of hexon assay to determine the lifecycle of ColoAd1

To determine the complete life cycle time of ColoAd1 from HEK293 cells, infectious viral particle release into the supernatant was quantified using the optimised infectivity assay (section 3.3.5). Figure 3-10 shows that the amount of infectious particles detected in the supernatant increased after 33 hours and plateaued after 48 hours. This suggested that ColoAd1 lifecycle from infection to lytic release was 48 hours.

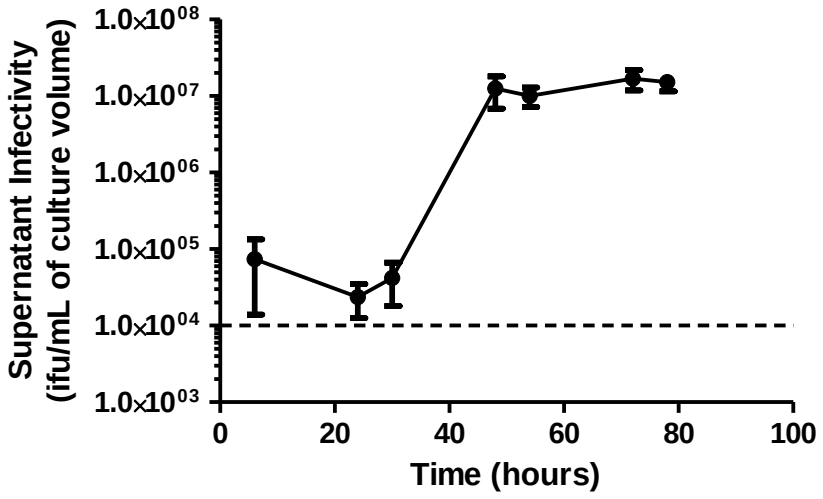

Figure 3-10: Infectious particle release of ColoAd1 into cell culture supernatant

Adherent HEK293 cells were seeded overnight in a 96 well plate at 10,000cells/well before infection in triplicate with ColoAd1 at MOI 1 (520vp/cell). After 6, 24, 30, 48, 54, 72 and 78 hours, cells and supernatant were removed from the well and microcentrifued to pellet cellular debris before taking a sample of the supernatant, which was stored at -80°C until performing a single infectivity assay by hexon staining. Mean of triplicates with standard deviation shown.

3.3.7 Assessment of total yield in adherent and suspension HEK293 cells

For manufacturing purposes, a seed stock would be used to inoculate a known amount of cells, optimised to maximise total yield (from cells and supernatant) to harvest at a specific time after infection. In addition, suspension cells are preferred when manufacturing to GMP to enable process scale-up. Therefore, to assess the effect of MOI on total yield for a manufacturing process, adherent HEK293 cells were infected with ColoAd1 at 3 different MOIs and compared to total yield in suspension HEK293 cells. At MOI 0.1, suspension cells appeared to show a lower amount of genome production than at higher MOIs (MOI 1 and 10). Total genome yield in suspension cells at MOI 0.1 was also lower than in adherent cells, with the former plateauing at 1 x 10^{11}gc/mL and the later plateauing 100 fold lower (Figure 3-11). However, yield of infectious particles was independent of MOI in suspension cells. In adherent cells, infectious particle yield was slightly more dependent on MOI (Figure 3-12).

A: Adherent HEK293

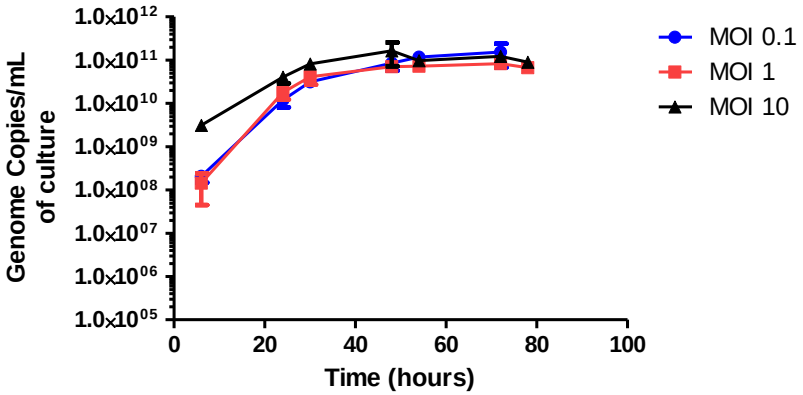

B: Suspension HEK293

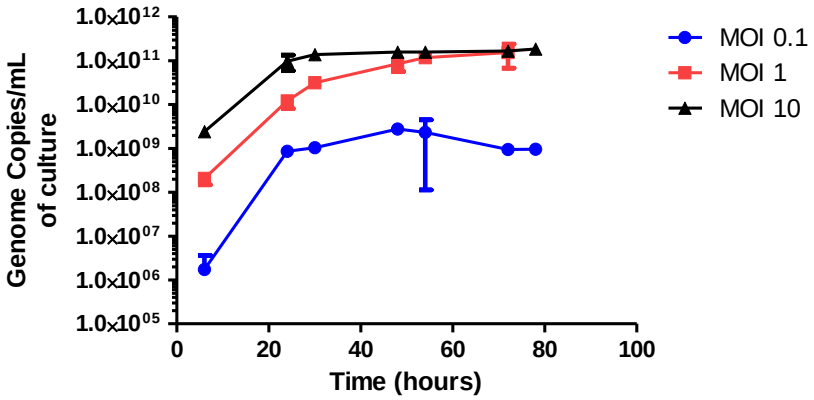

Figure 3-11: Total genome yield of ColoAd1 in adherent and suspension HEK293 cells

Adherent HEK293 cells (**A**) were seeded at 1,000,000 cells/well in a 24 well plate for 2 hours, or suspension HEK293 cells (**B**) were seeded at 1,000,000 cells/mL in 125mL shake flasks. Then cells were infected with ColoAd1 in triplicate at MOI 10 (5200vp/cell), MOI 1 (520vp/cell), MOI 0.1 (52vp/cell) or mock infected. After 6, 24, 30, 48, 72 and 78 hours, cells and supernatant were removed from each well, or flask, before storage at -80°C. Genome copy number was subsequently determined by QPCR. Mean of triplicates with standard deviation shown.

A: Adherent HEK293

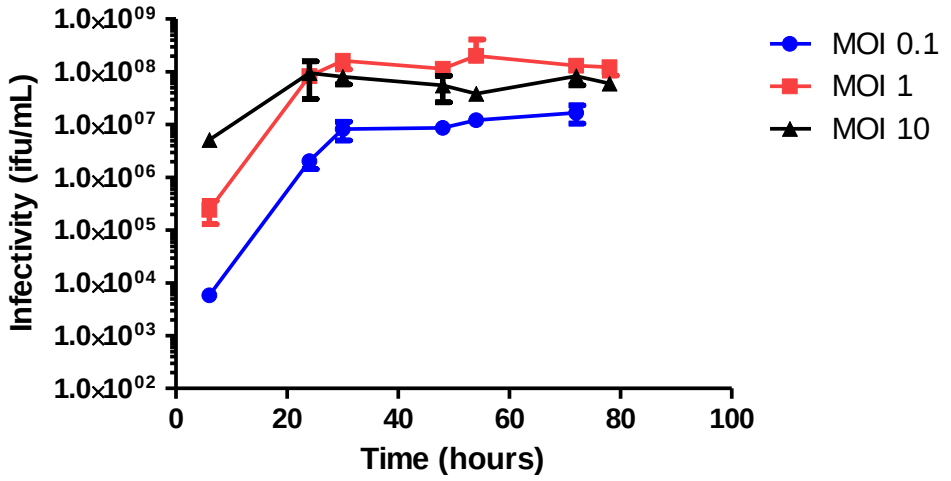

B: Suspension HEK293

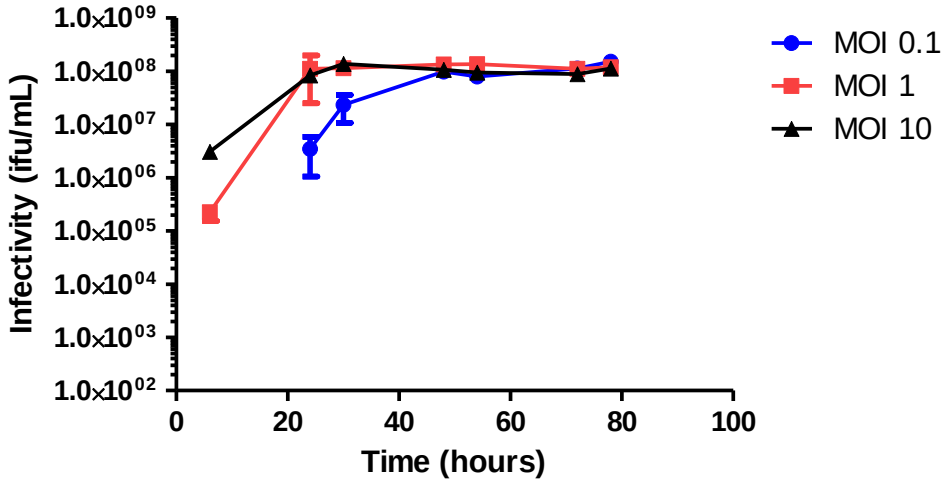

Figure 3-12: Total infectious particle yield of ColoAd1 in adherent and suspension HEK293 cells

Adherent HEK293 cells (**A**) were seeded at 1,000,000 cells/well in a 24 well plate for 2 hours, or suspension HEK293 cells (**B**) were seeded at 1,000,000 cells/mL in 125mL shake flasks. Then cells were infected with ColoAd1 in triplicate at MOI 10 (5200vp/cell), MOI 1 (520vp/cell), MOI 0.1 (52vp/cell) or mock infected. After 6, 24, 30, 48, 72 and 78 hours, cells and supernatant were removed from each well, or flask, before storage at -80°C and infectious particle number subsequently determined by hexon staining. Mean of triplicates with standard deviation shown.

Figure 3-11 and Figure 3-12 only consider the volumetric yield of ColoAd1 (the amount of virus produced per unit culture volume per unit time). Maximising the specific titre (the amount of virus produced per cell) is a mechanism of increasing the volumetric titre. To determine whether HEK293 cells continue to divide during ColoAd1 infection, cells were infected and subsequently stained with trypan blue, a dye impermeable to viable cell membranes, and live or dead cells counted using a haemocytometer and light microscope. HEK293 cells infected with both ColoAd1 and Ad11p appeared to double after 6 hours compared to the uninfected control cells (Figure 3-13A). This effect also occurred at 2 other MOIs (data not shown). However, 24 hours after infection, total cell numbers remained the same or less than the uninfected negative control (Figure 3-13A). In addition HEK293 viability, as determined by trypan blue staining, decreased slightly earlier for ColoAd1 than Ad11p (Figure 3-13B)

FACS was also used to determine cell division during ColoAd1 and Ad11p infection. HEK293 cells were stained with CFSE, a cell permeable dye that is converted to a florescent dye by intracellular esterases, and then infected with ColoAd1 or Ad11p or mock infected. After 48 hours, cells were fixed and the amount of CFSE stained remaining determined. The results also suggested that HEK293 cells did not divide more than once.

A: Total HEK293 cell counts

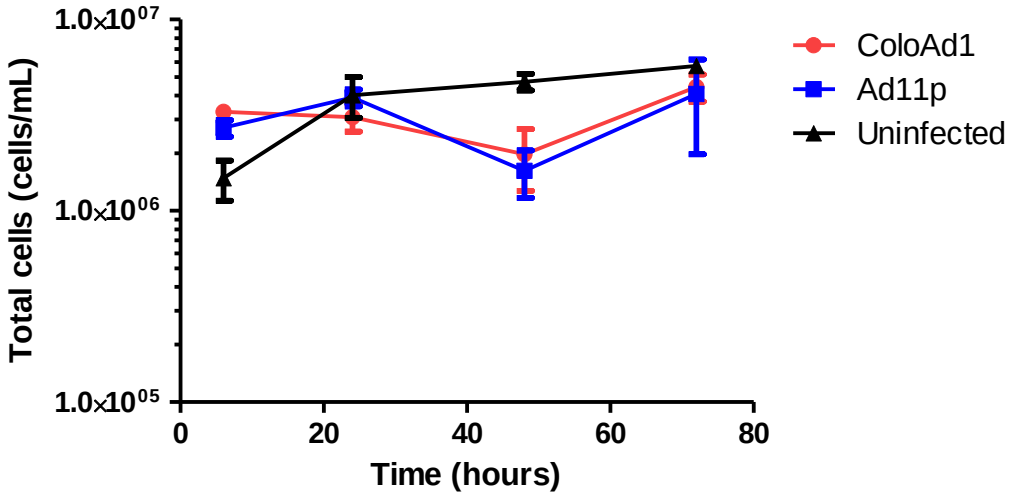

B: HEK293 cell viability

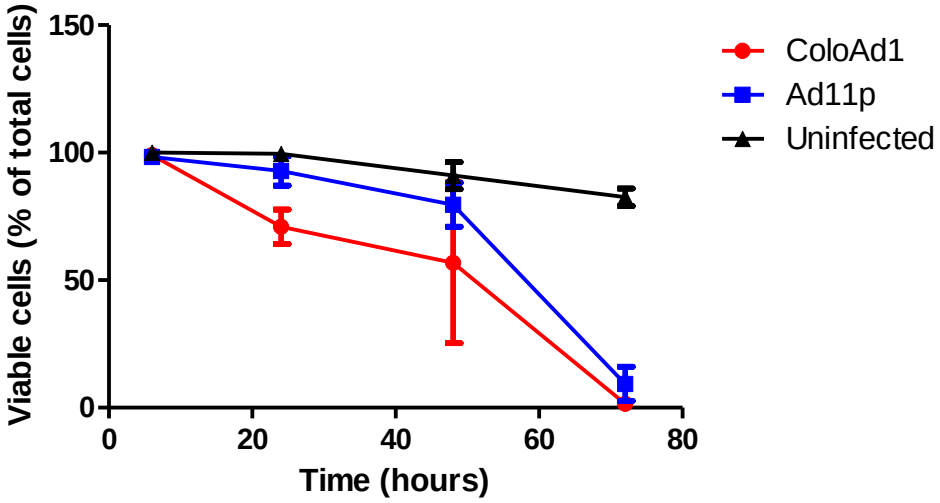

Figure 3-13: Adherent HEK293 cell growth and viability after infection

Adherent HEK293 cells were seeded overnight in 24 well plates at 350,000 cells/well before infection in triplicate with ColoAd1 or Ad11p at MOI 1(520vp/cell). After 6, 24, 48 and 72 hours, cells were removed using a cell scraper, microcentrifuged, and resuspended in 0.2mL PBS before staining with trypan blue to count viable unstained cells and non-viable stained cells using a microscope and haemocytometer. Data expressed as total cells (viable and non-viable) per mL (**A**) and viable cells as a fraction of total cells counted (**B**). Means of triplicates with standard deviation shown.

3.4 Discussion

Results from this chapter indicate that the differences in replication between ColoAd1 and Ad11p arise during the late phase of replication. Adherent HEK293 cells express high levels of the uptake receptors required for Group B adenovirus binding and internalisation (CD46 and DSG-2). Suspension HEK293 cells express CD46 to a high degree but express lower levels of DSG-2 than adherent HEK293 cells. The cellular uptake of ColoAd1 is the same as Ad11p on HEK293 cells. ColoAd1 replicates its genome to slightly higher copy numbers than Ad11p and releases particles into the supernatant earlier than Ad11p. The particles released are infectious and capable of spread through a monolayer of adherent HEK293 cells, as determined by staining for hexon protein, with spread occurring earlier for ColoAd1 than Ad11p. Finally, the total volumetric yield of ColoAd1 particles is independent of MOI in adherent HEK293 cells but dependent on MOI in suspension HEK293 cells, with total volumetric yield of infectious particles having the inverse relationship.

Overall, given that the differences in the replication lifecycles of ColoAd1 and Ad11p were thought to arise intracellularly, the intracellular response of HEK293 cells to ColoAd1 infection was investigated next.

4 Identifying Ways to Enhance ColoAd1 Production From HEK293 Cells

4.1 Introduction

Studies in Chapter 3 showed that the differences in the lifecycles of ColoAd1 and Ad11p occurred intracellularly, during the late phase of infection, after the onset of viral DNA replication. One consequence of this is that cell death observed for ColoAd1 occurred slightly earlier than wild type Ad11p, and although this may lead to a therapeutic benefit, in a bioprocessing setting it potentially limits virus productivity. It might therefore be advantageous to prolong infected cell viability to allow time to enhance manufacturing yield of ColoAd1.

During virus production it may be important that the cell does not experience stress due to excessive energy consumption. Adenosine 5' monophosphate-activated protein kinase (AMPK) functions as the main cellular energy sensor is a heterotrimeric protein, consisting of a catalytic α subunit and two regulatory β and γ subunits [148]. AMPK is activated, by a high ratio of AMP/ATP, which switches the cell from an anabolic environment to a catabolic environment, effectively preserving cellular energy levels. Phosphorylation of AMPKα at Thr-172 is required for activation [149]. The crystal structure of AMPK revealed that AMP or ADP binding to the regulatory subunit induced conformational changes that enhanced phosphorylation of Thr-172 by upstream kinases and also inhibited dephosphorylation by phosphatases [150]. LKB1 and CaMKK2 have been identified as kinases capable of phosphorylating AMPKα at Thr-172 [151]. PP2A and PP2C have also been identified as phosphatases capable of

dephosphorylating Thr-172 [152]. Overall, AMPK activation and downstream signalling pathways act to maintain the energy balance within the cell, by inhibiting excessive anabolic processes that consume ATP and, when necessary, enhancing catabolic processes to generate ATP [148].

Some viruses are capable of manipulating AMPK activity during cell infection, most likely to benefit the virus life cycle [153]. For example, HIV-1, Hepatitis C Virus (HCV) [154] and human cytomegalovirus (CMV) all inhibit AMPK [155] while other viruses such as Simian virus 40 (SV40) [156] and avian reovirus activate AMPK [157]. It is unclear whether adenovirus manipulates AMPK directly during infection. However, one of the downstream effectors targeted by AMPK is mTORC1 and Ad5 proteins E4orf1 and E4orf4 have been shown to activate mTORC1 during virus infection, most likely to maintain protein production independent of falling cellular ATP levels. Ad11p appears to have a similar E4 sequence as Ad5; suggesting E4 protein functions may be similar as in Ad5. However, as ColoAd1 lacks E4orf4, it was hypothesised that ColoAd1 and Ad11p would have different AMPK induced effects on mTORC1. Figure 4-1 shows the AMPK/mTORC1 signalling pathway investigated in this chapter.

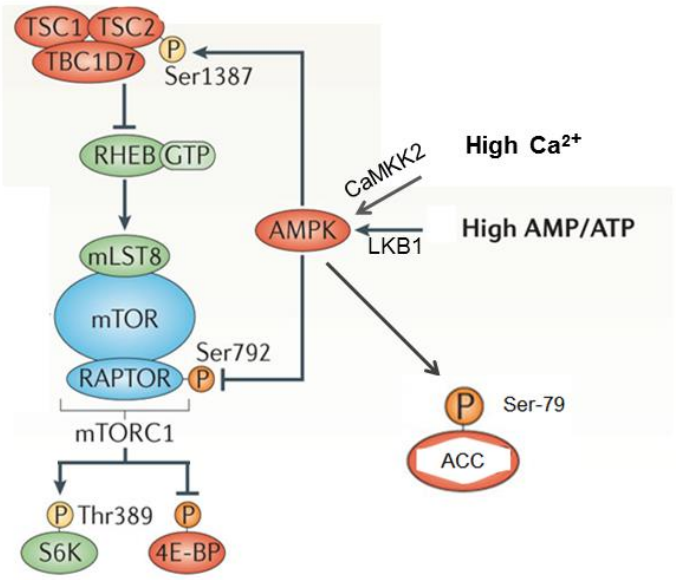

Figure 4-1: AMPK induced signalling on the mTORC1 pathway

AMPK is activated by phosphorylation of AMPKα subunit at Thr-172 in response to a high AMP/ATP ratio or by cytoplasmic calcium. Once activated, AMPK phosphorylates RAPTOR at Ser792 to directly inhibit mTORC1 and AMPK phosphorylates TCS2 at Ser1387 to indirectly inhibit mTORC1. AMPK also phosphorylates ACC at Ser79 to inhibit ACC activity in fatty acid synthesis. Phosphorylation events that function as inhibitory signals are depicted in orange and activating signals in yellow. Proteins depicted in red inhibit mTORC1 activity and proteins depicted in green activate mTORC1. Adapted by permission from Macmillan Publishers Ltd: Nature Reviews Molecular Cell Biology, copyright 2014 [158].

4.2 Aims

It was hypothesised that extending the viability of ColoAd1 infected HEK293 cells would allow time for enhancement of ColoAd1 particle production. To address this hypothesis the aims of this chapter were:

- To measure intracellular ATP during ColoAd1 and Ad11p infection of HEK293 cells.
- To determine the amount of AMPK phosphorylation and activation in ColoAd1 and Ad11p infected HEK293 cells, interpreting any differences in terms of the changed genetic makeup of ColoAd1.
- To manipulate AMPK phosphorylation and activation in ColoAd1 and Ad11p infected HEK293 cells by using pharmacological interventions.
- To delay ColoAd1 induced ATP depletion by enhancing ATP production, in order to enhance HEK293 cell viability.

4.3 Results

4.3.1 ColoAd1 infection induces ATP depletion earlier than Ad11p infection

Intracellular ATP levels were measured during ColoAd1 and Ad11p infection of HEK293 cells to determine cellular energy levels. The depletion of ATP precedes ADP and AMP accumulation. At MOI 10, intracellular ATP began depleting soon after infection with the steepest decrease occurring between 20 and 40 hours (Figure 4-2). At this time, the difference between ColoAd1 and Ad11 was subtle but significant with a 5 hour difference in time to 50% intracellular ATP relative to the uninfected control. At lower MOIs of 1 and 0.1 the onset of ATP depletion was later at about 30 and 50 hours respectively, although the rate of depletion after initiation was comparable. The difference between ColoAd1 and Ad11p at MOI 0.1 was more substantial than at MOI 10. This could have been due to the difference in the lifecycle time between ColoAd1 and Ad11p.

A

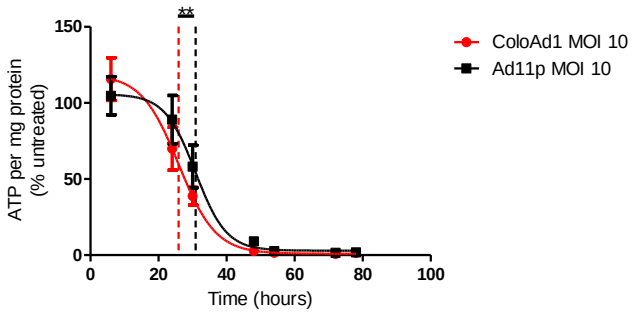

B

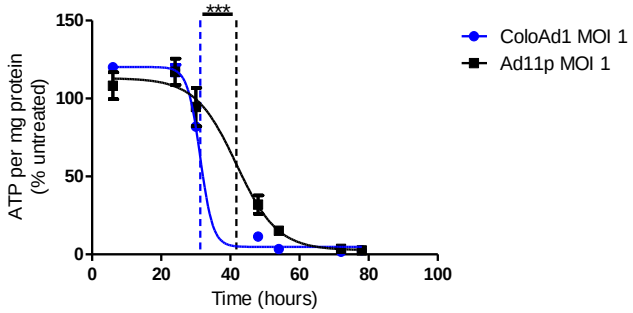

C

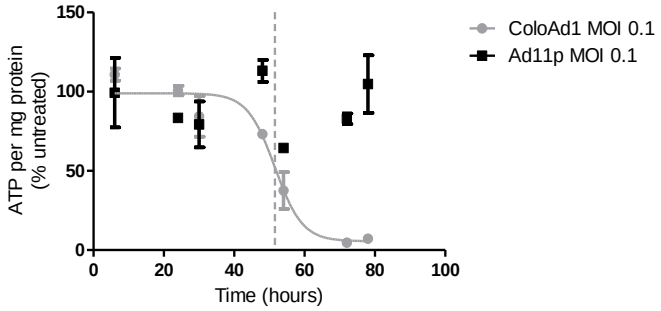

Figure 4-2: ColoAd1 depletes intracellular ATP earlier than Ad11p in HEK293 cells

Adherent HEK293 cells were infected with ColoAd1 and Ad11p at (**A**) MOI 10 (5200vp/cell), (**B**) MOI 1 (520vp/cell) and (**C**) MOI 0.1 (52vp/cell). After 6, 24, 30, 48, 54, 72 and 78 hours, cells were collected. Extracellular ATP was removed and intracellular ATP determined using a luciferase assay system (see Materials and Methods). The amount of protein present in all samples was determined using the BCA assay system. Then intracellular ATP normalised per mg of protein and expressed as a percentage of normalised uninfected control cells at each time point. Non-linear logistic fit (four-parameter) was performed on data points at each MOI. Dotted lines indicate the EC50 for each non-linear regression analysis and the significance of the difference in EC50 between ColoAd1 and Ad11p at each MOI determined using a student's T-test (unpaired). Means of triplicates with standard deviation shown.

4.3.2 AMPK phosphorylation status in virally infected HEK293 cells

Since ColoAd1 infection depleted intracellular ATP earlier than Ad11p infection (Figure 4-2), next it was considered whether infected HEK293 cells were capable of detecting the virally-induced ATP depletion. As AMPK is the major intracellular energy sensor, HEK293 cells were infected with ColoAd1 or Ad11p and the phosphorylation of AMPK at Thr-172 determined by Western blot. In addition, phosphorylation of ACC at Ser-79 was used to confirm the functional activity of AMPK resulting from Thr-172 phosphorylation.

Background phosphorylation of AMPK and ACC in HEK293 cells at 0 hours was low (Figure 4-3), suggesting that HEK293 cells were not metabolically stressed. After 24 hours, ColoAd1 infected cells had increased ACC phosphorylation compared to both uninfected cells and Ad11p infected cells. However, this did not correspond with a detectable increase in AMPK phosphorylation. This may mean that ACC phosphorylation was a more sensitive indicator of AMPK activity than phosphorylation status of AMPK itself.

After 30 hours, AMPK phosphorylation at Thr-172 in ColoAd1 infected cells was greater than AMPK phosphorylation in both untreated cells and Ad11p infected cells. This may have been due to the more rapid depletion of ATP by ColoAd1, leading to AMPK activation, or it might reflect the loss of E4orf4 protein in ColoAd1 compared to Ad11p. The phosphorylation of AMPK at this time corresponded with increased

phosphorylation of ACC at Ser-79 in ColoAd1 infected cells compared to uninfected and Ad11p infected cells.

Phosphorylation and activation of AMPK also eventually occurs in Ad11p infected HEK293 cells, 54 hours after infection. This coincides with ATP depletion in Ad11p infected HEK293 cells at the same MOI, suggesting AMPK may be activated by depleting ATP levels. It is also possible that E4orf4 is less active at this (late) stage of the Ad11p life cycle.

Overall, Figure 4-3 suggests that AMPK phosphorylation and activation occurs earlier in HEK293 cells infected with ColoAd1 than Ad11p. The reason for AMPK phosphorylation and activation is not certain, but the timing of AMPK phosphorylation in ColoAd1 and Ad11p infected HEK293 cells corresponds with the onset of ATP depletion seen in Figure 4-2, suggesting that falling ATP levels may contribute. However, AMPK can also be activated by the upstream kinase CaMKK2 in response to calcium [159]. CaMKK2 activity is inhibited by death associated protein kinase (DAPK) mediated phosphorylation at Ser-508 [160]. Indeed, at each time point after infection CaMKK2 appeared to be less phosphorylated at Ser-508 in ColoAd1 infected HEK293 cells compared to Ad11p and uninfected control cells, suggesting that AMPK activation could be mediated by calcium in HEK293 cells infected with ColoAd1 but not Ad11p (Figure 4-4).

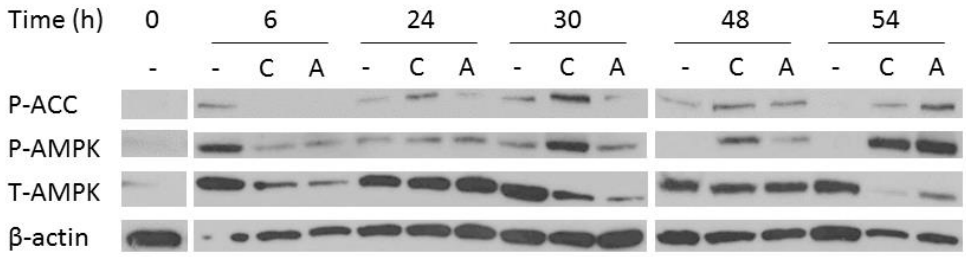

Figure 4-3: ColoAd1 induces AMPK phosphorylation and activation earlier than Ad11p in HEK293 cells

Adherent HEK293 cells were seeded at 500,000cells/well in a 6-well plate. The next day, cells were either mock infected (-) or infected at MOI 1 (520vp/cell) with ColoAd1 (C) or Ad11p (A). Cells were then harvested at 0, 6, 24, 30, 48 and 54 hours post infection and re-suspended in lysis buffer containing phosphatase inhibitor before loading 25µg protein on a 10% Tris-Glycine SDS gel, transferring to PVDF membrane and probing for phosphorylation of AMPKα at Thr-172 (P-AMPK) and ACC at Ser-79 (P-ACC). Endogenous levels of AMPKα was determined (T-AMPK) and β-actin used as a loading control.

Next, the downstream effects of AMPK activation were considered, which act to both inhibit ATP consuming processes and enhance ATP producing processes [148]. The effect of AMPK signalling on mTORC1 signalling was considered because E4orf4 is thought to interact with this pathway [121]. mTORC1 is centrally involved in the regulation of cap-dependent protein translation and cells cease most of their protein production when mTORC1 is inactivated. mTORC1 activity is normally regulated by the TSC1/TSC2 complex. Phosphorylation of TSC2 by AMPK at Ser-1387 acts to indirectly inhibit mTORC1 activity [161]. In addition, mTORC1 is also regulated by the phosphorylation status of its constituent subunit, Raptor. AMPK induced phosphorylation of Raptor at Ser-792 inhibits mTORC1 activity [162]. Inhibition of the mTORC1 complex then inhibits phosphorylation of S6K and 4EBP1 to inhibit cap dependent protein translation [161]. Therefore, the phosphorylation status of TSC2 and Raptor was determined during ColoAd1 and Ad11p infection.

Figure 4-4 shows the downstream effects of AMPK signalling in HEK293 cells infected with ColoAd1 and Ad11p. Interestingly, 24 hours after infection, in the absence of AMPK phosphorylation, Raptor and TSC2 were phosphorylated to higher levels than the untreated control. This suggested that in the absence of detectable AMPK activation, phosphorylation of TSC2 and Raptor was possible in virally infected HEK293 cells. This may represent a viral mechanism to manipulate mTORC1 signalling and protein translation, perhaps indicating that both viruses had largely switched to cap-independent translation by this time.

After 30 hours, it is difficult to draw conclusions from the control lane as the β-actin loading control appeared unreliable. As seen before, phosphorylation of AMPK in ColoAd1 infected cells was greater than in Ad11p infected cells, however, TSC2 and Raptor showed roughly equal phosphorylation in ColoAd1 and Ad11p infected cells. This gives further indication that the viruses had suppressed mTORC1 activity, most likely as part of a switch to cap-independent protein translation. It is interesting that both viruses seem able to do this without activation of AMPK.

As expected after 48 hours, phosphorylation of AMPK and ACC in ColoAd1 infected cells is greater than in Ad11p infected cells, and both virally infected cells have more AMPK phosphorylation than the untreated control cells. Unexpectedly, TSC2 phosphorylation at Ser-1387 is reduced in virally infected cells compared to the untreated control. This suggested that at this late time in the virus life cycle, ColoAd1 and Ad11p were capable of preventing the phosphorylation of TSC2 induced by AMPK. The same effect was seen 54 hours after infection.

Overall, there appears to be no connection between AMPK phosphorylation status and phosphorylation of TSC2 and Raptor in ColoAd1 or Ad11p infected HEK293 cells. In the absence of AMPK phosphorylation and activation, there is enhanced phosphorylation of TSC2 and Raptor at the sites normally phosphorylated by AMPK, whereas in the presence of AMPK phosphorylation and activation there is decreased phosphorylation of TSC2 and Raptor. This would cause mTORC1 inhibition and activation, respectively. However, mTORC1 activation is known to occur in adenovirus infected cells via the activity of E4orf1 and E4orf4 [121]. These data suggest that both viruses have mechanisms to deregulate AMPK-mediated phosphorylation of TSC2 and Raptor, and that both viruses must induce their own mechanisms for controlling mTORC1 activity instead. The main differences between ColoAd1 and Ad11p-infected cells relate to AMPK phosphorylation, but this appeared to have little downstream consequence on the mTORC1 pathway. To probe the effect of AMPK activation further, pharmacological inhibitors and activators of AMPK were used in the presence and absence of ColoAd1 and Ad11p.

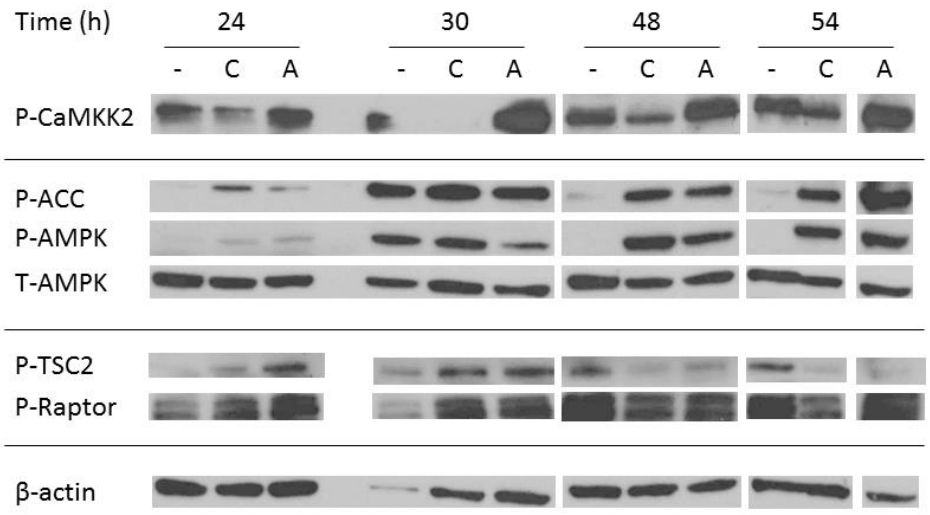

Figure 4-4: Downstream signalling of AMPK in ColoAd1 or Ad11p infected HEK293 cells
Adherent HEK293 cells were seeded at 500,000cells/well in a 6-well plate. The next day, cells were either mock infected (-) or infected at MOI 1 (520vp/cell) with ColoAd1 (C) or Ad11p (A). Cells were harvested at 24, 30, 48 and 54 hours post infection and re-suspended in lysis buffer containing phosphatase inhibitor before loading 25µg protein on a 10% Tris-Glycine SDS gel, transferring to PVDF membrane and probing for phosphorylation of AMPKα at Thr-172 (P-AMPK), ACC at Ser-79 (P-ACC), TSC2 at Ser-1387 (P-TSC2), Raptor at Ser-792 (P-Raptor) and CaMKK2 at Ser-508 (P-CaMKK2). Endogenous levels of AMPKα was determined (T-AMPK) and β-actin used as a loading control.

4.3.3 Pharmacological manipulation of AMPK phosphorylation and activation

Metformin is known to activate AMPK and compound C inhibits AMPK activity [163]. Therefore, these compounds were used in virally infected HEK293 cells at the onset of virally induced ATP depletion (24 hours after infection, Figure 4-2) to determine their effect on AMPK phosphorylation, activation and subsequent phosphorylation of TSC2 and Raptor.

Concentrations of metformin and compound C were chosen based on their toxicity to HEK293 cells (Figure 4-5). Dose response curves of metformin and compound C

treated HEK293 cells for 24 hours showed that HEK293 cells were highly sensitive to compound C treatment, whereas metformin required much higher concentrations to reduce HEK293 cell viability. Metformin is a hydrophilic base that is poorly permeable through cell membranes by passive diffusion. Instead, metformin requires uptake via Oct1/Oct2 cationic membrane transporters [164]. This could explain the high concentrations of metformin required to reduce HEK293 cell viability, and the difference in response between cell lines, where there may be a difference in expression of the membrane receptor required for uptake. In contrast, compound C is highly membrane permeable and reduces the viability of HEK293 cells at all concentrations tested (Figure 4-5).

The activity of metformin and compound C was then determined on the renal cell carcinoma cell line, RCC4-EV, that normally expresses higher levels of phosphorylated AMPK than HEK293 cells. As expected, treatment of RRC4-EV cells with 1.2mM or 3.6mM metformin for 24 hours increased AMPK phosphorylation and activation compared to the untreated control cells (Figure 4-6 A). Conversely, treatment with 2µM or 4µM compound C for 24 hours decreased AMPK phosphorylation and activation compared to the untreated control cells (Figure 4-6 A). Therefore, metformin and compound C were both active at their lowest concentrations (1.2mM and 2µM, respectively) on RCC4-EV cells. Given that these concentrations both induced some toxicity on HEK293 cells, as determined by MTS, the functional activity of these compounds towards AMPK was determined in HEK293 cells.

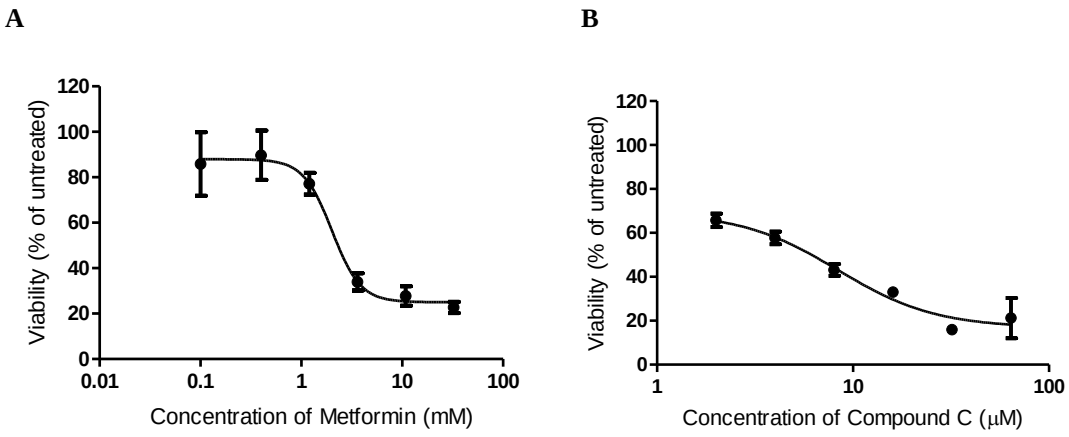

Figure 4-5: Effect of metformin and compound C on HEK293 viability

Adherent HEK293 cells were seeded at 10,000 cells/well in a 96 well plate. The following day, cells were treated in triplicate with 6 different concentrations of metformin (**A**) or compound C (**B**), or mock treated. After 24 hours, viability was determined using the MTS assay system (see Materials and Methods) and viability expressed relative to mock treated control (untreated) cells. Data was analysed using non-constrained non-linear curve fit. Mean of triplicate measurements shown, with error bars indicating standard deviation.

A

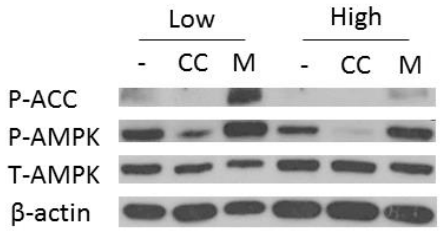

B

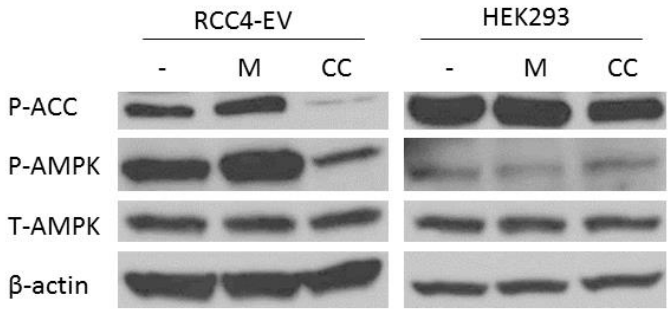

Figure 4-6 Effect of metformin and compound C on AMPK activation

A) RCC4-EV cells were seeded overnight in a 6 well plate at 500,000cells/well before treatment with compound C (CC) or metformin (M) at respective final concentrations of 2μM and 1.2mM (low), 4μM and 3.6mM (high), or mock treated (-). After 24 hours, supernatant was removed and cells suspended in cell lysis buffer containing phosphatase inhibitor, before loading 30μg protein on a 10% Tris-Glycine SDS gel, transferring to PVDF membrane and probing for phosphorylation of AMPKα at Thr-172 (P-AMPK) and ACC at Ser-79 (P-ACC). Endogenous levels of AMPKα was determined (T-AMPK) and β-actin used as a loading control.

B) RCC4-EV and adherent HEK293 cells were seeded overnight in a 6 well plate at 500,000cells/well before treatment with compound C (CC) or metformin (M) at respective final concentrations of 2μM and 1.2mM, or mock treated (-). After 24 hours, supernatant was removed and cells suspended in cell lysis buffer containing phosphatase inhibitor, before loading 25μg protein on a 10% Tris-Glycine SDS gel, transferring to PVDF membrane and probing for phosphorylation of AMPKα at Thr-172 (P-AMPK) and ACC at Ser-79 (P-ACC). Endogenous levels of AMPKα was determined (T-AMPK) and β-actin used as a loading control.

Surprisingly, in HEK293 cells there was no detectable activation or inhibition of AMPK phosphorylation by 1.2mM metformin or 2μM compound C (Figure 4-6 B). However, given that AMPK activation increased during viral infection, the effect of metformin and compound C was determined at the point in viral replication when AMPK phosphorylation and activation was maximal in an attempt to manipulate AMPK signalling (30 hours, as shown in Figure 4-3).

4.3.4 Combining metformin and compound C with virus infection

In this experiment, ColoAd1 and Ad11p infected HEK293 cells were treated with metformin and compound C 24 hours after infection, at the point where virally induced ATP depletion started to occur. Then, 30 hours after ColoAd1 infection there was no detectable phosphorylation of AMPK at Thr-172 (Figure 4-7), as seen previously (Figure 4-3). However, perhaps the additional mock treatment 24 hours after infection prevented AMPK phosphorylation. As a result, low AMPK phosphorylation made it difficult to determine the level of AMPK inhibition, if any, exerted by compound C. However, 48 hours after ColoAd1 infection AMPK phosphorylation at Thr-172 was detectable but compound C did not appear to inhibit AMPK or ACC phosphorylation. This suggested that compound C was not effective at inhibiting AMPK in ColoAd1 infected HEK293 cells.

In addition, 30 hours after infection compound C unexpectedly increased ACC phosphorylation in ColoAd1 infected HEK293 cells compared to the mock treated infected control cells. There was also a marginal increase in TSC2 phosphorylation at Ser-1387 (Figure 4-7) but no detectable increase in Raptor phosphorylation (Figure

4-7). Taken together this suggests that compound C actually enhances some functions of AMPK in ColoAd1 infected HEK293 cells but may reflect off-target effects of the compound.

Interestingly, 30 hours after Ad11p infection, compound C treatment decreased phosphorylation of TSC2 and Raptor compared to the untreated infected control (Figure 4-7). However, it was difficult to attribute this effect to AMPK, as AMPK and ACC phosphorylation was not detectable but does suggest that compound C inhibits some functions of AMPK in Ad11p infected HEK293 cells. The fact that the effect of compound C was more pronounced 30 hours after infection (6 hours after compound C treatment) compared to 48 hours after treatment (24 hours after compound C treatment), suggests that compound C may have a short mode of action in HEK293 cells and, therefore, perhaps there was an undetectable effect of compound C on AMPK phosphorylation 30 hours after infection (6 hours after treatment).

ColoAd1, and not Ad11p, enhanced AMPK phosphorylation at Thr-172 in the presence of metformin at both time points after infection, as compared to their respective untreated controls (Figure 4-7). This corresponded with enhanced ACC phosphorylation, suggesting that metformin increased both the phosphorylation and activation of AMPK in ColoAd1 infected cells. In contrast, Ad11p infected HEK293 cells appeared to be resistant to AMPK phosphorylation and activation by metformin (Figure 4-7). Despite this, TSC2 phosphorylation increased slightly in Ad11p infected HEK293 cells treated with metformin (Figure 4-7).

A

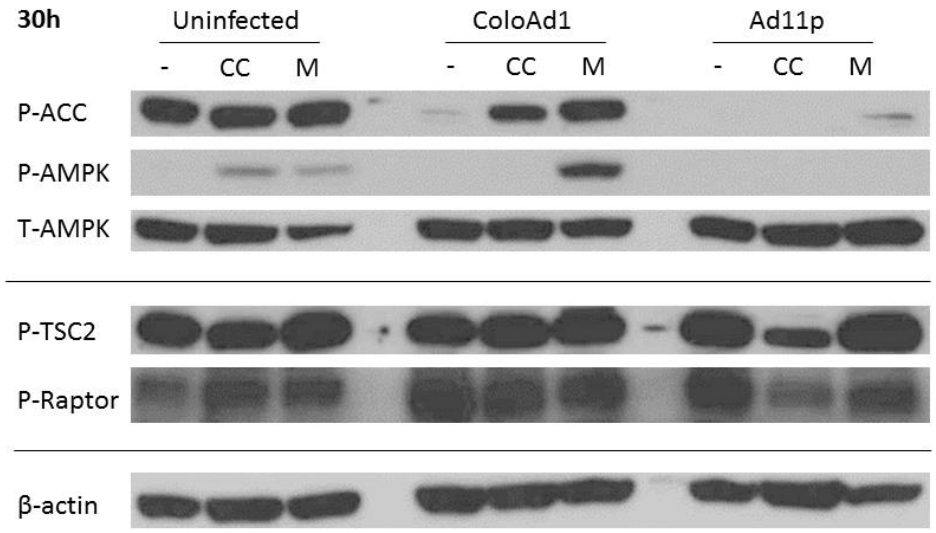

B

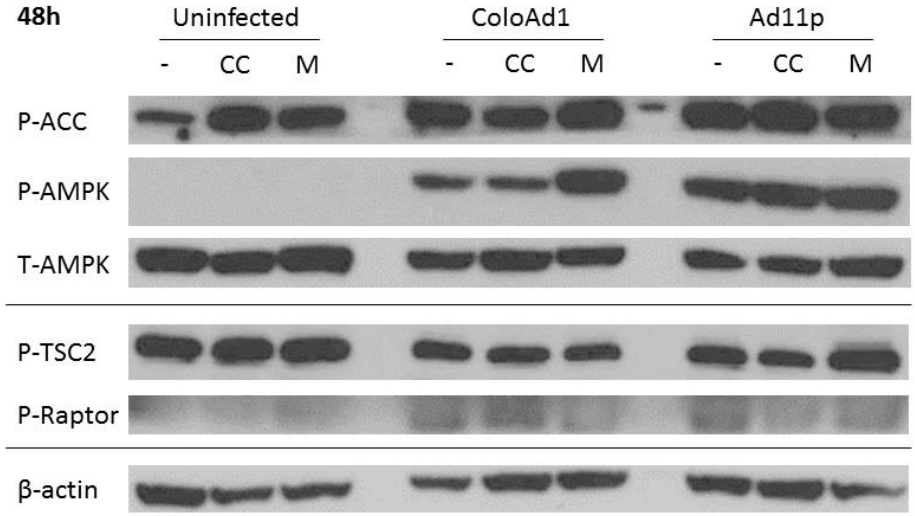

Figure 4-7 Effect of metformin and compound C on AMPK activation during ColoAd1 and Ad11p infection in HEK293 cells

Adherent HEK293 cells were seeded at 500,000cells/well in a 6-well plate. The next day, cells were either mock infected or infected at MOI 1 (520vp/cell) of ColoAd1 or Ad11p. After 24 hours, cells were treated with 1.2mM metformin (M) to give a final concentration of 1.2mM or treated with compound C (CC) to give a final concentration of 2µM. Cells were harvested 30hours (**A**) or 48 hours (**B**) after infection and re-suspended in lysis buffer containing phosphatase inhibitor, before loading 25µg protein on a 10% Tris-Glycine SDS gel, transferring to PVDF membrane and probing for phosphorylation of AMPKα at Thr-172 (P-AMPK), ACC at Ser-79 (P-ACC,) TSC2 at Ser-1387 (P-TSC2) and Raptor at Ser-792 (P-Raptor). Endogenous levels of AMPKα was determined (T-AMPK) and β-actin used as a loading control.

Overall, metformin enhanced AMPK phosphorylation and activation in ColoAd1 infected HEK293 cells, but this does not translate into enhanced Raptor or TSC2 phosphorylation. In contrast, Ad11p infected HEK293 cells appeared resistant to metformin induced AMPK phosphorylation and activation. This suggested that ColoAd1 infected HEK293 cells were capable of AMPK activation, whereas Ad11p infected HEK293 cells were not. Then both viruses were able to uncouple the downstream phosphorylation effect of AMPK on TSC2 and Raptor.

These findings were also tested in the RCC4-EV cell line as they had high background levels of AMPK phosphorylation from which to detect AMPK inhibition by compound C. A similar effect was seen as in HEK293 cells (data not shown). Interestingly, in addition to expressing high levels of phosphorylated AMPK, the RCC4-EV cell line gave an inverse relationship between ColoAd1 and Ad11p IC50 where the IC50 of Ad11p was less than the IC50 of ColoAd1 (Figure 4-8).

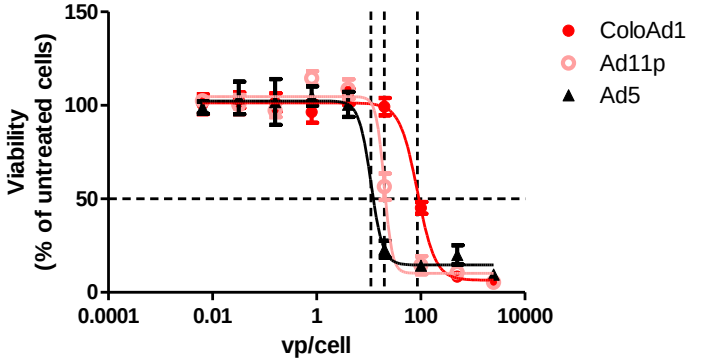

Virus	Cell line	IC50 (vp/cell)
ColoAd1	RCC4-EV	86.45
Ad11p	RCC4-EV	19.86
Ad5	RCC4-EV	11.05

Figure 4-8 IC50 of ColoAd1 is higher than Ad11p on RCC4-EV cell line

RCC4-EV cells were seeded overnight in a 96 well plate at 10,000 cells/well and then infected with 5-fold serial dilutions of each virus type (ColoAd1, Ad11p and Ad5). Viability (normalised to untreated control cells) was determined 5 days after infection using the MTS assay (see Materials and Methods). Means of 3 independent experiments with standard deviation shown. Non-linear curve fit (four parameter) is shown with dotted lines indicating IC50 values for each data set.

Finally, to determine whether metformin or compound C were able to prevent ColoAd1 or Ad11p induced lysis of HEK293 cells, the effect of each treatment on the IC50 of ColoAd1 and Ad11p was determined. The IC50 of ColoAd1 and Ad11p infected HEK293 cells decreased when cells were treated with metformin 24 hours after infection (Figure 4-9), suggesting that metformin enhanced adenovirus induced lysis. In contrast, compound C increased the IC50 of ColoAd1 infected HEK293 cells from 16.2vp/cell to 21.7vp/cell but Ad11p increased the IC50 by a greater degree from 146vp/cell to 215vp/cell (Figure 4-9). This suggested that compound C enhanced the viability of Ad11p infected HEK293 cells to a greater degree than ColoAd1.

A

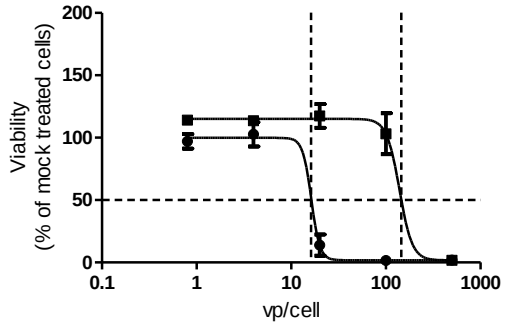

Virus	Treatment	IC50 (vp/cell)
ColoAd1	None	16.2
Ad11p	None	146

B

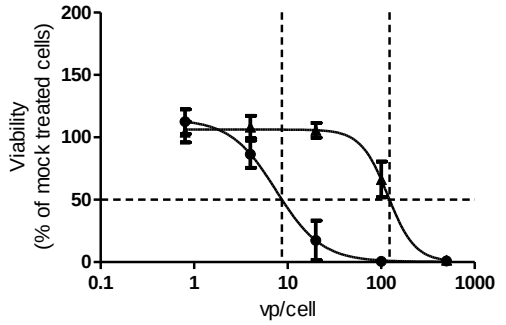

Virus	Treatment	IC50 (vp/cell)
ColoAd1	Metformin	8.70
Ad11p	Metformin	123

C

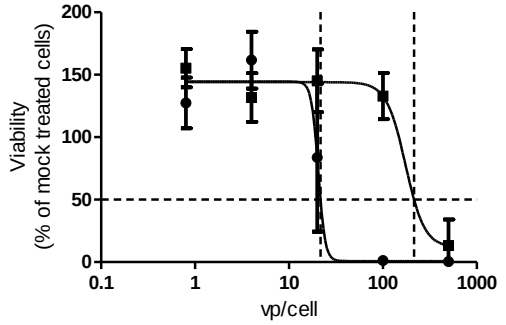

Virus	Treatment	IC50 (vp/cell)
ColoAd1	CC	21.7
Ad11p	CC	215

Figure 4-9: Effect of metformin and compound C on ColoAd1 and Ad11p infected HEK293 cell viability

Adherent HEK293 cells were seeded overnight in 96 well plates at 10,000 cells/well, and then infected with ColoAd1 or Ad11p, or mock infected. After 24 hours, cells were mock treated (**A**), treated with 1.2mM metformin (**B**) or treated with 2µM compound C (**C**). Viability (normalised to mock treated control cells) was determined using the MTS assay 3 days after infection (see Materials and Methods). Means of triplicate measurements with error bars showing standard deviation. Each data set was analysed using a four parameter non-linear curve fit.

4.3.5 Pharmacological manipulation of mTORC1

Taken together, the results from this chapter so far suggest that HEK293 cells respond to virally induced ATP depletion by AMPK activation and that cells infected with ColoAd1 or Ad11p are not responsive to AMPK induced signalling in the mTORC1 pathway. To confirm this, the mTORC1 inhibitor, rapamycin, was used to determine the impact of mTORC1 inhibition on ColoAd1 replication. ColoAd1 genome production significantly decreased in the presence of rapamycin (Figure 4-10) suggesting that ColoAd1 requires mTORC1 activity, and associated cap-dependent protein translation, for efficient replication. In addition, ColoAd1 infected HEK293 cells had significantly reduced viability in the presence of rapamycin compared to without (Figure 4-11B), even though rapamycin alone had no effect on HEK293 cell viability (Figure 4-11A).

It is possible that the effect of rapamycin may be time dependent as, after 48 hours, the viability of ColoAd1 infected HEK293 cells did not significantly change in the presence of rapamycin compared to without (Figure 4-12B), even though rapamycin alone reduced HEK293 cell viability by at least 50% at this time point (Figure 4-12A). This suggested that rapamycin treatment may be more effective during the late phase of adenovirus replication.

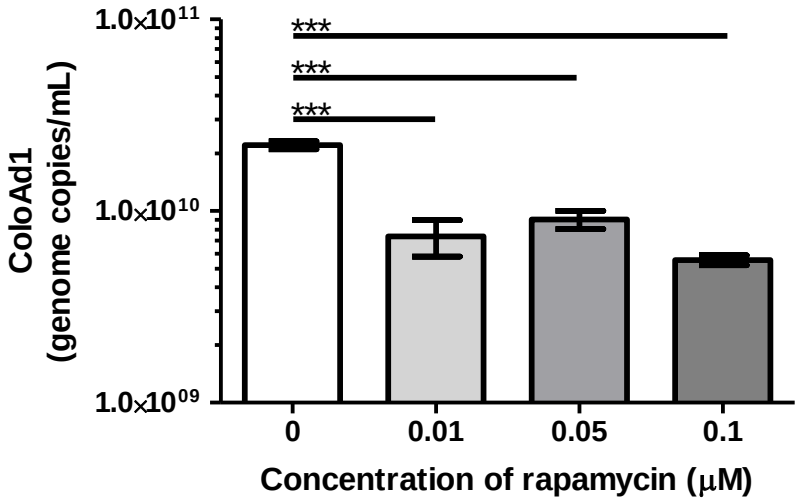

Figure 4-10: Rapamycin significantly decreases ColoAd1 genomes 48 hours after infection

Adherent HEK293 cells were seeded at 10,000 cells/well in 96 well plate and incubated overnight, before infection with ColoAd1 at MOI 1 (520vp/cell). After 3 hours, cells were mock treated or treated with rapamycin to give final concentrations of 0.01μM, 0.05μM or 0.1μM. 48 hours after infection, cells were removed by scraping and combined with the supernatant before storage at -80°C, until DNA extraction was performed and copies of ColoAd1 genome determined by QPCR (see Materials and Methods). Error bars show standard deviation. One way ANOVA with Dunnets post-test was performed against untreated ColoAd1 infected cells. ** P = 0.034. N = 3 for mock and ColoAd1 controls. N = 2 for each rapamycin treatment.

A: Uninfected

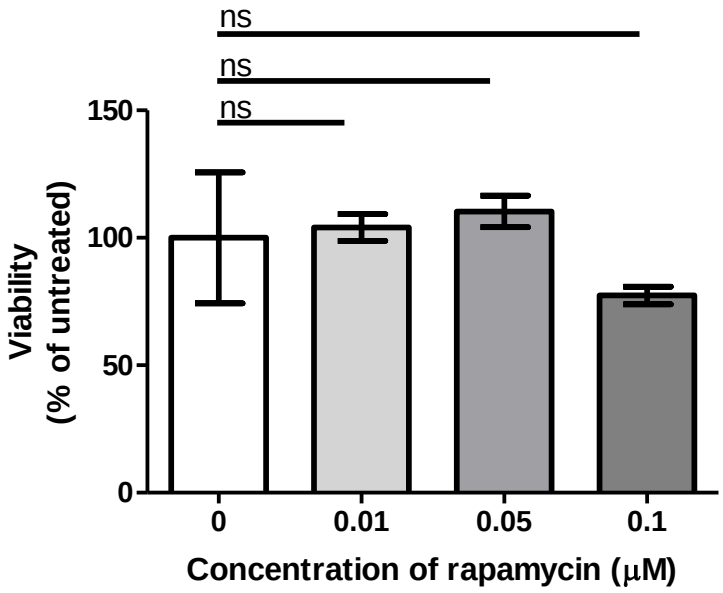

B: ColoAd1

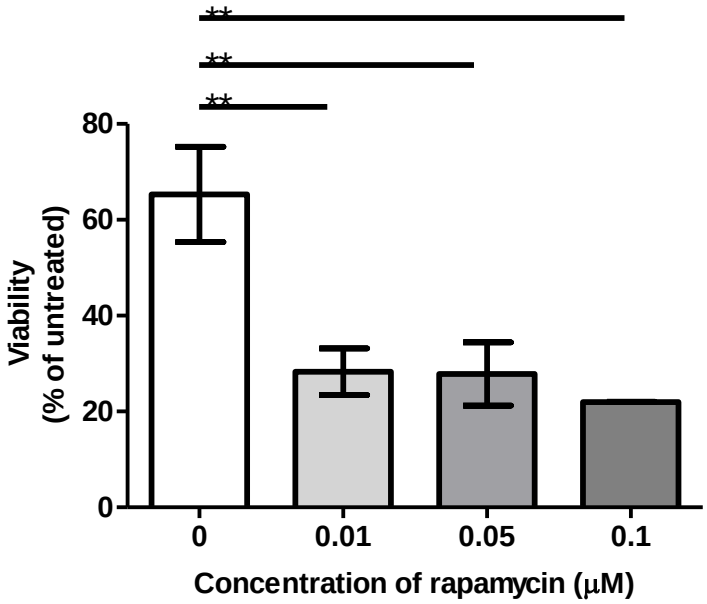

Figure 4-11: Rapamycin has no effect on HEK293 cell viability and reduces ColoAd1 infected cell viability after 24 hours

Adherent HEK293 cells were seeded at 10,000 cells/well in 96 well plate and incubated overnight. Cells were then **(A)** mock infected or **(B)** infected with ColoAd1 at MOI 1 (520vp/cell). After 3 hours, cells were treated with rapamycin to give final concentrations of 0.01μM, 0.05μM or 0.1μM. The MTS assay was performed 24 hours after infection and the viability of cells relative to uninfected, untreated (mock) cells determined. Error bars show standard deviation. One way ANOVA with Dunnets post-test was performed to determine the effect of rapamycin treatment on HEK293 cell viability (A) or ColoAd1 infected HEK293 cell viability (B). ** P = 0.034. N = 3 for mock and ColoAd1 controls. N = 2 for each rapamycin treatment.

A: Uninfected

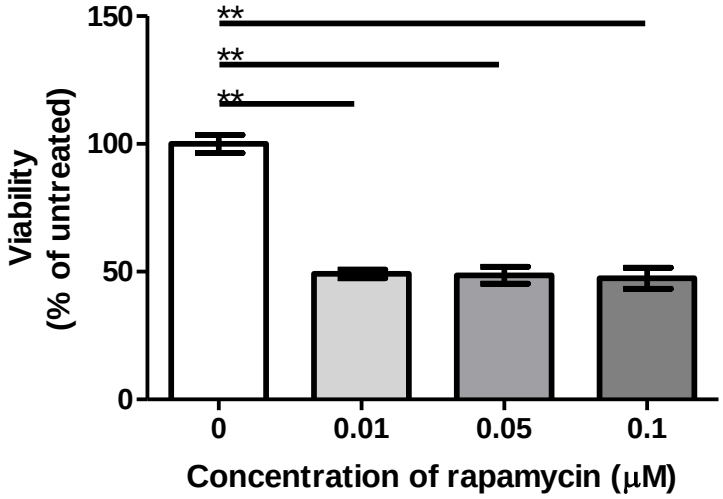

B: ColoAd1

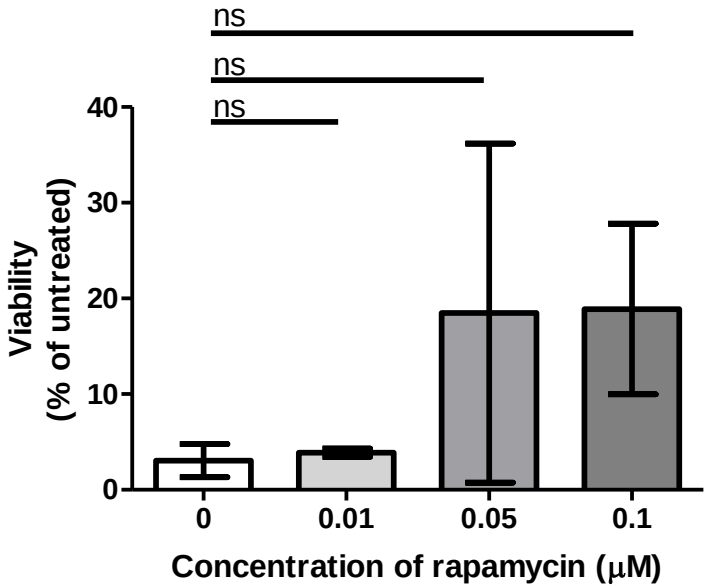

Figure 4-12: Rapamycin reduces HEK293 cell viability and has no effect on ColoAd1 infected cell viability after 48 hours

Adherent HEK293 cells were seeded at 10,000 cells/well in 96 well plate and incubated overnight. Cells were then **(A)** mock infected or **(B)** infected with ColoAd1 at MOI 1 (520vp/cell). After 3 hours, cells were treated with rapamycin to give final concentrations of 0.01μM, 0.05μM or 0.1μM. The MTS assay was performed 48 hours after infection and the viability of cells relative to uninfected, untreated (mock) cells determined. Error bars show standard deviation. One way ANOVA with Dunnets post-test was performed to determine the effect of rapamycin treatment on HEK293 cell viability (A) or ColoAd1 infected HEK293 cell viability (B). ** P = 0.034. N = 3 for mock and ColoAd1 controls. N = 2 for each rapamycin treatment.

4.4 Discussion

As ATP is not stored within the cell, depletion of intracellular ATP in ColoAd1 infected HEK293 cells was either due to increased ATP consumption with supply of ATP not meeting demand, or there could have been some degree of virally induced inhibition of ATP synthesis. The reason for intracellular ATP levels being lower in ColoAd1 than Ad11p infected HEK293 cells was not identified, although it could have resulted from the enhanced genome replication observed for ColoAd1 (Figure 3-5). The energy demands of Ad5 DNA replication have been characterised [165] and E4orf4 has been shown to limit viral replication [119]. Therefore, as ColoAd1 lacks E4orf4, ColoAd1 may be less able than Ad11p to control the energy consuming process of genome replication.

ColoAd1 appears to activate AMPK at the onset of virally induced ATP depletion, whereas Ad11p shows a delayed response in AMPK activation. This could be due to the delay in ATP depletion observed for Ad11p or could result from the genetic differences between ColoAd1 and Ad11p. Therefore, AMPK activation could be a passive response of the cell to virus replication or could be induced by viral proteins, either directly or indirectly. The mechanism of AMPK activation remains controversial. The current hypothesis is that ADP and AMP binding to AMPK enhances allosteric activation by LKB1 but also decreases allosteric inhibition by phosphatases [148]. In addition, AMPK can be activated by calcium calmodulin kinase kinase II (CaMKK2), which is activated by a rise in cytoplasmic calcium [159]. In this respect, investigation of ATP levels and AMPK activation in the LKB1-null cell line, A549, would be useful to determine the contribution of CaMKK2 on AMPK activation in ColoAd1 and Ad11p infected HEK293 cells.

In any case, AMPK induced phosphorylation of TSC2 and Raptor appears to be avoided by both ColoAd1 and Ad11p. This is in accordance with the hypothesis that adenovirus activates mTORC1, especially in the absence of nutrients, mediated by E4orf1/E4orf4 proteins [121]. More specifically, in the absence of nutrients E4orf1 mimics PI3K signalling to increase p70S6K phosphorylation and E4orf4 acts on the mTOR pathway downstream of AMPK to enhance 4EBP1 phosphorylation [121]. In this respect, perhaps the effect of AMPK activation observed on the phosphorylation of TSC2 and Raptor may be better investigated in nutrient deprived HEK293 cells.

For both ColoAd1 and Ad11p, the fall in intracellular ATP (Figure 4-2) occurred during the late phase of the virus lifecycle, after the accumulation of replicated viral genomes (Figure 3-5). A defining feature of the late phase of adenovirus infection is the shut off of host cell translation. This is achieved partly by E1B 55-kDa forming a complex with E4orf6 to mediate the selective export of viral mRNA [166]. Despite this, cytoplasmic viral mRNAs remain only about 20% of the total cytoplasmic pool so adenovirus also shuts off host translation to encourage translation of late viral mRNAs to produce the structural proteins required for adenovirus packaging. However, all eukaryotic mRNA, including adenoviral mRNA, is capped with 7-methyl-GTP at the 5’-end and polyadenylated at the 3’-end [167] so there are no obvious structural differences between viral and host mRNA. Instead, the host cell selectively translates adenoviral mRNA via tripartite leader sequences in late viral mRNAs, which direct ribosome shunting for viral mRNA translation in the absence of cap dependent translation initiation [114].

Cap dependent translation initiation (reviewed in [168]) is an ATP consuming process that requires the formation of the eukaryotic initiation factor 4F complex (eIF4F) at the 5'-end of mRNA. The eIF4F complex consists of:

- eukaryotic initiation factor 4E (eIF4E) cap binding protein
- eukaryotic initiation factor 4A (eIF4A) ATP-dependent RNA helicase
- eukaryotic initiation factor 4G (eIF4G) large scaffold protein

In a fully assembled eIF4F complex, unwinding of the mRNA secondary structure by eIF4A begins in the 5'-untranslated region (5'-UTR) and is an ATP consuming process that allows ribosome scanning for the start codon [169]. Given that Ad11p is capable of maintaining higher levels of ATP than ColoAd1, it is possible that ColoAd1 lacks the ability to inhibit cap dependent translation initiation to induce earlier ATP depletion or that Ad11p is capable of more efficient inhibition of cap dependent translation initiation to conserve ATP.

Many viruses are capable of manipulating cap dependent translation to their advantage for replication, reviewed in [170]. Some viruses, such as encephalomyocaditis virus, shut off host protein translation by decreasing 4EBP1 phosphorylation [171]. Other viruses such as herpes virus activate cap dependent translation [172]. Adenovirus activates cap dependent translation early in replication, by hyperphosphorylation of the 4EBP1 and 4EBP2, and E4orf4 may mediate this effect in nutrient deprived conditions [121, 173]. In addition, E1A is thought to induce p70S6K expression and E4orf1 enhances p70S6K phosphorylation by mimicking PI3K/Akt signalling [121]. However, dephosphorylation of eIF4E contributes to the inhibition of cap dependent translation

initiation during the late phase of adenovirus replication [174, 175]. Given that the AMPK signalling observed in this chapter was not coupled to mTORC1 signalling, it is likely that ColoAd1 and Ad11p manipulate mTORC1 signalling to permit productive viral replication.

Pharmacological agents can also activate AMPK. Metformin was used to activate AMPK in this chapter. Meformin activates AMPK by inhibiting complex I in the electron transport chain [176]. Although, there is also some evidence that metformin can inhibit mTORC1, independently of AMPK [177]. Activation of AMPK with metformin in the presence of ColoAd1 but not Ad11p, suggested that either ColoAd1 potentiates metformin induced AMPK activation or that Ad11p was capable of inhibiting metformin induced phosphorylation of AMPK. In contrast, compound C was not able to inhibit ColoAd1 induced AMPK activity on any substrate but it did appear to prevent AMPK induced phosphorylation of TSC2 in HEK293 cells.

Investigation of the host cell factors that determine the difference in IC50 between ColoAd1 and Ad11p on RCC4-EV might help determine the mechanism of action for ColoAd1. RCC4-EV cells fail to express functional VHL, the protein which is responsible for the ubiquitination and proteasomal degradation of HIF1α [178]. High levels of HIF1α enhance 4EBP1 gene expression [179]. The phosphorylation status of 4EBP1 determines cap dependent translation initiation. Ad11p contains E4orf4 that has been shown to enhance 4EBP1 phosphorylation [121]. However, ColoAd1 lacks E4orf4 so would presumably be unable to enhance 4EBP1 phosphorylation, especially in RCC4-EV cells that presumably express high levels of 4EBP1. Therefore, investigating

the phosphorylation status of 4EBP1 in RCC4-EV cells may further our understanding of the host cell factors that contribute to ColoAd1 mechanism of action.

Overall, AMPK activation had no effect on the mTORC1 pathway in ColoAd1- or Ad11p-infected HEK293 cells. HCMV is also capable of circumventing AMPK-mediated inhibition of mTOR [155]. However, as ColoAd1 responds to AMPK activation, it is possible that the downstream signalling of AMPK activation on alternative pathways would be beneficial to maintain intracellular ATP levels in ColoAd1 infected HEK293 cells. AMPK also acts to activate ATP producing processes, such as glycolysis. The next chapter will consider whether it is possible to enhance ATP producing processes in an attempt to delay the fall in ATP observed in ColoAd1 infected HEK293 cells.

5 Manipulating Metabolic Pathways in ColoAd1 Infected HEK293 Cells

5.1 Introduction

In 1924, Warburg observed that cancer cells predominantly metabolise glucose to produce lactate, even in the presence of sufficient oxygen [180]. This phenomenon, termed aerobic glycolysis, has gained much attention since then and is now regarded as one of the hallmarks of cancer [10]. Many cells cultured *in vitro* also have a strong preference for aerobic glycolysis despite retaining oxidative phosphorylation capabilities. At first this seems paradoxical, as metabolism of glucose to lactate yields less ATP than metabolism of glucose by oxidative phosphorylation. However, cancer cells compensate for this deficit by increasing the glycolytic rate and this can occur by:

1) Increased glucose uptake by increased expression of glucose transporters, particularly GLUT-1 and/or GLUT-3 [181, 182]. This has been exploited to allow the clinical detection of tumours by fluorodeoxyglucose positron emission tomography (FDG-PET) with FDG [183].
2) Increased expression and activity of glycolytic enzymes. For example, cancer cells often over express hexokinase (HK), especially the mitochondrial bound isoezyme, HK-2, where normal cells do not [184, 185].

These compensatory mechanisms underlying aerobic glycolysis are thought to allow the cell to generate adequate levels of ATP as well as provide sufficient carbon source for anabolism to benefit cell division [186]. In some ways the metabolic requirements of proliferating cells are similar to the metabolic requirements of viruses, where both need to maintain energy levels in addition to producing nucleotides, amino acids, and lipids for replication or virus particle production [187].

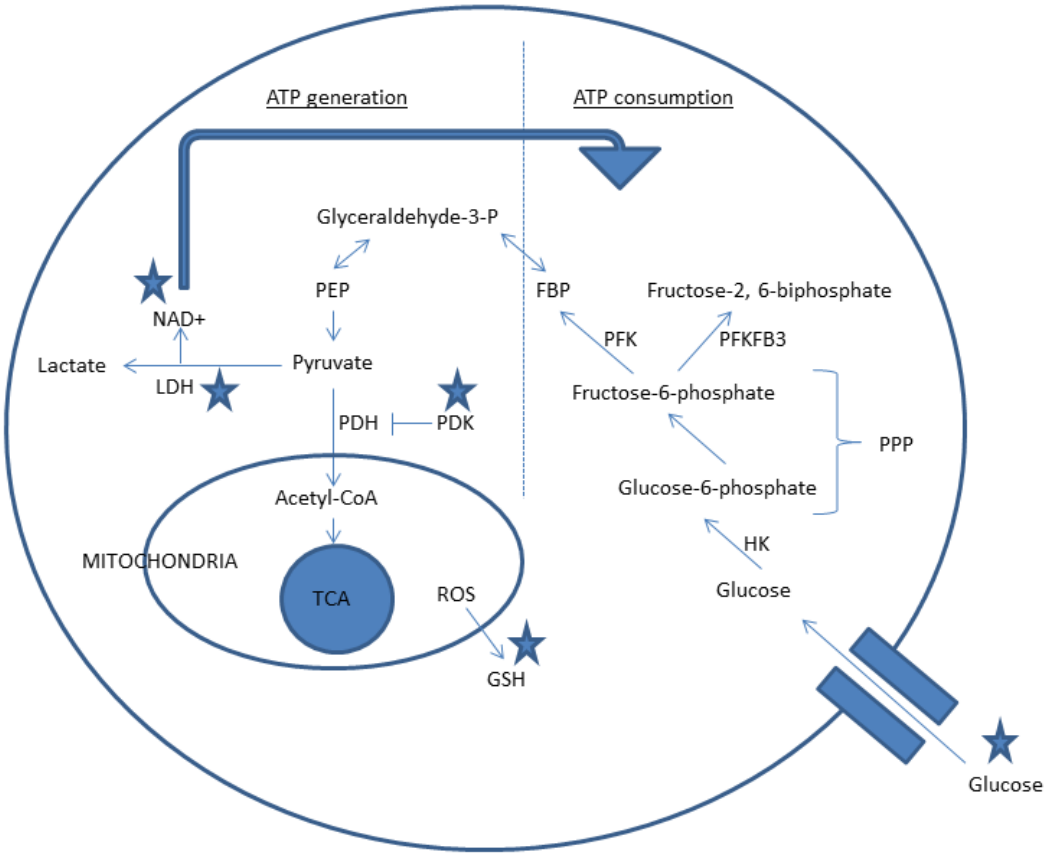

Figure 5-1 Points of intervention to boost ColoAd1 infected cell viability and yield

Depicted is the cellular uptake of glucose through glucose transporters, such as GLUT-1 or GLUT-3, in the plasma membrane and subsequent cytoplasmic metabolism before mitochondrial metabolism via the TCA cycle and oxidative phosphorylation. Points of intervention are marked with *. Hexokinase (HK), 6-phosphofructo-2-kinase/fructose-2,6-biphosphatase 3 (PFKFB3), Phosphofructokinase (PFK), Fructose 1, 6-bisphosphate (FBP), Glyceraldehyde-3-phosphate (Glyceraldehyde-3-P), Phosphoenolpyruvate (PEP), Lactate dehydrogenase (LDH), Pyruvate dehydrogenase (PDH), Pyruvate dehydrogenase kinase (PDK), Reactive oxygen species (ROS), tricarboxylic acid cycle (TCA) and Glutathione (GSH). Adapted from [187].

5.2 Aims

We developed the hypothesis that ColoAd1 would require glycolysis during the early phase of infection and that enhancing intracellular ATP levels by boosting intermediates required for oxidative phosphorylation may delay ColoAd1 induced ATP depletion. In this way, the aim was to maintain infected cell viability and enhance ColoAd1 yield. The points of intervention that are considered in this chapter are described in Figure 5-1.

- To determine whether ColoAd1 infected HEK293 cells have a preference for aerobic glycolysis.
- To explore the possibility of preventing ColoAd1 induced ATP depletion by promoting ATP generation via oxidative phosphorylation.
- To identify pharmacological agents that may promote survival of ColoAd1 infected HEK293 cells and enhance the total genome yield.

5.3 Results

5.3.1 Galactose decreases ColoAd1 genome production

To determine whether ColoAd1 was reliant on glycolysis, galactose was used as the energy source instead of glucose. The metabolism of galactose to pyruvate, by glycolysis, yields no net ATP so the cell relies totally on ATP production by mitochondrial oxidative phosphorylation [188].

HEK293 cells were incubated for 24 hours in media containing glucose, galactose or no glucose (see Table 5-1) before infection with ColoAd1 or Ad11p to determine the effect of glycolysis on virus production. Galactose significantly decreased the genome copies

of ColoAd1 produced 48 hours after infection (Figure 5-2 A) although this effect was harder to discern in Ad11p, perhaps because fewer particles were produced (Figure 5-2 B). This suggests that ColoAd1 replication relies on the products of glycolysis and if these products are consumed by oxidative phosphorylation then many fewer genomes are produced, despite the greater production of ATP. Galactose did not significantly increase intracellular ATP in ColoAd1 infected HEK293 cells, although there was a trend towards increased intracellular ATP in ColoAd1 infected HEK293 cells (Figure 5-3A) that was not seen in Ad11p infected HEK293 cells (Figure 5-3B). However, perhaps the timing of measurement was not optimal for Ad11p as ATP depletion due to viral replication had not begun.

Overall, the need for the products of glycolytic metabolism of galactose to be consumed in oxidative phosphorylation for ATP generation appeared to be detrimental to ColoAd1 replication yield, although surprisingly this did not appear to significantly enhance the intracellular ATP levels compared to the non-inhibited control.

	DMEM	Glucose/Galactose (mM)	Glutamine (mM)	Pyruvate (mM)
Control	D5786	25mM	2mM	N/A
TCA & Glycolysis (control)	11966-025	25mM/0mM	2mM	1mM
TCA only (galactose)	11966-025	0mM/10mM	2mM	1mM
TCA only (no glucose)	11966-025	0mM/0mM	2mM	1mM

Table 5-1: Details of cell culture conditions for Figure 5-2 and Figure 5-3

A: ColoAd1

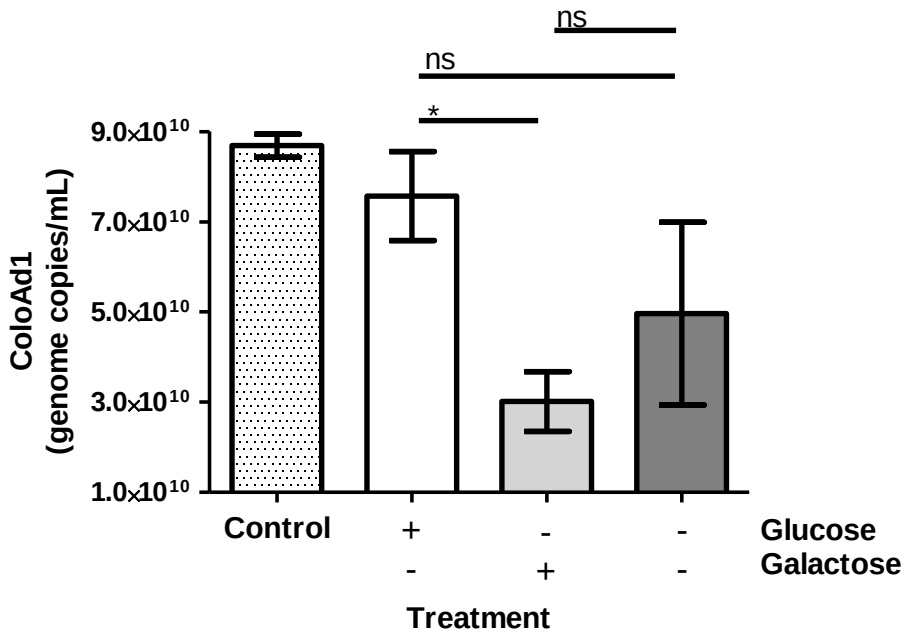

B: Ad11p

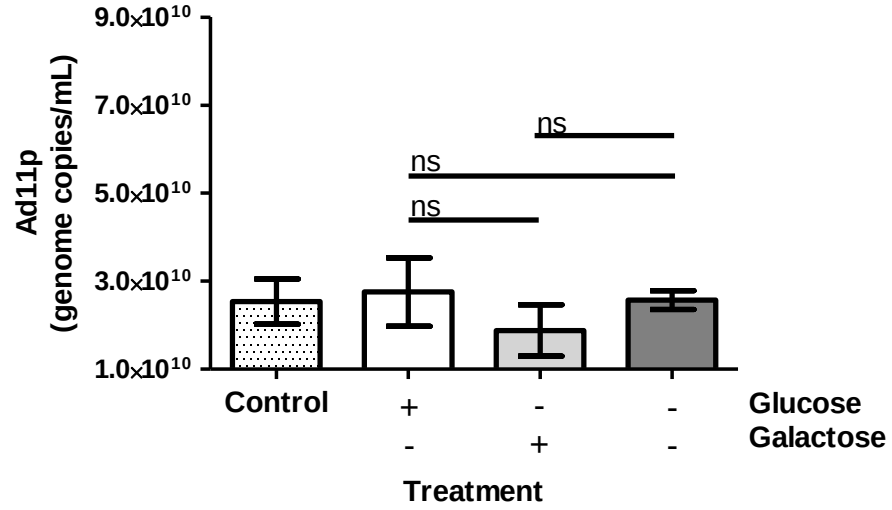

Figure 5-2: Galactose decreases ColoAd1 but not Ad11p genome yield 48 hours after infection

Adherent HEK293 cells were seeded overnight in 96 well plates at 10,000cells/well before exchanging media to contain either 25mM glucose (+/-), 10mM galactose (-/+), neither (-/-) or standard media conditions (control). After 24hours, cells were mock infected or infected in triplicate with ColoAd1 (**A**) or Ad11p (**B**) at 520vp/cell, diluted in the corresponding media (see Table 5-1). 48 hours after infection, supernatant and cells were removed from each well, before storage at -80°C. After DNA extraction (Promega) total genome copies were determined by QPCR and expressed per mL of culture volume. Mean of triplicate measurements with standard deviation shown. One-way ANOVA with Dunnett's post-test was performed to determine the significance of any effect of glucose removal on virus genome yield, where ns = no significant difference ($P>0.05$) and * = $P<0.05$.

A: ColoAd1

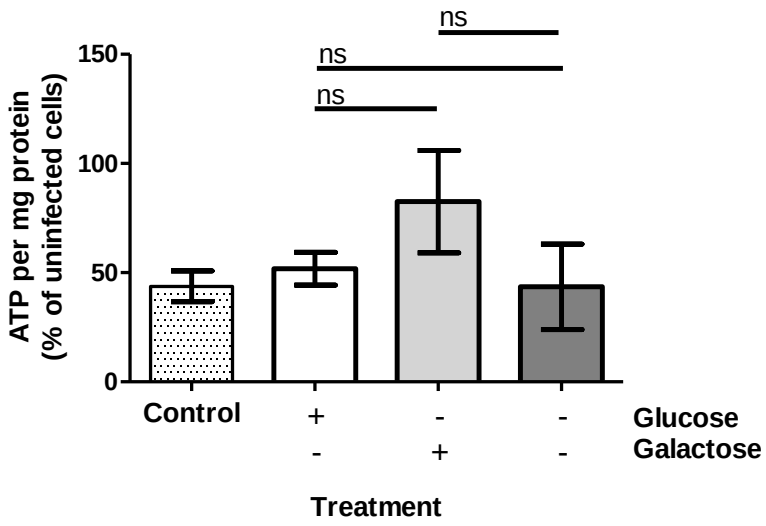

B: Ad11p

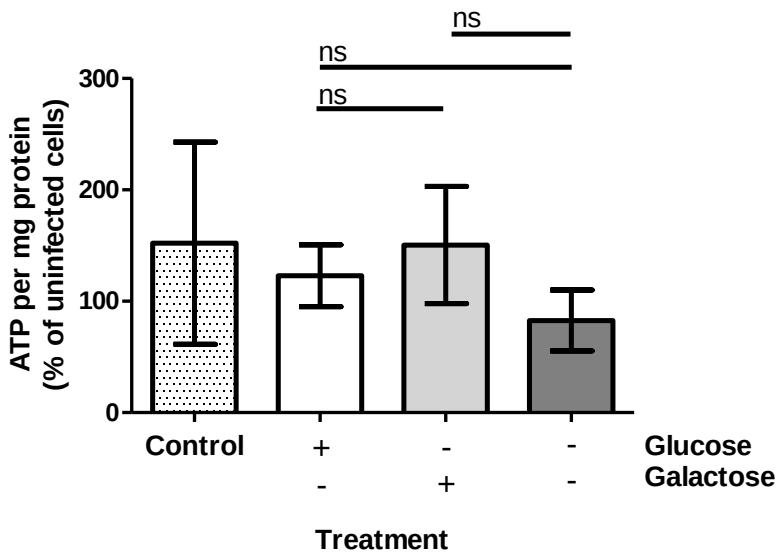

Figure 5-3: Galactose has no effect on intracellular ATP of HEK293 cells infected with ColoAd1 or Ad11p 48 hours after infection

Adherent HEK293 cells were seeded overnight in 96 well plates at 10,000cells/well before exchanging media to contain either 25mM glucose (+/-), 10mM galactose (-/+), neither (-/-) or standard media conditions (control). After 24hours, cells were mock infected or infected in triplicate with ColoAd1 (**A**) or Ad11p (**B**) at 520vp/cell, diluted in the corresponding media (see Table 5-1). 48 hours after infection, cells were removed from each well and ATP assay performed (see Materials and Methods) with data normalised per mg of protein as determined by BCA assay. One-way ANOVA with Dunnett's post-test was performed to determine the significance of any effect of glucose removal on intracellular ATP, where ns = no significant difference ($P>0.05$).

5.3.2 Effect of sodium oxamate on ColoAd1 infected HEK293 cells

Bypassing glycolytic ATP production with galactose appeared to protect against ColoAd1 induced intracellular ATP depletion. To assess whether this was due to enhanced generation of ATP by oxidative phosphorylation, pharmacological agents were used to encourage the cell to metabolise pyruvate for oxidative phosphorylation instead of lactate production.

Inhibition of lactate dehydrogenase using sodium oxamate was first considered. Figure 5-4 shows that sodium oxamate significantly ($P<0.01$) enhanced the viability of ColoAd1 infected HEK293 cells 24 hours after infection (Figure 5-4A) but not after 48 hours (Figure 5-4B). Surprisingly, sodium oxamate had no effect on the intracellular ATP levels of ColoAd1 infected HEK293 cells 24 or 48 hours after infection (Figure 5-5), and also had no effect on ColoAd1 genome replication (Figure 5-6). This suggested that sodium oxamate increased the metabolic activity of ColoAd1 infected HEK293 cells during the early phase of viral replication (as indicated by the enhanced viability determined by MTS after 24 hours), which conferred protection against ColoAd1 induced cell death (after 24 hours) but not later (after 48 hours). In addition, the enhanced infected cell viability early (after 24 hours) did not confer any benefit in ColoAd1 genome yield later (after 48 hours). Therefore, as this early effect of enhanced infected cell viability was desired, it was hypothesised that feeding more pyruvate into the TCA cycle for oxidative phosphorylation, would enhance ColoAd1 infected cell viability.

A: 24 hours after infection

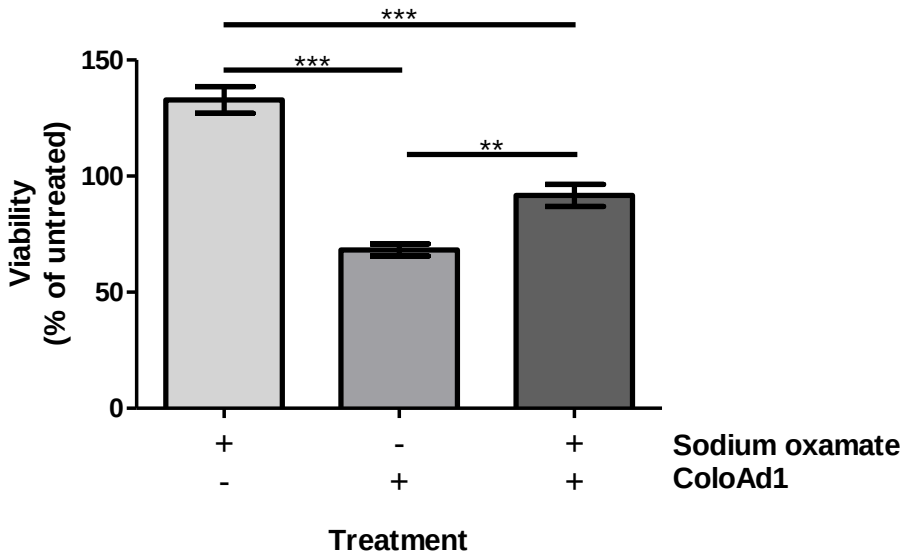

B: 48 hours after infection

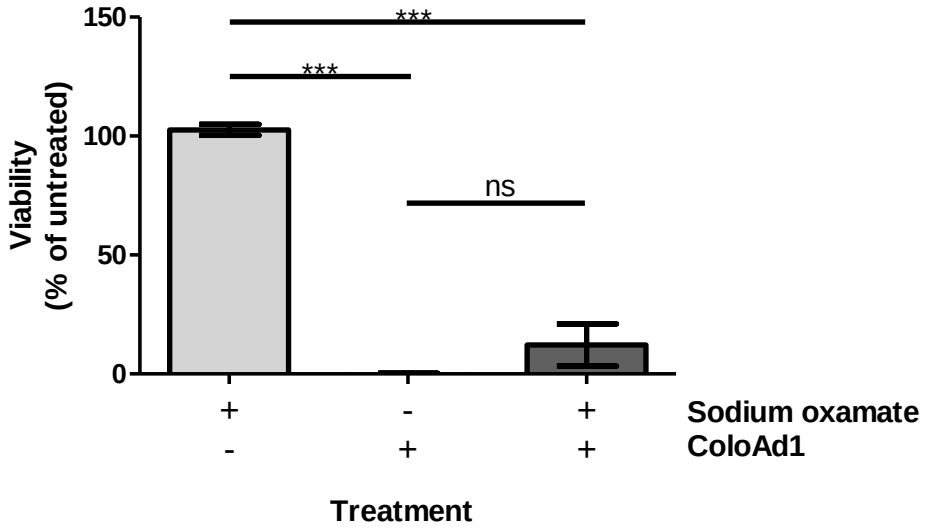

Figure 5-4: Effect of sodium oxamate on HEK293 cell viability with and without ColoAd1

Adherent HEK293 cells were seeded overnight in 96 well plates at 10,000cells/well, before mock infection (-) or infection with ColoAd1 (+) at MOI 1 (520vp/cell). After 3 hours, cells were either mock treated (-) or treated with sodium oxamate (+) to give a final concentration of 1mM. HEK293 cell viability was determined after 24 hours (**A**) or 48 hours (**B**) using the MTS assay (see Materials and Methods) and normalised to the viability of untreated, uninfected cells. Mean of triplicate measurements with standard deviation shown. One-way ANOVA with Tukey's multiple comparison post-test was performed to determine the significance of any effect of sodium oxamate on the viability of ColoAd1 infected HEK293 cells, where ns = not signficant ($P>0.05$), ** = $P<0.01$, and *** = $P<0.0001$.

A: 24 hours after infection

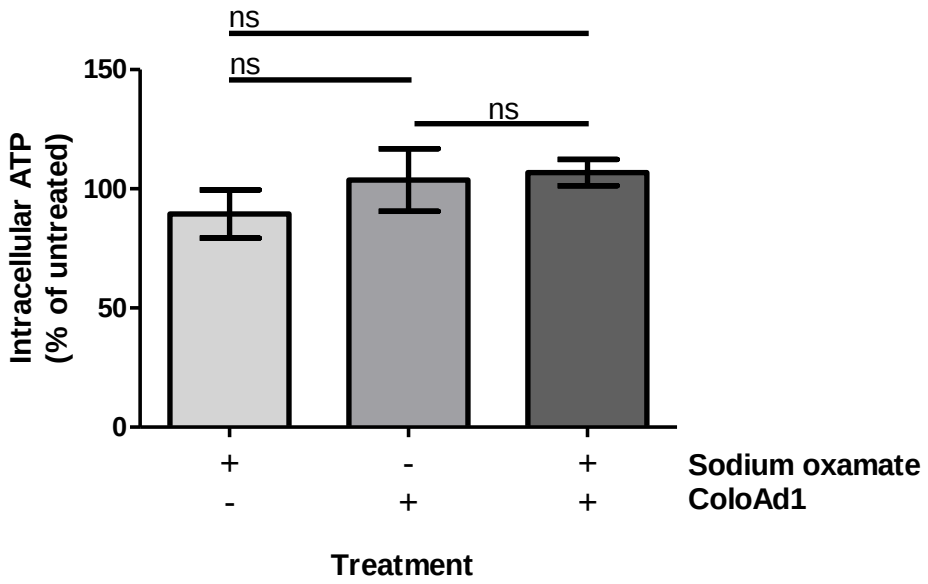

B: 48 hours after infection

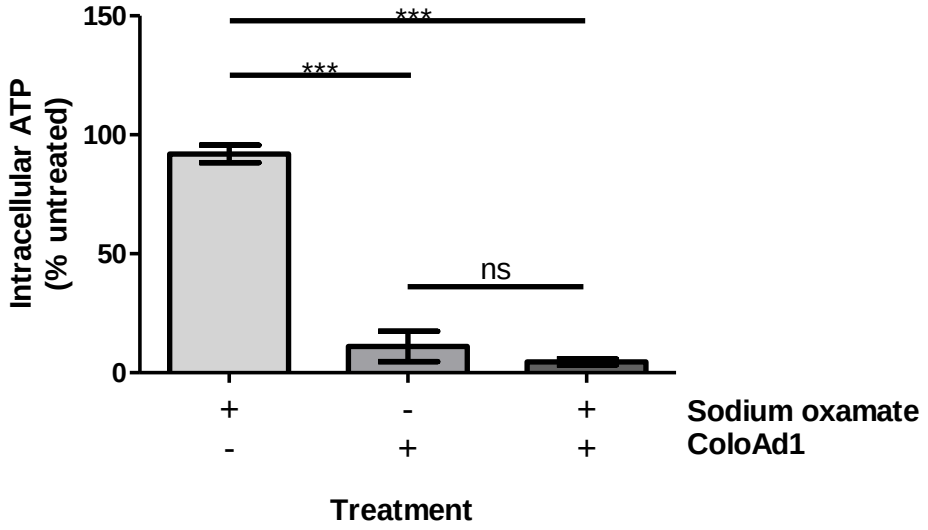

Figure 5-5: Effect of sodium oxamate on intracellular ATP of HEK293 cells

Adherent HEK293 cells were seeded overnight in 96 well plates at 10,000cells/well, before mock infection (-) or infection with ColoAd1 (+) at MOI 1 (520vp/cell). After 3 hours, cells were either mock treated (-) or treated with sodium oxamate (+) to give a final concentration of 1mM. Intracellular ATP was determined after 24 hours (**A**) or 48 hours (**B**) using the intracellular ATP assay (see Materials and Methods) and ATP normalised to the intracellular ATP of uninfected, untreated cells. Mean of triplicate measurements with standard deviation shown. One-way ANOVA with Tukey's multiple comparison post-test was performed to determine the significance of any effect of sodium oxamate on the intracellular ATP of ColoAd1 infected HEK293 cells, where ns = no significant difference ($P>0.05$) and *** = $P<0.0001$.

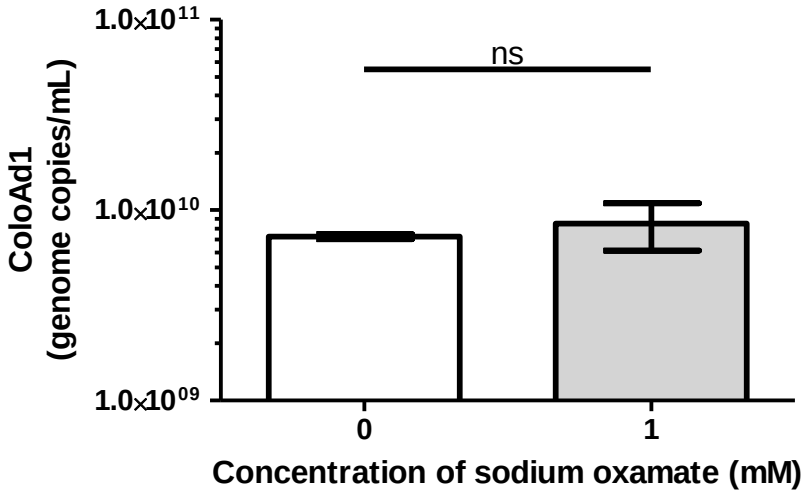

Figure 5-6: Effect of sodium oxamate on ColoAd1 genome yield 48 hours after infection

Adherent HEK293 cells were seeded overnight in 96 well plates at 10,000cells/well, before infection with ColoAd1 at MOI 1 (520vp/cell) for 3 hours, followed by treatment with sodium oxamate. 48 hours after infection, cells and supernatant were collected and stored at -80°C before DNA extraction and QPCR to determine genome copy number expressed per mL of culture volume (see Materials and Methods). Mean of triplicate measurements with standard deviation shown. Unpaired students T-Test was performed to determine the significance of any effect of sodium oxamate on ColoAd1 genome yield, where ns = no significant difference ($P>0.05$).

5.3.3 Effect of DCA on ColoAd1 infected HEK293 cells

The small molecule PDK inhibitor, dichloroacetate (DCA), increases the flux of pyruvate into the mitochondria for oxidative phosphorylation [189]. A range of DCA concentrations were tested to determine toxicity on HEK293 cells. Increasing DCA concentrations showed a trend towards decreasing HEK293 cell viability, with 25mM DCA significantly reducing HEK293 cell viability after 48 hours compared to the untreated control (Figure 5-7 A). However, DCA treatment of ColoAd1 infected HEK293 cells had no significant effect on ColoAd1 infected cell viability after 48 hours compared to the infected mock treated HEK293 cells (Figure 5-7 B). This suggests that ColoAd1 protects HEK293 cells against DCA induced cell death, especially at 25mM.

DCA had no significant effect on ColoAd1 genome yield after 48 hours, although there was a trend where low concentrations of DCA (<10mM) appeared to enhance ColoAd1 genome yield and higher concentrations of DCA (25mM) had a genome yield that was similar to the infected mock treated control (Figure 5-8). In any case, DCA does not appear to have a detrimental effect on ColoAd1 genome yield (Figure 5-8). In addition, it was also observed that ColoAd1 infected HEK293 cells treated with DCA maintained a higher culture pH than mock-treated ColoAd1 infected cells, as indicated by the colour of the phenol red containing culture media. This effect presumably occurred by DCA enhancing pyruvate flux into the mitochondria for oxidative phosphorylation, thus, preventing pyruvate conversion to lactate.

Overall, given that both sodium oxamate and DCA had marginal effects alone, perhaps they would perform better in combination to prevent lactic acid accumulation and

encourage pyruvate to enter the TCA cycle. Either way, it appears that both sodium oxamate and DCA are better at promoting survival of ColoAd1 infected HEK293 cells with no significant effects on ColoAd1 genome yield. Therefore, perhaps enhancing glycolysis and pentose phosphate pathway is a better mechanism of increasing ColoAd1 yield.

A: DCA Only

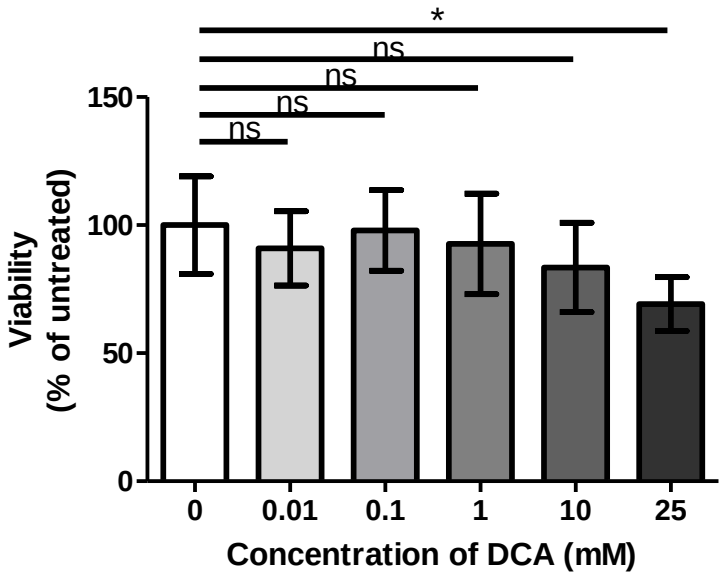

B: DCA with ColoAd1

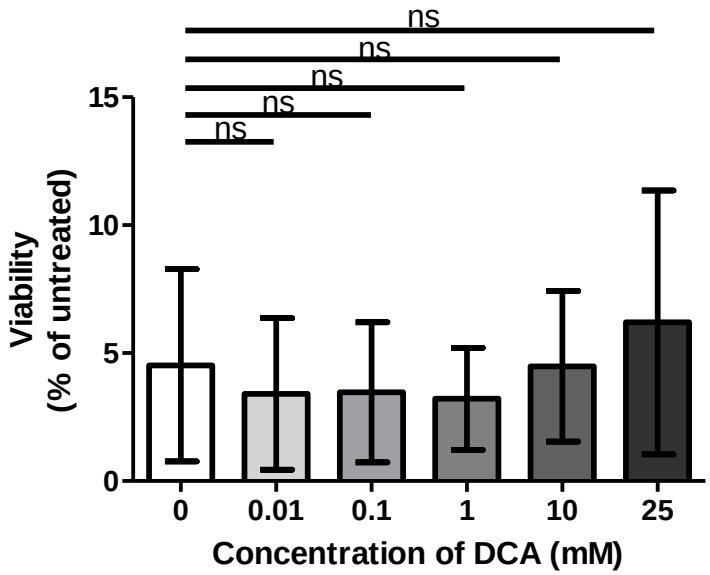

Figure 5-7: Effect of DCA on HEK293 cell viability with and without ColoAd1 48 hours after infection

Adherent HEK293 cells were seeded overnight in 96 well plates at 10,000cells/well, before mock infection (**A**) or infection with ColoAd1 (**B**) at MOI 1 (520vp/cell) for 3 hours, followed by treatment with dichloroacetate (DCA) to give a final concentration of 0, 0.01, 0.1, 1, 10 or 25mM. HEK293 cell viability was determined 48 hours after infection using the MTS assay (see Materials and Methods) and normalised to the viability of uninfected, untreated cells. Mean of triplicate measurements from 2 independent experiments with standard deviation shown. One-way ANOVA with Dunnett's post-test was performed to determine the significance of any effect of DCA on HEK293 cell viability in the absence or presence of ColoAd1, where * = $P < 0.05$ and ns = no significant difference ($P>0.05$).

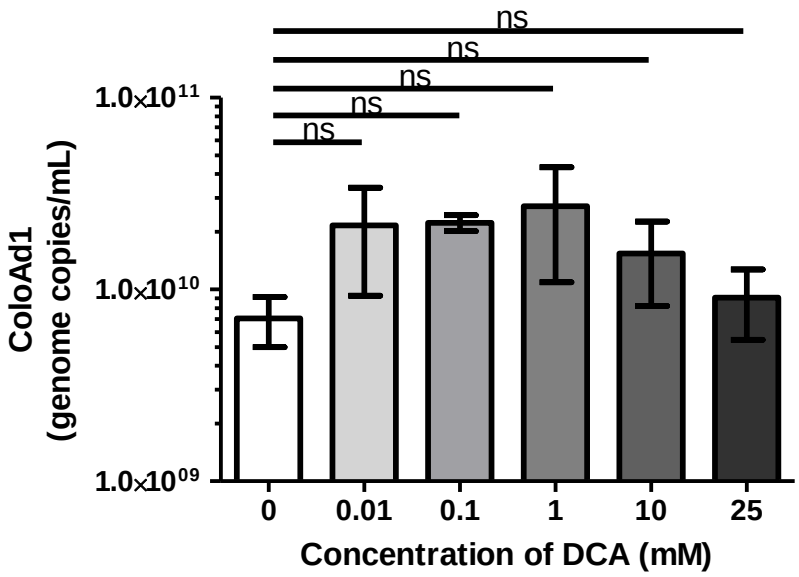

Figure 5-8: Effect of DCA on ColoAd1 genome yield 48 hours after infection

Adherent HEK293 cells were seeded overnight in 96 well plates at 10,000cells/well, before infection with ColoAd1 at MOI 1 (520vp/cell) for 3 hours, followed by treatment with dichloroacetate (DCA) to give a final concentration of 0, 0.01, 0.1, 1, 10 or 25mM. Then 48 hours after infection, cells and supernatant were collected and stored at -80°C before DNA extraction and QPCR to determine genome copy number expressed per mL of culture volume (see Materials and Methods). Mean of triplicate measurements from 2 independent experiments with standard deviation shown. One-way ANOVA with Dunnett's post-test was performed to determine the significance of any effect of DCA on ColoAd1 genome yield, where ns = no significant difference ($P>0.05$).

5.3.4 Effect of nicotinamide on ColoAd1 infected HEK293 cells

One of the major factors limiting glycolytic flux is the availability of nicotinamide adenine dinucleotide (NAD+) [190]. The cell regenerates NAD+ back from NADH by the conversion of pyruvate to lactate or by NADH shuttles. Nicotinamide is a precursor of NAD+, therefore, it was hypothesised that enhancing the availability of NAD+, by the addition of nicotinamide, might enhance glycolysis and ColoAd1 genome yield.

Nicotinamide significantly enhanced the viability of ColoAd1 infected HEK293 cells after 24 hours compared to the untreated control, although this effect was not obvious after 48 hours (Figure 5-9). This effect confirms the hypothesis that cell viability can be enhanced during ColoAd1 infection. Interestingly, nicotinamide had no significant effect on the intracellular ATP levels of ColoAd1 infected HEK293 cells (Figure 5-10). Nicotinamide also had no significant effect on ColoAd1 genome yield after 48 hours (Figure 5-11). Therefore, like sodium oxamate and DCA, nicotinamide appeared to have a more significant effect on mitochondrial metabolism and cell viability rather than ColoAd1 genome yield.

A: 24 hours after infection

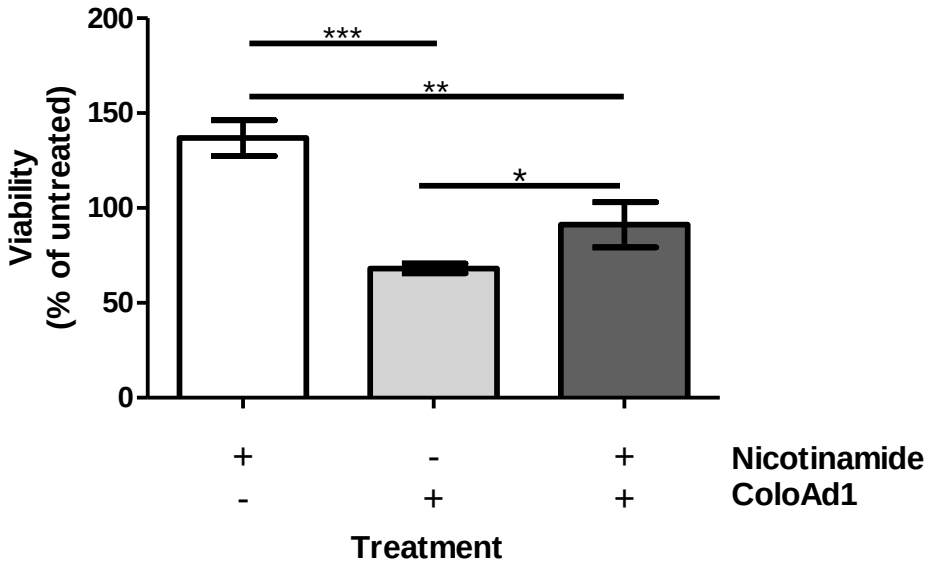

B: 48 hours after infection

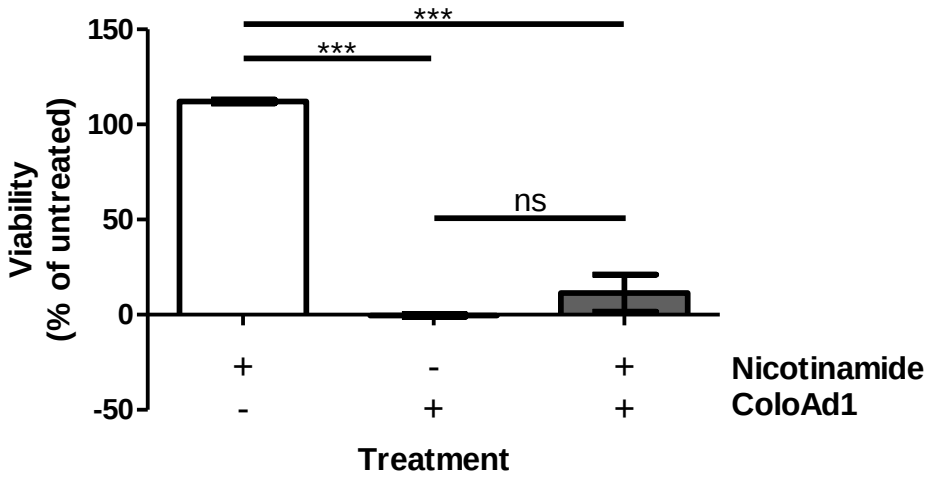

Figure 5-9: Effect of nicotinamide on ColoAd1 infected cell viability by MTS

Adherent HEK293 cells were seeded overnight in 96 well plates at 10,000cells/well, before mock infection (-) or infection with ColoAd1 (+) at MOI 1 (520vp/cell) for 3 hours, followed by mock treatment (-) or treatment with nicotinamide (+) to give a final concentration of 1mM. HEK293 cell viability was determined after 24 hours (**A**) or 48 hours (**B**) using the MTS assay (see Materials and Methods) and normalised to the viability of uninfected, untreated cells. Mean of triplicate measurements with standard deviation shown. One-way ANOVA with Tukey's multiple comparison post-test was performed to determine the significance of any effect of nicotinamide on HEK293 cell viability in the absence or presence of ColoAd1, where ns = no significant difference ($P>0.05$), ** = $P<0.01$, and *** = $P<0.0001$.

A: 24 hours after infection

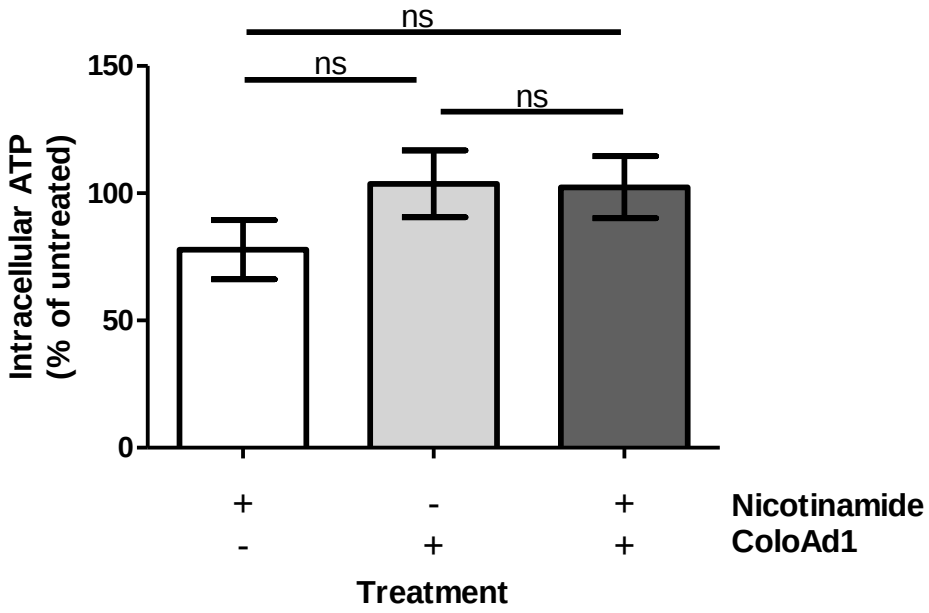

B: 48 hours after infection

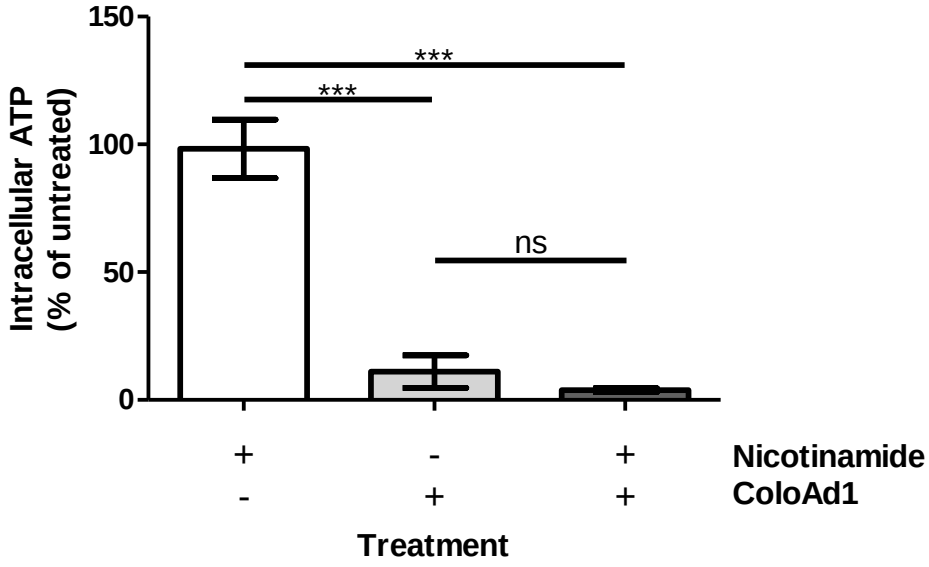

Figure 5-10: Effect of nicotinamide on intracellular ATP of ColoAd1 infected HEK293 cells

Adherent HEK293 cells were seeded overnight in 96 well plates at 10,000cells/well, before mock infection (-) or infection with ColoAd1 (+) at MOI 1 (520vp/cell) for 3 hours, followed by mock treatment (-) treatment with nicotinamide (+) to give a final concentration of 1mM. Intracellular ATP was determined after 24 hours (**A**) and 48 hours (**B**) using the ATP assay (see Materials and Methods) and normalised to mock infected, mock treated HEK293 cells. Mean of triplicate measurements with standard deviation shown. One-way ANOVA with Tukey's multiple comparison post-test was performed to determine the significance of any effect of nicotinamide on intracellular ATP of ColoAd1 infected HEK293 cells, where ns = no significant difference ($P>0.05$) and *** = $P<0.0001$.

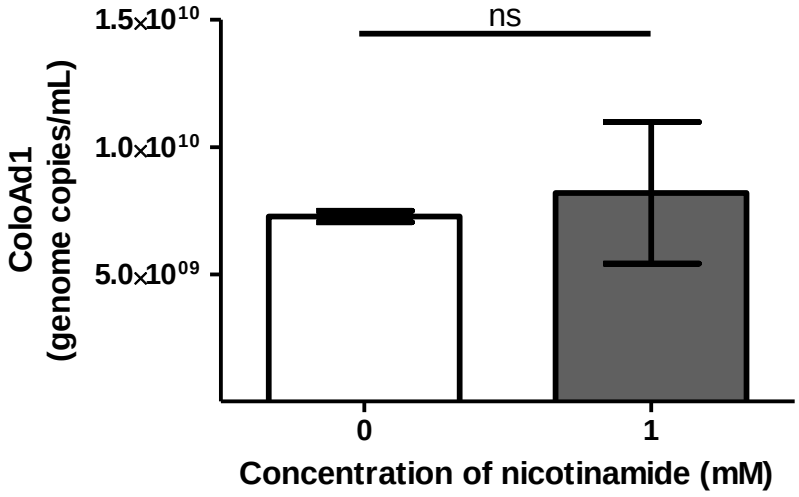

Figure 5-11: Effect of nicotinamide on ColoAd1 genome yield 48 hours after infection

Adherent HEK293 cells were seeded overnight in 96 well plates at 10,000cells/well, before infection with ColoAd1 for 3 hours, followed by mock treatment or treatment with nicotinamide to give a final concentration of 1mM. Then 48 hours after infection, cells and supernatant were collected and stored at -80°C before DNA extraction and QPCR to determine genome copy number expressed per mL of culture volume (see Materials and Methods). Mean of triplicate measurements with standard deviation shown. Unpaired students T-Test was performed to determine the significance of any effect of nicotinamide on ColoAd1 genome yield, where ns = no significant difference ($P>0.05$).

5.3.5 Effect of N-Acetyl L-Cysteine on ColoAd1 infected HEK293 cells

N-acetyl L-cysteine (NAC) has been shown to enhance Ad5 productivity from suspension HEK293 cells [191], although the exact mechanism was not examined. NAC is an aminothiol that acts as an anti-oxidant once it has been converted to cysteine and glutathione (GSH) within the cytoplasm of the cell. The main intracellular stores of GSH are in the nucleus, endoplasmic reticulum and mitochondria where it exists in different oxidised or reduced form depending on its function [192]. The main source of intracellular reactive oxygen species (ROS) is by superoxide leakage from complex I, II and III of the electron transport chain and some of these superoxides are mopped up by mitochondrial GSH [192]. Recently, the more cell permeable form of NAC, N-acetyl L-cysteine amide (NACA), was found to prevent ROS induced apoptosis and enhance oncolytic adenovirus progeny production in neural stem cells [193]. Therefore, the effect of NAC on ColoAd1 replication was investigated.

NAC significantly increased the viability of ColoAd1 infected HEK293 cells after 48 hours compared to mock treated ColoAd1 infected HEK293 cells (Figure 5-12). Surprisingly, NAC also significantly decreased ColoAd1 genome yield from HEK293 cells (Figure 5-13). However, given that there was only a 2-fold reduction in genome yield with a 10-fold enhancement of cell viability by MTS, this pharmacological intervention may show enhanced yield beyond 48 hours. In addition, CPE appeared delayed in ColoAd1 infected HEK293 cells treated with NAC compared to without (data not shown) suggesting a delay in replication kinetics of ColoAd1 in the presence of NAC.

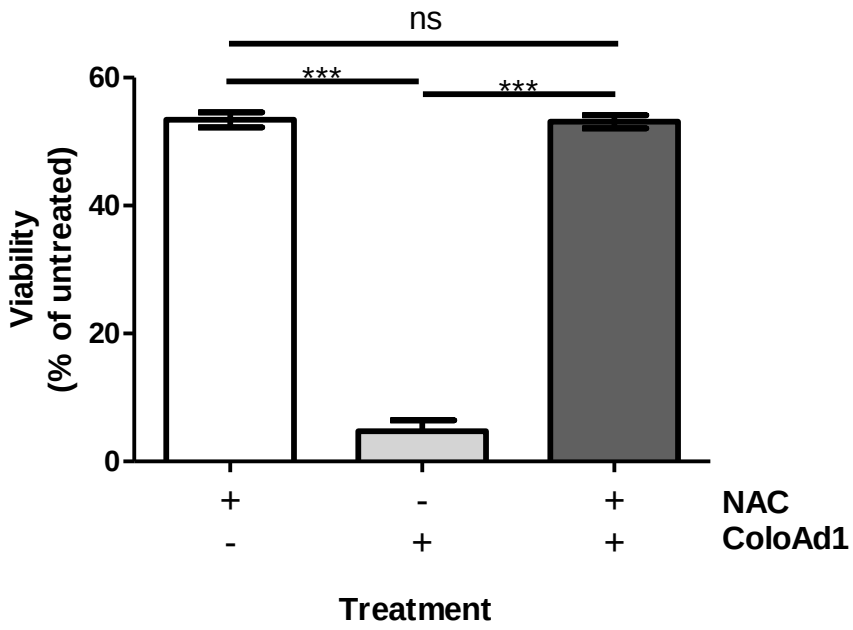

Figure 5-12: Effect of NAC on HEK293 cell viability after 48 hours with and without ColoAd1

Adherent HEK293 cells were seeded overnight in 96 well plates at 10,000cells/well, before mock infection (-) or infection with ColoAd1 (+) at MOI 1 (520vp/cell) for 3 hours, followed by mock treatment (-) or treatment with N-acetyl L-cysteine (NAC) to give a final concentration of 1mM (+). HEK293 cell viability was determined 48 hours after infection using the MTS assay (see Materials and Methods) and normalised to mock infected, mock treated HEK293 cells. Mean of triplicate measurements with standard deviation shown. One-way ANOVA with Tukey's multiple comparison post-test was performed to determine the significance of any effect of NAC on ColoAd1 infected HEK293 cell viability, where ns = no significant difference ($P>0.05$) and *** = $P<0.0001$.

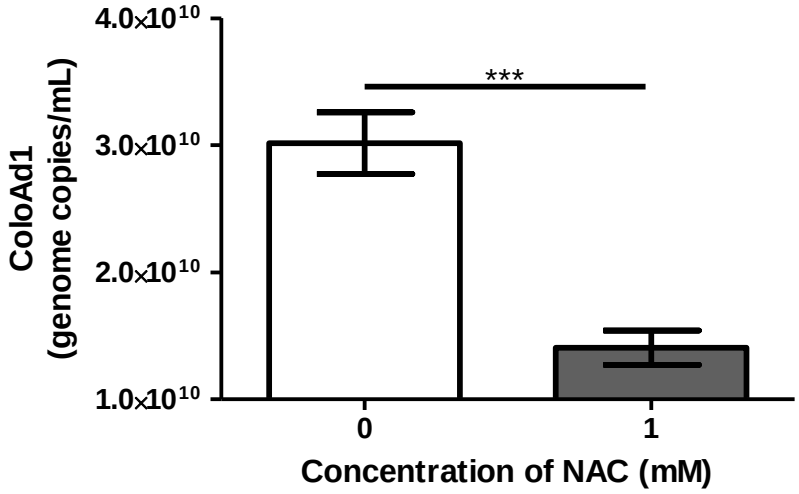

Figure 5-13: Effect of NAC on ColoAd1 genome yield from HEK293 cells after 48 hours

Adherent HEK293 cells were seeded overnight in 96 well plates at 10,000cells/well, before infection with ColoAd1 for 3 hours, followed by treatment with N-acetyl L-cysteine (NAC) to give a final concentration of 1mM. Then 48 hours after infection, cells and supernatant were collected and stored at -80°C before DNA extraction and QPCR to determine total genome copy number expressed per mL of culture volume (see Materials and Methods). Mean of triplicate measurements with standard deviation shown. Unpaired T-Test was performed to determine the significance of any effect of NAC on ColoAd1 genome yield, where ns = no significant difference ($P>0.05$) and *** = $P<0.0001$.

5.3.6 Effect of calcium chloride on ColoAd1 infected HEK293 suspension cells

Other groups have observed that calcium chloride increases the yield of Ad5, especially at high cell densities in HEK293 suspension cell culture [136]. Calcium chloride has also been shown to improve CMV infectivity [194]. Calcium chloride is often removed from the culture media as a means of preventing suspension cell aggregation [195]. Therefore, these studies were performed in HEK293 suspension cells. Calcium chloride added to suspension HEK293 cells at a final concentration of 1mM significantly increased the yield of ColoAd1 genomes but not the yield of infectious particles associated with the supernatant of the suspension cell culture (Figure 5-15) but not the cells (Figure 5-14), without significantly changing suspension HEK293 cell viability (Figure 5-16). The reason for this is unclear. It is possible that extracellular calcium chloride could change intracellular calcium signalling pathways or change the amount of intracellular calcium stored.

A: ColoAd1 genome copies from the cells

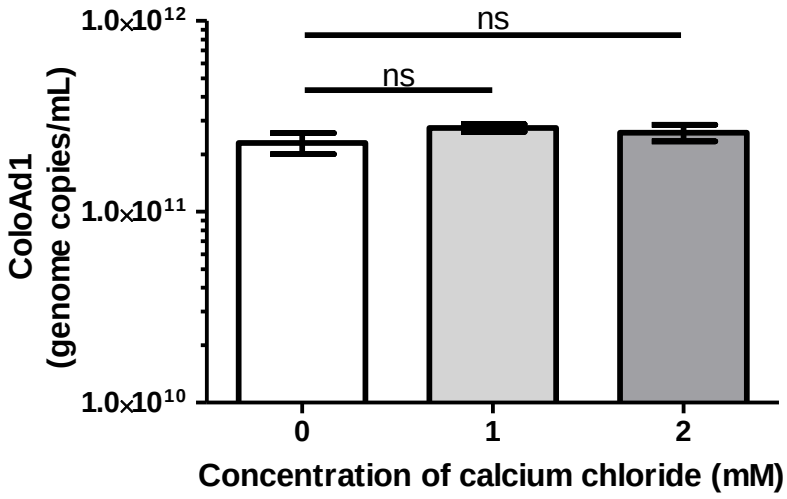

B: ColoAd1 infectious particles from the cells

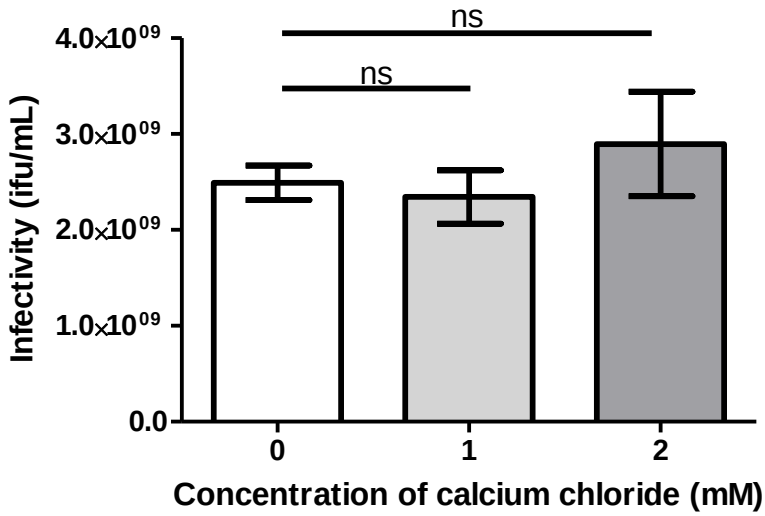

Figure 5-14: Effect of calcium chloride on ColoAd1 yield from HEK293 suspension cells

Suspension HEK293 cells were infected at 2 x 10^6cells/mL at MOI 10 (5200vp/cell) for 2 hours in 125mL Erylemeyer shake flasks in triplicate, before adding CD293 media or CD293 media containing calcium chloride to give a final concentration of 1mM or 2mM at a cell density of 1 x 10^6 cells/mL. Cells and supernatant were collected 33 hours after infection and separated by centrifugation. From the cells, ColoAd1 genome copies (**A**) were determined by QPCR and infectious particles (**B**) determined by hexon staining (see Materials and Methods). Mean of triplicate measurements with standard deviation shown. One-way ANOVA with Tukey's multiple comparison post-test was performed to determine the significance of any effect of calcium chloride on ColoAd1 yield, where ns = no significant difference ($P>0.05$).

A: ColoAd1 genome copies from the supernatant

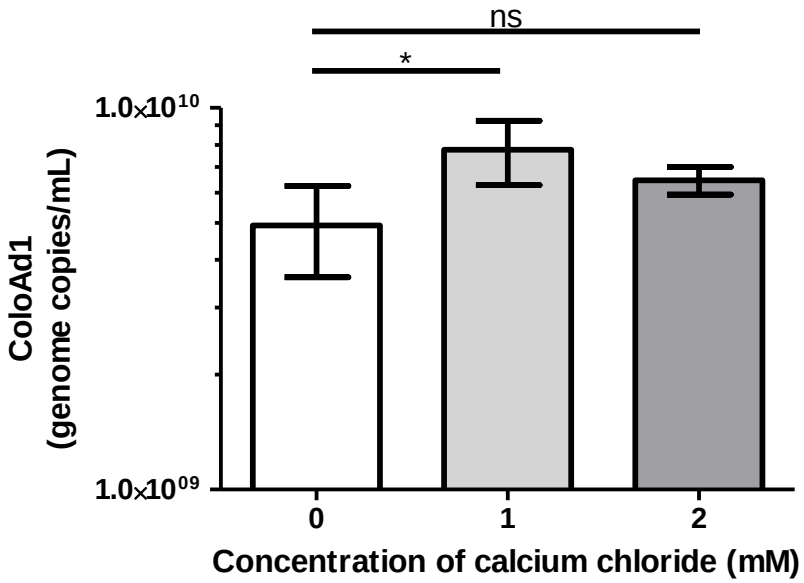

B: ColoAd1 infectious particles from the supernatant

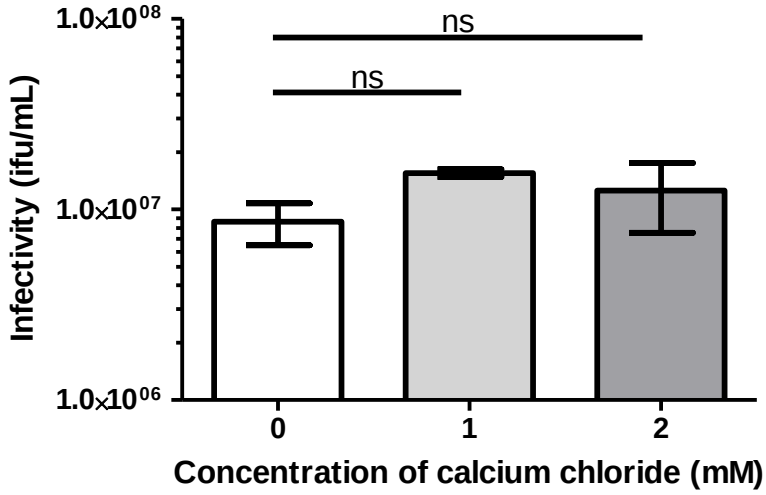

Figure 5-15: Effect of calcium chloride on ColoAd1 yield from the supernatant of infected suspension HEK293 cells

Suspension HEK293 cells were infected at 2 x 10^6cells/mL at MOI 10 (5200vp/cell) for 2 hours in 125mL Erylemeyer shake flasks in triplicate, before adding CD293 media containing calcium chloride to give a final concentration of 1mM or 2mM with a cell density of 1 x 10^6 cells/mL. Cells and supernatant were collected 33 hours after infection and separated by centrifugation. From the supernatant, ColoAd1 genome copies (**A**) were determined by QPCR and infectious particles (**B**) determined by hexon staining (see Materials and Methods). Mean of triplicate measurements with standard deviation shown. One-way ANOVA with Tukey's multiple comparison post-test was performed to determine the significance of any effect of calcium chloride on ColoAd1 yield, where ns = no significant difference ($P>0.05$) and * = $P<0.05$.

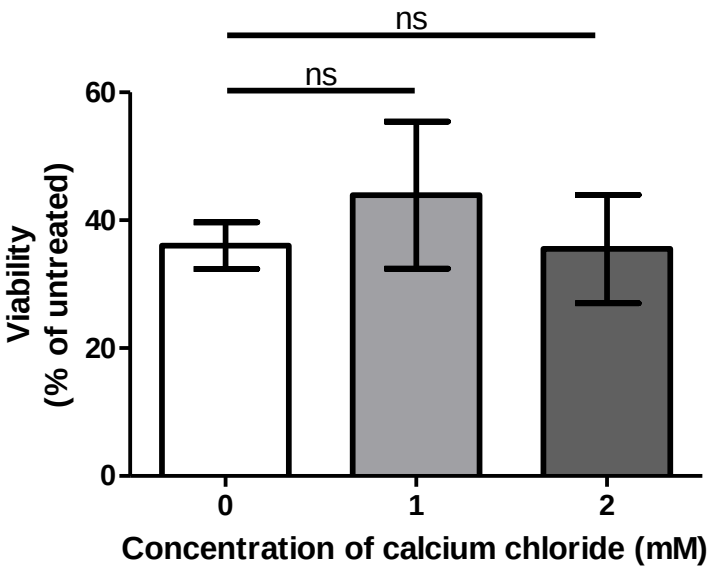

Figure 5-16: Effect of calcium chloride on suspension HEK293 cell viability by MTS 33 hours after infection with ColoAd1

Suspension HEK293 cells were infected at 2 x 10^6cells/mL at MOI 10 (5200vp/cell) for 2 hours in 125mL Erlenmeyer shake flasks in triplicate, before adding CD293 media containing calcium chloride to give a final concentration of 1 or 2mM with a cell density of 1 x 10^6 cells/mL. Cells and supernatant were collected 33 hours after infection and separated by centrifugation. The cells were incubated with MTS reagent and cell viability normalised to uninfected, untreated suspension HEK293 cells. One-way ANOVA with Tukey's multiple comparison post-test was performed to determine the significance of any effect of calcium chloride on ColoAd1 infected suspension HEK293 cell viability, where ns = no significant difference ($P>0.05$).

5.4 Discussion

The metabolic requirements of adenovirus producing cells are likely to vary at different stages of the virus life cycle. Accordingly, the effects of the pharmacological interventions proposed here are perhaps best considered in distinct phases of viral replication. It may also be important to consider the timing of the addition of these agents to infected cells. First, ColoAd1 genome replication appears to require glycolysis for enhanced yield. Perhaps agents that enhance the glycolytic rate should be considered 6 - 24 hours after infection when ColoAd1 genome replication is rapid (Figure 3-5). Alternatively, perhaps the cells should be pre-conditioned for optimum glycolysis before infection. Previous studies have pre-conditioned cells in galactose media for 15 passages, which is much longer than the 24 hours pre-conditioning performed in these studies [196].

Inhibition of LDH with sodium oxamate increased the viability of ColoAd1 infected HEK293 cells, suggesting that the accumulation of metabolic waste products, particularly lactate, was detrimental to infected HEK293 cell viability. In support of this, increased glucose consumption and lactate production rates are observed after infection of HEK293 cells with adenoviral vectors [137]. Further, metabolic flux analysis of HEK293 suspension cell cultures have shown that cell productivity is linked to the metabolic state of cells [138]. To circumvent the accumulation of detrimental metabolic waste products and maintain cells in an optimal metabolically active state, cell cultures are continuously perfused in large scale bioreactors [197].

The use of NAC suggested that infected HEK293 cell viability can be rescued with the use of anti-oxidants. Mitochondria are the main source of intracellular, in particular reactive oxygen species (ROS). There is evidence that other viruses increase ROS, presumably to benefit viral replication. HCV expresses a core protein that inhibits mitochondrial electron transport and increases ROS [198]. Determining the effect of NAC on Ad11p infected cell viability may elucidate if ROS was induced specifically by ColoAd1 and a further comparison of the response to Ad5 would be interesting, especially given that Ad5 based adenoviral vector yield increased in the presence of NAC but effects on cell viability were not reported [191].

In this chapter, DCA had no significant effect on ColoAd1 infected HEK293 cell viability or ColoAd1 genome yield, although there was a trend where 0.01mM - 0.1mM DCA increased ColoAd1 genome yield compared to the untreated control and perhaps these concentrations warrant further investigation. In support of this, inhibition of LDH by 0.5mM DCA has been observed in A549 cells and, at this concentration, DCA could selectively inhibit the proliferation of cancer cells without affecting normal cells *in vitro* [199]. The clinical use of DCA as a cancer treatment has also been controversial. DCA was originally approved to treat lactate acidosis and it proved safe and effective [200]. Since then, DCA has been tested in a small set of patients with glioblastoma multiforme but it appeared to have neurotoxicity at higher doses [201]. If DCA enhances ColoAd1 yield then this could also have a clinical impact and perhaps the effect of combining ColoAd1 and DCA in tumour cells, such as A549 or HT29 cells, would be interesting to persue.

In this chapter, it was shown that calcium chloride had significant effects on ColoAd1 genome yield from the supernatant but not the cells. The mechanism for this is unknown. However, the calcium ion, like ROS, is also involved in necrotic cell death. Given that calcium chloride increased the amount of ColoAd1 detected from the supernatant and not the cells, it may indicate more efficient release of viral particles in the presence of calcium. Therefore, perhaps the calcium ion plays an important role in efficient viral particle release. It would also be important to clarify the role of calcium chloride and CAMKK2 activity, on AMPK activation seen in Chapter 4. Perhaps calcium signalling, as opposed to ATP signalling, plays a more important role in ColoAd1 induced cell death.

Overall, there appears to be link between cell viability and the yield of genomes. If viability is rescued then genome yield decreases, and vice versus. This suggests that infected HEK293 cells die when they reach a certain threshold. Whether the infected cell is capable of detecting this threshold and how the cell responds remains to be determined. It is also likely that the Warburg effect plays a role in ColoAd1 genome replication. The enhanced glycolytic rate of cells exhibiting the Warburg effect is likely to enhance ColoAd1 genome replication.

6 Human Kinase Profiling to Identify Kinases That Enhance ColoAd1 Replication

6.1 Introduction

As established in Chapter 4, ColoAd1 manipulates intracellular signalling pathways in different ways to Ad11p. Kinases are critical components of intracellular signalling pathways. Therefore, it is hypothesised that there will be some critical and non-critical kinases required for efficient ColoAd1 replication. The lack of a biomarker for ColoAd1 replication, lead us to consider screening methods to identify the critical kinases required for ColoAd1 replication in HEK293 cells.

The post transcriptional silencing of genes by small interfering RNAs was first discovered in plants [202] and later in cultured mammalian cells [203]. RNA interference (RNAi) occurs naturally as a mechanism of defence against RNA containing viruses, and as a mechanism to selectively knock down the expression of specific genes. Dicer, a multi-domain RNase III-related endonuclease, binds dsRNA and cleaves both strands to form dsRNA fragments that are approximately 21-22 nucleotides in length with an overhang of 2 nucleotides at each 3' end [204]. The strands of these dsRNA fragments are then separated apart by an ATP dependent process, and each strand is subsequently incorporated into the cytoplasmic RNA-induced silencing complex (RISC) containing argonate (ago) proteins [204]. One strand is then cleaved by Ago2 endonuclease and released, with the other strand acting as a template to degrade complementary mRNA sequences [204].

Since then, two main methods of gene silencing have evolved with the use of chemically synthesised double-stranded small interfering RNA (siRNA) or vectors encoding short hairpin RNA (shRNA). siRNA achieves gene silencing by dsRNA fragments directly interacting with the RISC after transfection [205]. shRNA achieves gene silencing by expressing shRNA from lentiviral vectors. Reverse transcription of the RNA containing lentiviral genome in the nucleus produces pre-shRNA that interact with Drosha to produce pre shRNA, which is exported from the nucleus and is processed in the cytoplasm to produce mature shRNA that interacts with RISC [205]. shRNA is often used for permanent efficient gene silencing *in vitro*, however siRNA mediated gene silencing was selected as permanent gene silencing was not required for the initial identification of kinases affecting ColoAd1 replication.

6.2 Aims

- To develop a protocol to screen a library of 720 siRNAs targeting the human kinome.
- To identify kinases that enhance ColoAd1 genome production in HEK293 cells and, conversely, to identify kinases that are required for genome production in HEK293 cells.
- Further, to identify kinases that enhance ColoAd1 genome production and increase HEK293 cell viability.

6.3 Results

6.3.1 Optimisation of siRNA transfection conditions

First, the transfection conditions required to deliver siRNA into HEK293 cells were optimised to ensure that transfection occurred with minimal toxicity and maximal knockdown of the target protein. Two different transfection reagents, Lipofectamine 2000 and Dharmafect-1, were investigated to deliver siRNA targeting β-actin to HEK293 cells and subsequent knockdown of β-actin determined by western blot. Transfection of a non-targeted siRNA with Lipofectamine 2000 was found to be less toxic to HEK293 cells than transfection with Dharmafect-1 (Figure 6-1). Different concentrations of siRNA were tested with different concentrations of transfection reagent to obtain maximal knockdown. It was found that reverse transfection with Lipofectamine 2000 at 0.3μL per reaction, with a final siRNA concentration of 30nM, gave the most effective knock down of β-actin (Figure 6-1). Under these conditions, transfection of the siRNA death control also gave the most effective loss of cell viability (Figure 6-1). Therefore, these conditions defined the protocol for transfection (see Materials and Methods).

A: Cell viability

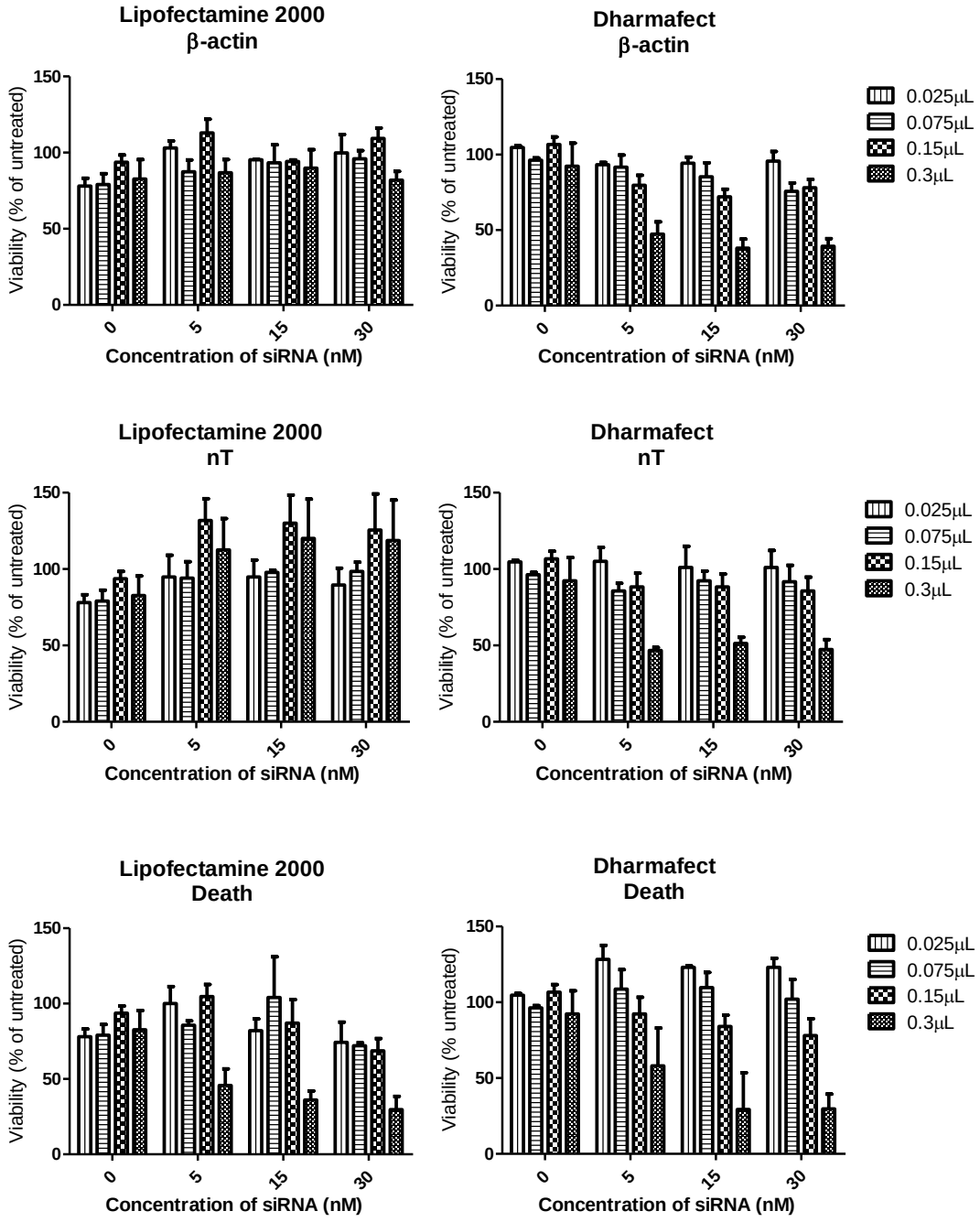

B: Western blot

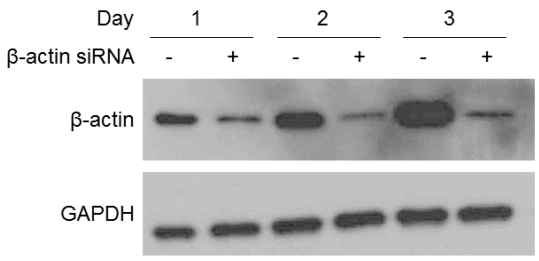

Figure 6-1: Optimisation of transfection conditions

HEK293 cells were reverse transfected at 8000cells/well with Lipofectamine 2000 or Dharmafect-1 transfection reagents at a range of concentrations (0.025 – 0.3µL/well) with siRNAs targeting β-actin, non-targeted or a death siRNA control, at concentrations ranging from 5-30nM. The effect of transfection on cell viability was determined by resazurin assay after 3 days (A) and Western blot (B) confirmed that the transfection of siRNA targeting β-actin using optimal conditions of 0.3µL Lipofectamine 2000 and 30nM siRNA produced a time dependent knockdown of protein.

6.3.2 Identifying positive control for screen

To identify a positive control for the screen, data was reviewed from a screen that had been performed in our laboratory (Dr Clemens Thoma) where the aim of that screen was to identify siRNA targets that enhanced the viability of adenovirus infected ovarian cancer cells. The hits from that screen were compared to a screen performed in HEK293 cells [206]. This approach identified seven siRNA targets as potential positive controls for this screen. These siRNAs were tested; however, they did not enhance ColoAd1 genome yield compared to the infected cells treated with non-targeted siRNA (Figure 6-2). However, the positive control simply produces the effect desired from the screen hits and the screen would not be required if hits were already known. Therefore, the screen was performed as a preliminary development screen, without a positive control.

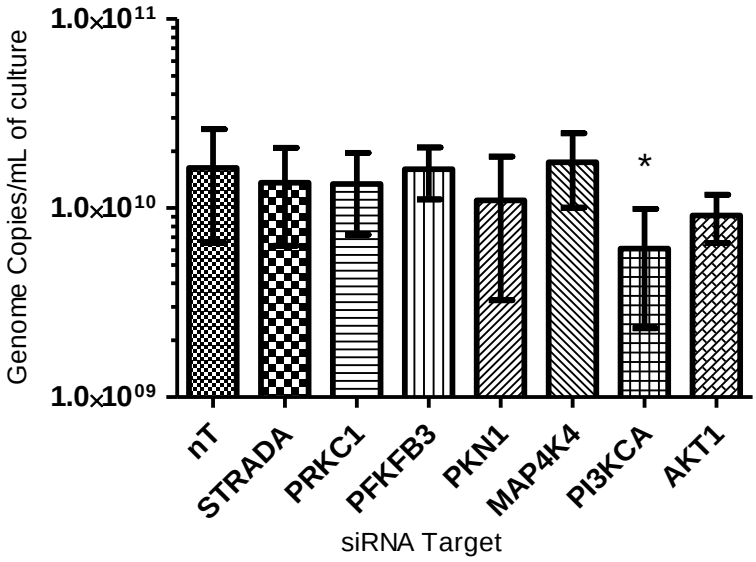

Figure 6-2: Identifying positive controls for the screen

HEK293 cells were reverse transfected with siRNA or non-targeted siRNA (nT) for 3 days according to the optimised protocol (see Materials and Methods) before infection at 520vp/cell with ColoAd1.After 48 hours, cells and supernatant were stored at -80°C before extraction of viral DNA and quantification by QPCR. N=3 independent experiments. One way ANOVA was performed with Dunnet's post-test to compare the significance of the differences between the non-targeted siRNA and the test siRNA. * = P <0.05.

6.3.3 Normalisation to cell number at infection

The aim of the screen was to identify targets that would enhance ColoAd1 total genome yield per cell. Therefore, different methods of quantitating cell number were considered. As the primary readout for the screen was QPCR for viral genome copies, multiplexed QPCR was considered to determine viral genomes and host cell DNA in a single reaction. The TOP3 gene was identified as a target for host cell DNA quantification that was compatible with ColoAd1 primers and probes. After optimising the primer and probe concentrations for TOP3A in combination with ColoAd1 primer and probes, it was found that, as TOP3A was a low copy number gene, it was difficult to obtain a linear correlation between cell number as determined by counting and multiplexed QPCR. Instead, it was decided to determine cell number using the resazurin assay to determine cell viability relative to untreated cells.

6.3.4 Screen

The workflow for the screen is shown in Figure 6-3. Initially, the average CT values of duplicate measurements determined by QCPR were plotted to show the range in the data (Figure 6-4) and siRNA targets below the threshold CT of 17.33 indicated targets that may have enhanced ColoAd1 genome replication (Table 6-1). However, this analysis does not account for systematic error or inherent plate to plate variability, and makes it impossible to determine whether reduced CT values were significantly different from the CT of the non-targeted control. In addition, the 5 fold range of CT values was a concern but, again, could have represented plate to plate variability. Therefore, a more sophisticated analysis was sought. Many screens use the Z-score to normalise each data point to the non-targeted control on each plate or to the mean of each value on the plate [207]. The advantage of this method is that it removes systematic error so that data from different plates in the screen can be compared. The Z-score gives each siRNA a score of how far that value deviates from the mean of the plate, which makes it sensitive to outliers but the robust Z-score can overcome sensitivity to outliers by using the median instead of the mean should this be a problem.

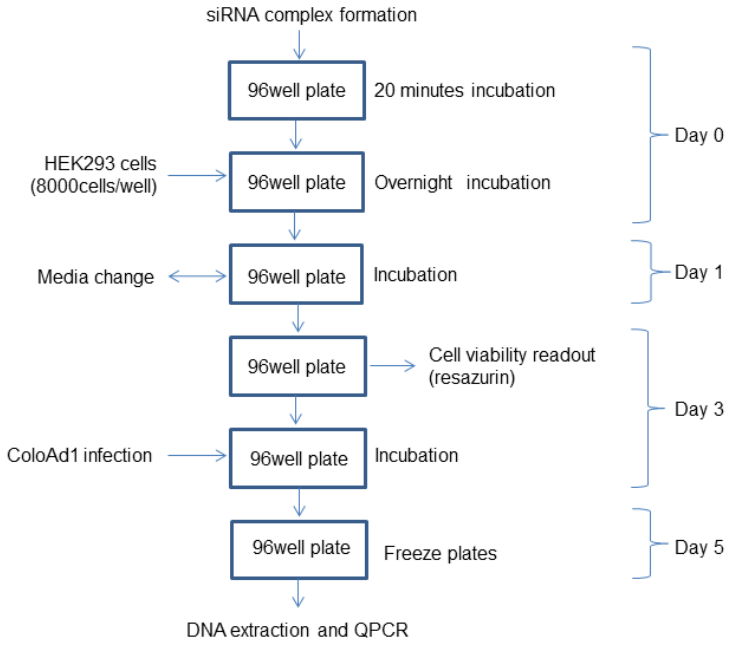

Figure 6-3: Workflow for screen

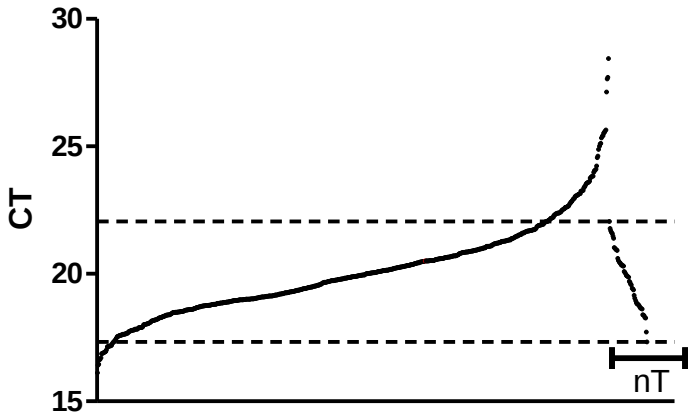

Figure 6-4: CT values determined by QPCR

The CT value of each well was determined by QPCR (see Materials and Methods) and the average CT from duplicate plates calculated before ordering. The dotted lines represent the highest and lowest CT values of ColoAd1 replication in cells transfected with the non-targeted siRNA. The individual CT values of replication in cells transfected with the non-targeted siRNA control are indicated (nT). CT values above and below these thresholds represent fewer and more genomes than the non-targeted control.

siRNA target (Gene symbol)	siRNA Target (name)	Gene ID	CT	Function of gene product
NEK1	NIMA-related kinase 1	4750	16.96	Cell cycle control DNA damage response
RP6-213H19.1	serine/threonine protein kinase 26	51765	16.94	Apoptosis
ILK	integrin-linked kinase	3611	16.94	Regulates integrin signalling
CALM2	calmodulin 2 (phosphorylase kinase, delta)	805	16.91	Calcium/calmodulin signalling
RIOK3	RIO kinase 3	8780	16.90	Ser/Thr kinase involved in spindle microtubles
EPHB4	EPH receptor B4	2050	16.88	Ephrin receptor
NTRK1	neurotrophic tyrosine kinase, receptor, type 1	4914	16.87	MAPK signalling
NME4	NME/NM23 nucleoside diphosphate kinase	4833	16.7	Catalyzes transfer of γ-phosphates, between nucleoside and dioxynucleoside tri- anddi-phosphates
PFKM	Phosphofructoskinase, muscle	5213	16.65	Subunit of the phosphofructokinase, which catalyzes the phosphorylation of fructose-6-phosphate to fructose-1,6-bisphosphate
CDK3	Cyclin-dependent kinase 3	1018	16.64	S-phase entry
TSKS	Testis-specific serine kinase substrate	60385	16.46	RAS and interferon signalling

Table 6-1: siRNA targets below the threshold CT of the non-targeted control

siRNA targets with average CT values less than 17 were identified from Figure 6-4 and function assigned using the Pubmed gene database (http://www.ncbi.nlm.nih.gov/gene).

6.3.5 Z-score analysis of replication

The first consideration was whether to normalise each value on the plate to the mean of the non-targeted siRNA or the mean of the plate. Normalising to the mean of the non-targeted siRNA is advantageous as this was the biological effect that needed to be compared to. However, the power of the statistical method is greater when using the mean of the plate because the n-number of the plate is greater than the n-number of the non-targeted control on each plate. Normalising to the mean of the plate does assume that the data is normally distributed.

Each replicate plate was normalised separately and targets greater than 2 standard deviations below the mean from each replicate identified (Table 6-2). Only one siRNA target, NTRK1, identified in Table 6-1 was also identified in Table 6-2. In addition, Z score analysis of individual replicates highlighted the fact that a hit identified in replicate 1 did not necessarily produce a hit in replicate 2. Therefore, a method was sought that would prioritise hits that were reproducible between duplicate measurements.

siRNA target (Gene Symbol)	siRNA target (Gene name)	Gene ID	Replicate	Function of gene product
STK32A	serine/threonine kinase 32A	202374	1	Unknown
CDK11	cyclin-dependent kinase 19	23097	1	Component of Mediator co-activator complex, required for activation of transcription
STYK1	serine/threonine/tyrosine kinase 1	55359	1	Cell proliferation, differentiation and survival
CDC2	cyclin-dependent kinase 1	983	1	M-phase promoting factor (MPF) required for G1/S and G2/M phase transition
NTRK1	neurotrophic tyrosine kinase, receptor, type 1	4914	2	MAPK signalling leading to differentiation
DLG3	discs, large homolog 3 (Drosophila)	1741	2	Negatively regulates cell proliferation
RPS6KL1	ribosomal protein S6 kinase-like 1	83694	2	Unknown
MAPKAPK5	mitogen-activated protein kinase-activated protein kinase 5	8550	2	Cellular stress response
ILK	integrin-linked kinase	3611	2	Integrin signalling
STK38L	serine/threonine kinase 38 like	23012	2	Insulin signalling and cell cycle progression
DCK	deoxycytidine kinase	1633	2	Deoxyribonucleoside phosphorylation
PKLR	pyruvate kinase, liver and RBC	5313	2	Glycolysis
MYO3A	myosin IIIA	53904	2	Actin bundling in sensory cells

Table 6-2: siRNA targets with CT values greater than 2 standard deviations below the mean

siRNA targets with Z scores less than -2 were identified from each replicate and function assigned using the Pubmed gene database (http://www.ncbi.nlm.nih.gov/gene).

6.3.6 Z-score and rank product analysis of replication per cell

Ultimately, although hits that increased viral replication were interesting, the identification of hits that increased genome replication per cell was ideal. Therefore, the cell viability at infection (as determined by resazurin assay) was used to normalise viral genomes. In addition, a method that accounted for the variability between replicates was sought to identify hits that reproducibly had the same effect on viral replication per cell. Therefore, the Rank Product analysis (see Materials and Methods) was used to identify hits that produced the lowest ratio (viral CT/cell) consistently between duplicates as a low CT value indicated a high viral genome yield.

The hits from Table 6-3 were confirmed to have CT values lower than the CT value of the non-targeted siRNA on that plate and cell viability greater than that of the non-targeted siRNA on that plate. It is interesting that four of these hits are involved in calcium signalling, given the conclusions made from the results in Chapter 4, where calcium chloride increased ColoAd1 genome yield.

siRNA target (Gene symbol)	siRNA target (Gene name)	Gene ID	Function of gene product	Calcium signalling implicated	Inhibitor of gene product
SGK	serum/glucocorticoid regulated kinase 1	6446	Cellular stress response [208]	Yes [208]	[209]
BAIAP1	membrane associated guanylate kinase	9223	Scaffolding protein at cell-cell junctions [210]	No	[211, 212]
STK17B	serine/threonine kinase 17b	9262	TGF-β signalling [213, 214]	Yes [215]	N/A
CSNK1D	casein kinase 1, delta	1453	Regulation of apoptosis, microtubule dynamics, chromosome segregation and DNA repair [216, 217]	No	[218]
NPR2	natriuretic peptide receptor 2	4882	Guanylyl cyclase activation upon ligand binding [219]	No	[220]
FASTK	Fas-activated serine/threonine kinase	10922	Fas-mediated apoptosis and alternative splicing regulation [221, 222]	Yes [223]	N/A
BCR	breakpoint cluster region	613	GTPase-activating protein for p21rac [224]	No	N/A
DAPK1	death-associated protein kinase 1	1612	Calmodulin dependent serine-theronine kinase mediating γ-interferon induced cell death [225]	Yes [226]	[227]

Table 6-3: Highest ranking siRNA targets with the lowest ratio of CT/cell

For each well of each plate, the CT value representing viral replication was divided by the cell viability at infection (viral CT/cell). The ratio of each well (viral CT/cell) was compared to average ratio of each plate by applying a Z score analysis. Then the Z score of each well was ranked as a product of the ratios from duplicate wells. The highest ranking products with the lowest ratio of CT/cell and the siRNA targets of those wells identified, with the function of the siRNA targets assigned using the Pubmed gene database (http://www.ncbi.nlm.nih.gov/gene).

6.4 Discussion

Many of the highest ranking siRNA targets that enhanced HEK293 cell viability and ColoAd1 genome yield, compared to the non-targeted siRNA control, were involved in calcium signalling (Table 6-3). The role of calcium in enhancing ColoAd1 genome replication remains interesting, considering that in Chapter 5 it was observed that calcium chloride enhanced ColoAd1 genome yield. Perhaps the addition of calcium chloride to suspension cell cultures modulated intracellular calcium signalling pathways to increase ColoAd1 yield from HEK293 cells. Interestingly, calcium signalling is most well studied in neuronal cells and it has been noted that HEK293 cells are neuronal like [228]. Therefore, HEK293 cells may be more susceptible to changes in intracellular calcium signalling pathways than other cell types.

The siRNA target that caused the most significant and consistent increase in ColoAd1 genomes per cell, compared to the non-targeted control, was *SGK*. In epithelial cells, SGK plays a role in ion transport [229]. Here, knockdown of *SGK* needs to be validated but if proven then perhaps *SGK* knockdown prevents activation of the cellular stress response. This suggests that the SGK mediated cellular stress response normally limits ColoAd1 yield from HEK293 cells. Interestingly, *SGK* gene expression is activated by store operated mitochondrial calcium signalling [208] and the results from Chapter 4 suggested that CaMKK2 was activated in ColoAd1 infected HEK293 cells.

Another siRNA target that had a significant and consistent effect on increasing ColoAd1 genomes per cell was DAPK. This target also remains interesting in the context of the results from Chapter 4. The site that DAPK phosphorylates on CaMMK2

is Ser511 [160]. In Chapter 4, it was observed that Ser511 phosphorylation was reduced in ColoAd1 infected HEK293 cells compared to Ad11p and uninfected cells (section 4.3.2). DAPK activity is negatively regulated by autophosphorylation of Ser308, which is located within the calcium/calmodulin regulatory domain of DAPK [230]. Therefore, phosphorylation of Ser308 inactivates DAPK. However, PP2A also dephosphorylates Ser308, which facilitates calcium/calmodulin induced DAPK activation [231]. Given that E4orf4 interacts with PP2A, it is possible that the difference in DAPK induced phosphorylation of CaMKK2 may be mediated by the presence and absence of E4orf4 in ColoAd1 and Ad11p respectively. Further studies are warranted to address this hypothesis.

Furthermore, the role of CaMKK2 would be interesting to determine, given that SGK expression is regulated by store-operated calcium entry [208] and given that AMPKα is phosphorylated and activated by CaMKK2 [159]. In chapter 4, it was observed AMPKα phosphorylation and activation earlier in ColoAd1 infected HEK293 cells compared to Ad11p (section 4.3.2). There are two kinases upstream of AMPKα, LKB1 and CaMKK2, that could be responsible for AMPKα activation in HEK293 cells. Therefore, CaMKK2 mediated AMPKα phosphorylation and activation may be better observed in an LKB1 negative cell line, such as A549s, to ensure AMPKα activation by CaMKK2 alone.

Results from this screen suggest that inhibition of calcium signalling is an important mechanism of enhancing HEK293 cell viability and ColoAd1 genome yield. Inhibitors of the targets identified in Table 6-3 have been identified from the literature and future

work could focus on using these inhibitors in HEK293 suspension cell cultures to increase ColoAd1 yield. Some of the targets also act in the same signalling pathway as already addressed in Chapter 4 and combining inhibitors may provide even greater increases in yield.

7 Discussion

During the course of this project oncolytic viruses have continued to progress through early and late stage clinical trials. The herpes based oncolytic virus T-VEC met its primary phase III trial endpoint and is likely to be approved in the future. Meanwhile ColoAd1 (now named Enadnotucirev) has completed the recruitment of a phase 1 safety study and two further studies have been initiated. The increased interest in this area will heighten demand on production of clinical grade material. For systemically administered viruses the demand is likely to be particularly high due to the numbers of viruses required to saturate clearance mechanisms and break through neutralising antibodies [232]. To date, ColoAd1 has proved safe by intravenous delivery of up to 6 x 10^{12}vp/dose. This is consistent with the dose achieved by intravenous administration of the Ad5 based oncolytic, GC7870 [57].

Currently, processes used to manufacture oncolytic adenoviruses are limited to batches due to the lytic replication lifecycle. This inherently limits the window of time when adenovirus can be produced. Therefore, increasing the yield from each batch remains an attractive strategy to meet clinical demand for adenovirus products. In addition, a large proportion of adenovirus produced from a batch is required for release testing [125]. Increasing yield per batch thus increases the amount of product available for clinical use. Many manufacturing processes published to date have also been based on the replication life cycle of Ad5, partly due to popular use of Ad5 for gene therapy and vaccine applications. Indeed, as of January 2014, 23.4% (n=478) of vectors used in gene therapy clinical trials were adenovirus (reference wiley.com), highlighting the requirement for high titre (10^{12} - 10^{13} viral particles/patient) clinical grade adenovirus for gene therapy purposes alone. However, the use of group B adenoviruses for such applications is also likely to

increase in the future as a strategy to circumvent antibody mediated neutralisation that limits the efficacy of Ad5 vectors *in vivo* [233]. Therefore, the main aim of this thesis was to identify methods and agents that could increase group B adenovirus yield from a batch manufacturing process.

This thesis focused on the group B oncolytic adenovirus, ColoAd1, to determine whether its inherent oncolytic capacity limited its yield during manufacture. Two approaches were taken to address this. In the first approach, biological differences observed between ColoAd1 and its wild type parental virus, Ad11p, were investigated. In the second approach, screening was used to identify factors limiting ColoAd1 yield from the manufacturing cell line, HEK293. During the course of this work new insights were gained into the cellular requirements for virus replication that may impact manufacturing processes but could also impart basic virology knowledge for the future development of oncolytic viruses, or identify targets for the development of anti-viral therapeutics.

7.1 Main findings

Overall, this thesis shows that ColoAd1 can replicate and produce particles from the HEK293 cell line to achieve adequate yield. The question of whether yield can be further increased from the HEK293 cell line by manipulating host cell signalling pathways, such as the AMPK/mTORC1 signalling pathway, or by manipulating host cell metabolism, has also been addressed. Table 7-1 summarises the main findings from the interventions used in this thesis to manipulate these cellular pathways.

Intervention	Result	Implication of intervention on bioprocess	GMP compliant intervention	Future work
Suspension HEK293 cells	-Slightly reduced DSG-2 receptor expression compared to adherent HEK293 cells -Yield similar to yield from adherent HEK293 cells	-Scalable cell culture process -Serum free cell culture medium	Yes	Determine optimal process conditions for suspension cell culture at larger scale (>1L)
Metformin	-Enhanced potency -Activation of AMPK in presence of ColoAd1 but not Ad11p	-Early virus induced cell death -Activate AMPK	Yes	Effect on yield not determined
Compound C	-No inhibition of ColoAd1 induced AMPK activation	-Not possible to manipulate cellular energy sensor during viral replication	N/A	N/A
Sodium oxamate	-Enhanced infected cell viability after 24 hours but not 48 hours -No effect on yield	-Inhibition of lactate dehydrogenase -Prevent lactate accumulation	Yes	Combine with DCA to enhance carbon flux into TCA cycle
DCA	-Enhanced infected cell viability after 24 hours but not 48 hours -Trend towards increased ColoAd1 genome yield	-Inhibition of PDK -Increased metabolism by oxidative phosphorylation	Yes	Combine with sodium oxamate
Nicotinamide	-Enhanced infected cell viability -No effect on yield	-Maintain NAD+ supply for glycolysis	Yes	Combine with agents that enhance glycolysis
Glycolysis	-Reduced yield when metabolism relies on glycolysis	-Maintain high glycolytic flux for enhanced yield	Yes	Combine with nicotinamide
NAC	-Enhanced infected cell viability after 48 hours -Reduced yield	-Extend harvest time	Yes	Combine with sodium oxamate and DCA
Calcium chloride	-Enhanced yield from supernatant	-Purify virus from supernatant to capture virus	Yes	Determine how calcium chloride affects capture of ColoAd1 from supernatant.

Figure 7-1 A table to show the main findings from the interventions used in this thesis

The interventions described were used with the aim of enhancing ColoAd1 yield from HEK293 cells. The result of each intervention is summarised and the implication that this would have on a future process used to manufacture ColoAd1 described.

7.1.1 ColoAd1 replication

The difference in the sensitivity of HEK293 cells to ColoAd1 and Ad11p was found to be due to intracellular factors after virus uptake. The cellular uptake of ColoAd1 was the same as Ad11p on HEK293 cells and differences in replication arose intracellularly, especially during the late phase of infection. ColoAd1 produced more genomes earlier, expressed hexon protein earlier and released particles earlier than Ad11p. Ultimately this means that the harvest time used for the manufacture of ColoAd1 would be earlier than wild-type Ad11p and Ad5, especially if harvesting only the cell fraction for downstream purification. ColoAd1 harvest time identified in these studies was MOI dependent. This contrasts to Ad5 infection, where yield is known to be MOI dependent up to MOI 5, after which MOI becomes independent [234].

At MOI 1, the cellular release of ColoAd1 into the supernatant was observed between 33 and 48 hours. During manufacture, harvesting virus from the supernatant would require ColoAd1 to be thermally stable. Adenovirus is widely accepted as being thermally stable. In addition, the thermal stability of Ad11p has been compared to Ad5 and shown to be stable at 37°C for up to 30 minutes, with the stability of Ad11p also being similar to Ad5 at 48°C [235]. Further, Ad11p shows extended stability at 37°C for up to 8 weeks [236]. Therefore, it may be possible to harvest productive ColoAd1 particles from the supernatant for downstream processing. In contrast, enveloped viruses are known to be less thermally stable. For example, the stability of oncolytic measles virus is a particular problem during processing [237].

It is not surprising that the uptake of ColoAd1 and Ad11p was the same on HEK293 cells. Group B adenoviruses are known to bind both CD46 and DSG-2 for cellular uptake [102, 103]. Both adherent and suspension HEK293 cells highly expressed the uptake receptors for group B adenovirus, CD46 and DSG-2, as well as the group C adenovirus receptors, CAR and αv-integrin. This suggested that group B adenoviruses could attach to HEK293 cells. However, suspension HEK293 cells expressed slightly lower levels of DSG-2 than adherent HEK293 cells. The impact of this on ColoAd1 production in HEK293 suspension cells has not been determined in this thesis. The degree to which group B adenoviruses access and use CD46 and/or DSG-2 for infection also remains controversial [238]. It has been shown with another group B adenovirus, Ad3, that DSG-2 binding promotes epithelial-to mesenchymal transition to open intercellular junctions for access to CD46 [103]. More specifically, excess viral capsid proteins, penton base and fibre proteins produced by Ad3 replication opens intercellular junctions for infection of epithelial cell monolayers [239]. However, as suspension HEK293 cells do not exist in an epithelial monolayer, it is unlikely that receptor access is problematic. Uptake on to suspension HEK293 cells was not determined in this thesis but it was shown that ColoAd1 particle yield from HEK293 suspension cells was similar to yield from adherent HEK293 cells. This is important because production of ColoAd1 in suspension cells ensures process scalability and removes serum requirements for the process to cost effectively meet GMP. Ultimately the interventions identified in this thesis, especially those in Table 7-1 and the kinases identified in Chapter 6, eventually need to be tested in suspension cells to ensure process scalability.

Despite presence of the receptor for infection, E1-deleted group B adenovirus vectors such as those derived from Ad35 or Ad11 fail to produce particles in HEK293 cells [240].

Importantly, this highlights the lack of *trans*-complementation between E1 from group B and group C adenoviruses for viral replication. However, Ad35 vectors containing E1A deletions but expressing wild-type E1B produce viral particles in PER.C6 cells [241]. These observations lead to the creation of cell lines, such as the CRE25G3 derived from HEK293 cells and PER.C6/55K derived from PER.C6 cells, both of which complement E1-deleted Ad35 by expressing Ad5 E1 and Ad35 E1B-55k [242]. In addition, E1-deficient Ad11 vectors can be produced in HEK293 cells that express Ad11 E1B-55k so *trans*-complementation can be achieved for particle production [235]. These examples highlight how, despite having receptors for cellular uptake, adenovirus replication can still fail if the intracellular environment is not conducive.

In any case, the differences in replication observed between ColoAd1 and Ad11p in HEK293 cells must have been due to the genetic differences between them, thus informing the potential mechanism of action for ColoAd1 replication in cancer cells. Importantly, ColoAd1 has a mutant E2B region, which contains multiple substitutions of the E2B region from Ad3, and E2B encodes the viral DNA polymerase [69]. The chimeric E2B gene in ColoAd1 may underlie the observation that ColoAd1 produces more genomes, earlier than Ad11p. The mutant DNA polymerase of ColoAd1 is hypothesised to bind the ITR of Ad11p better than the DNA polymerase of Ad11p, to permit more efficient DNA replication initiation with ColoAd1 [69]. It is the ITR sequences at each end of the adenovirus genome contain the minimal sequences required for DNA replication and they are the same between ColoAd1 and Ad11p [243]. Therefore, Ad11p mutants, containing the chimeric ColoAd1 E2B gene would be useful to address this hypothesis and inform the design of adenoviruses with enhanced replication capacity.

Overall, the main limitation of this work is that ColoAd1 replication studies were performed in comparison to wild-type Ad11p and Ad5, not Ad3. Further studies investigating ColoAd1 genome replication relative to Ad3 would begin to address the specific hypothesis that Ad3 E2B enhances Ad11p genome replication. In addition, ColoAd1 replication has been determined relative to Ad11p only in the HEK293 cell line because this is the cell line used for clinical manufacture. If an alternative cell line was used for manufacture then harvest times would need to be optimised in those cell lines.

7.1.2 AMPK activation in adenovirus infected cells

In chapter 4, it was observed that ColoAd1 infected HEK293 cells depleted ATP earlier than Ad11p infected HEK293 cells. By determining the host cell response to ATP depletion, the aim was to delay the onset of ATP depletion in ColoAd1 infected HEK293 cells by manipulating the host cell energy sensor, AMPK. Indeed, AMPK was phosphorylated and activated earlier in ColoAd1 infected HEK293 cells compared to Ad11p. AMPK activation has previously been implicated in the replication of group C adenoviruses such as Ad5 [121] but this is the first known report of AMPK activation observed during the replication of group B adenoviruses, particularly during Ad11p replication. Indeed, AMPK activation has been observed after infection of cells with other viruses. SV40 expresses the small-T antigen that activates AMPK by inhibition of PP2A [244]. Further, expression of the small-T antigen protects against cell death induced by glucose deprivation, suggesting that the small T-antigen activates AMPK to inhibit mTOR and activate autophagy to obtain cellular resources for replication [156]. The RNA containing virus, Reovirus, also activates AMPK to induce MAPK signalling for viral replication [157]. Thus, it is conceivable that ColoAd1 activates AMPK earlier to benefit viral replication and/or oncolysis.

In this thesis, metformin was used to activate AMPK in the presence or absence of the group B adenoviruses, Ad11p and ColoAd1. Metformin is a dimethylbiguanide that inhibits complex I of the electron transport chain to activate AMPK indirectly by inhibiting ATP production [163, 176]. AMPK was activated by metformin in the presence of ColoAd1 but not in the presence of Ad11p or in uninfected HEK293 cells, suggesting that complex I was more susceptible to inhibition by metformin in the presence of ColoAd1 than Ad11p. Interestingly, a recent study has shown that adenovirus, particularly bovine Ad3, disrupts the mitochondrial membrane potential, depletes cellular ATP and physically damages the mitochondrial membrane 24 hours after infection at MOI 5 [245]. The timing of ATP depletion was also consistent with the timing of ATP depletion observed with ColoAd1 at MOI 10 and MOI 1, and in their study correlated with reduced mitochondria function. Further, many viruses manipulate mitochondrial function to benefit viral replication (reviewed in [246]). The fact that the anti-oxidant NAC also significantly enhanced the viability of ColoAd1 infected HEK293 cells compared to without, suggests a role for ROS in ColoAd1 induced cell death. This further implicates the mitochondria in ColoAd1 induced cell death as the mitochondria are the main source of cellular ROS [247]. In addition, mitochondria perform important functions in the regulation of calcium [248]. This is significant since ColoAd1 induced AMPK activation coincided with ATP depletion and the data presented in this thesis also suggested that calcium signalling may also have played a role as CAMKK2 was less phosphorylated, and presumably more active, in ColoAd1 infected cells than Ad11p.

The indirect activation of AMPK by metformin via complex I inhibition limits the conclusions that can be made relating to AMPK activation in virally infected cells.

Alternative AMPK activators exist. AICAR is an AMP mimetic and is an allosteric activator of AMPK that, like Metformin, inhibits cancer cell proliferation [249, 250]. Metformin is also used clinically as an anti-diabetic agent with its use correlating with a reduced incidence of many cancers, including liver, pancreatic, colorectal and breast cancer [251]. In this thesis, metformin decreased the IC50 of both ColoAd1 and Ad11p, suggesting that the combination increased the potency of both adenoviruses. This is the first time that this has been reported for group B adenoviruses. Therefore, the combination of ColoAd1 and metformin warrants further study as it may enhance the potency of ColoAd1 *in vivo*.

Overall, it was established that AMPK could be activated but not inhibited in ColoAd1 infected HEK293 cells. The effect that this had on virus yield was not determined. The lack of inhibition of AMPK activation by compound C made it difficult to achieve the aim of preventing AMPK signalling in response to virally induced ATP depletion. Despite this, future work focusing on defining the cause of AMPK activation, or the cause of virally induced ATP depletion, in HEK293 cells may help delineate the oncolytic mechanism of ColoAd1, especially given that rapid ATP depletion is a hall mark of necrotic cell death [252] and that extracellular release of ATP is one of the hallmarks of immunogenic cell death [253] so both of these mechanisms may contribute to the oncolytic potency of ColoAd1 *in vivo*.

7.1.3 Calcium signalling in adenovirus infected cells

The importance of CaMKK2 has been implicated in separate studies in this thesis. Western blot analysis of ColoAd1 infected HEK293 cells suggested that CaMKK2 was more susceptible to activation in HEK293 cells infected with ColoAd1 compared to Ad11p. To

further address the contribution of CaMKK2 on AMPK phosphorylation and activation, studies in an LKB1 negative cell line, such as A549 or HeLa, would be useful. In addition, knockout of DAPK, the kinase upstream of CaMKK2 that inhibits CaMKK2 activity, enhanced ColoAd1 genome replication. This implicates DAPK in limiting ColoAd1 replication. Death associated protein kinases are also implicated in ischemic diseases and this has promoted the search for inhibitors against them [227].

In chapter 5 it was observed that calcium chloride enhanced ColoAd1 yield from the supernatant. Taken together with the findings from chapter 6, this confirms the hypothesis that it is possible to manipulate the upstream cell culture process to increase ColoAd1 yield. This result is also consistent with the effect of calcium chloride on Ad5 yield from suspension cells [136]. Further, the addition of calcium chloride after infection is a simple, cost-effective GMP compliant method of increasing ColoAd1 yield from suspension HEK293 cells, although this intervention would require capture of ColoAd1 from the supernatant for downstream purification.

7.1.4 Insights into loss of E4orf4 function in ColoAd1

In chapter 4, the differences in AMPK activation observed between ColoAd1 and Ad11p may have been mediated by E4orf4. Expression of E4orf4 from plasmid DNA or expression vectors in model systems, such as yeast, induces cytotoxicity that although informative of function may not be relevant in the setting of viral replication [254, 255]. However, such studies have been useful to show that E4orf4 binds the regulatory subunit of the Ser/Thr phosphatase PP2A, specifically B55α [256]. E4orf4 is also known to contain nuclear localisation signals [117, 257]. Further, it has been shown that during viral replication PP2A becomes localised to the nucleus [121]. It is not clear what effect this

relocation has on PP2A function. It is possible that relocation of PP2A to the nucleus increases PP2A activity towards nuclear substrates and simultaneously decreases PP2A activity towards cytoplasmic substrates, simply by changing the ability of PP2A to access its substrates. Indeed, p70S6K phosphorylation increases with PP2A relocation to the nucleus [121] and SR protein phosphorylation decreases [120]. Ultimately, an E4orf4 inducible HEK293 cell line would be useful to compensate for the lack of E4orf4 in ColoAd1 and help to determine the contribution, if any, of E4orf4 towards the observed differences in AMPK phosphorylation between ColoAd1 and Ad11p, especially as PP2A regulates the phosphorylation of AMPK at Thr-172 [256, 258].

It is important to note that most, if not all, known E4orf4 functions have been determined with E4orf4 from Ad5 or Ad2. However, there is only 48% amino acid sequence homology between the E4orf4 of Ad5 and Ad11p. The residues in E4orf4 that are required for PP2A binding will be critical in determining whether Ad5 and Ad11p E4orf4 have the same functions. Indeed, some studies have mapped the E4orf4 residues required for PP2A binding using deletion mutants [254, 259]. Other studies have characterised the residues in the B55α subunit of PP2A that may interact with E4orf4 [256]. In ColoAd1, the first 60 nucleotides of *E4orf4* are intact and code for the E4orf4 of Ad11p but after the deletion multiple stop codons are present. The first 20 amino acids of Ad11p E4orf4 are only 45% homologous with that of Ad5. In addition, the functional PP2A binding region exists after the deletion in ColoAd1 so it would be unlikely that ColoAd1 expresses functional E4orf4 protein capable of binding PP2A. Future work needs to confirm this and establish if Ad11p E4orf is capable of binding PP2A to induce the same effects as Ad5 or Ad2 Ad11p.

The lack of E4orf4 interaction with the regulatory B subunit of PP2A may mediate ColoAd1 cancer selectivity. PP2A has also been linked to cancer development. Normal PP2A activity inhibits proliferative signalling pathways and loss of PP2A function contributes to transformation [260]. Decreased expression of the B56α subunit of PP2A has been associated with melanoma [261]. The B55α subunit can be found mutated in some breast cancers [262]. In other cancers, such as AML, PP2A activity is inhibited by transforming mutations in *c-kit* [263]. Therefore, determining the functional consequences of E4orf4 interaction with PP2A could contribute to ColoAd1 biomarker selection that would be important for patient selection in clinical trials.

7.1.5 ColoAd1 and HEK293 cell metabolism

Many of the agents tested in Chapter 5 were intended to increase ATP production via the TCA cycle and electron transport chain. This is based on the assumption that ColoAd1 does not interfere with the TCA cycle. Some agents, such as sodium oxamate, and nicotinamide, enhanced ColoAd1 infected cell viability but had no effect on ColoAd1 genome production, whereas, galactose significantly decreased ColoAd1 genome production, suggesting that glycolysis was required for optimal yield. Taken together, this indicated that glycolysis affected yield more than cellular energy levels. Given that cellular nucleotide synthesis occurs from the intermediates produced during glycolysis, this suggested that glycolysis and the availability of building blocks for nucleotide or protein synthesis are more important for viral replication than cellular energy levels. In this respect, the glycolytic rate of the cell line may determine susceptibility to efficient virus production. Indeed, ovarian cancer cell lines have high glycolytic rates and could prove more productive than HEK293 cells [264]. New methods that measure the glycolytic rate may also be useful. Bittner et al, have developed a high resolution method that determines the glycolytic rate at a single-cell level, which has proved useful to study the metabolic

requirements of pluripotent stem cells [265]. Further, maintaining the glycolytic rate of cells during infection may maintain optimal production and these observations may help inform media feeding strategies in large bioreactors.

7.2 Future directions

7.2.1 Cell metabolism and cancer

A revival in the study of metabolic changes that underpin the Warburg effect has identified targets of new anticancer therapies [266]. The similarities between tumour and virally infected cells provide an interesting niche for this oncolytic approach. Removing redundant genes from viruses that control cellular resources are likely to attenuate them in normal cells without impacting in cancer cell potency. Furthermore, rationale combinations of drugs to manipulate energy and synthesis pathways could help to improve both the activity and selectivity of viruses in the clinic.

7.2.2 Future development of oncolytic adenoviruses

Different methods of generating oncolytic viruses were discussed in this thesis and it was argued that bioselection generates mutant viruses with desired phenotypes that would not otherwise be predicted due to the complex interactions that a virus has with a host cell. Bioselection of oncolytic viruses in 3-dimentional models, such as spheroids, may further enhance potency. Spheroids have the advantage of mimicking the environment of a tumour mass more effectively than monolayer cell culture and have already been used to study the replication and penetration of Ad5 [267]. In addition, combinations of oncolytic viruses with drugs that target metabolic pathways could be used to manipulate viral replication as required, either therapeutically or *in vitro*.

7.2.3 Exploring alternative or modified cell lines for adenovirus manufacture

Given the metabolic implications that glycolysis has on ColoAd1 yield; it is likely that some cell lines would be more productive than HEK293 cells. The glycolytic rate could therefore become a marker for high yielding cell lines. Metabolic flux analysis of ovarian cancer cell lines has identified a highly glycolytic cell line [264]. Investigation of yield in alternative cell lines, would certainly improve knowledge of the host cell factors that limit yield. Alternatively, permanent knockdown of the hits identified from the siRNA screen in HEK93 cells might produce a higher yielding, ColoAd1 specific cell line. This would be an attractive solution if ColoAd1 progresses through clinical trials to market but would require production of GMP compliant cell banks of these cell lines. Combining kinase knockout from the host cell line with the interventions described in Table 7-1 may also enhance yield further.

7.2.4 Improvements in upstream manufacturing yields

Improvements in the yield of synthetic proteins and monoclonal antibodies have been made over the last few decades [268]. Small scale microwell bioreactors that mimic large scale suspension cell culture would be useful to probe multiple parameters to improve yield. Designed experiments can also quickly identify optimal conditions in a single experiment, instead of changing one condition at a time. This approach would significantly speed up the time that it takes to optimise a process but assumes that the parameters that limit yield are known. The results from this thesis have alluded to some parameters that may impact yield, such as the cellular rate of glycolysis, mitochondrial function and culture pH resulting from lactate accumulation.

7.2.5 Impact on downstream purification process

Increasing the packaging of ColoAd1 DNA into functional viral particles would be of importance from a bioprocessing perspective. Increasing viral genomes without increasing viral particle titre reduces the efficiency of the manufacturing process and generates more DNA that must be removed from the final product, thus, burdening the purification process. Contaminating cellular DNA is a particular problem with virus purification processes. The highly negatively charged DNA strongly binds cation exchange columns and limits the capacity of anion exchange columns to bind the viral product [269]. Methods to reduce such contamination would also be extremely important to investigate.

7.2.6 Antivirals for adenovirus

The self-limited nature of most adenovirus infections has not produced a great need for anti-viral therapies. However, adenoviral infections in immunocompromised patients are a significant problem and can become life-threatening. At the moment treatment options for adenoviral infections are limited to nucleoside or nucleotide analogues, such as cidofovir and ribavirin. Indeed, cidofovir inhibits ColoAd1 replication [270]. Other targets for anti-adenovirus therapy have been the adenovirus DNA polymerase. However, the siRNA targets that inhibited ColoAd1 replication in the screen performed in Chapter 6 could become novel targets for the development of antivirals against adenovirus infections.

7.3 Summary

Overall, oncolytic viruses are becoming established as potent and effective anti-cancer agents, so it is reasonable to expect that some of the findings from this thesis will ultimately be incorporated in to the design and manufacture of next generation oncolytic adenoviruses.

8 References

1. Mistry, M., et al., *Cancer incidence in the United Kingdom: projections to the year 2030.* British Journal of Cancer, 2011. **105**: p. 1795–1803.
2. Rosenburg, S., A., *Progress in human tumour immunology and immunotherapy.* Nature, 2001. **411**: p. 380-384.
3. Pardoll, D.M., *The blockade of immune checkpoints in cancer immunotherapy.* Nature Reviews Cancer, 2013. **12**(4): p. 252-264.
4. Siegel, R., et al., *Cancer statistics 2014.* CA: A Cancer Journal for Clinicians, 2014. **64**(1): p. 9-29.
5. Baskar, R., et al., *Cancer and Radiation Therapy: Current Advances and Future Directions.* International Journal of Medical Sciences, 2012. **9**(3): p. 193-199.
6. Luqmani, Y., A., *Mechanisms of drug resistance in cancer chemotherapy.* Medical Principles and Practices, 2005. **14**(Suppl 1): p. 35-48.
7. Baltimore, D., *Expression of animal virus genomes.* Microbiology and Molecular Biology Reviews, 1971. **35**(3): p. 235.
8. Futreal, P., A., et al., *A census of human cancer genes.* Nature Reviews Cancer, 2004. **4**: p. 177-183.
9. Hanahan, D. and R. Weinberg, A., *The Hallmarks of Cancer.* Cell, 2000. **100**(1): p. 57-70.
10. Hanahan, D. and R. Weinberg, A., *Hallmarks of Cancer: The Next Generation.* Cell, 2011. **144**(5): p. 646–674.
11. Rous, P., *A sarcoma of the fowl transmissible by an agent separable from the tumor cells.* The Journal of Experimental Medicine, 1911. **13**(4): p. 397-411.
12. Stehelin, D., et al., *DNA related to the transforming gene(s) of avian sarcoma viruses is present in normal avian DNA.* Nature, 1976. **260**: p. 170-173.
13. Hunter, T. and B. Sefton, M., *Transforming gene product of Rous sarcoma virus phosphorylates tyrosine.* Proceedings of the National Academy of Sciences of the United States of America, 1980. **77**(3): p. 1311-1315.
14. Spector, D., H., Varmus, H E., and J. Bishop, M., *Nucleotide sequences related to the transforming gene of avian sarcoma virus are present in DNA of uninfected vertebrates.* Proceedings of the National Academy of Sciences of the United States of America, 1978. **75**(9): p. 4102-4106.
15. Irby, R., B. and T. Yeatman, J., *Role of Src expression and activation in human cancer.* Oncogene, 2000. **19**: p. 5636-5642.
16. Sheiness, D., L. Fanschier, and J. Bishop, M., *Identification of nucleotide sequences which may encode the oncogenic capacity of avian retrovirus MC29.* Journal of Viriology, 1978. **28**(2): p. 600-610.
17. Malmumbres, M. and Barbacid, *RAS oncogenes: the first 30 years.* Nature Reviews Cancer, 2003. **3**: p. 459-465.
18. Lane, D., P. and L. Crawford, V., *T antigen is bound to a host protein in SV40-transformed cells.* Nature, 1979. **278**(5701): p. 261-263.

19. Lane, D., P., *p53, guardian of the genome.* Nature, 1992. **358**: p. 15-16.

20. Sarnow, P., et al., *Adenovirus E1b-58kd tumor antigen and SV40 large tumor antigen are physically associated with the same 54 kd cellular protein in transformed cells.* Cell, 1982. **28**(2): p. 387-394.

21. Lechner, M., S. and L. Laimins, A., *Inhibition of p53 DNA binding by human papillomavirus E6 proteins.* Journal of VIirology, 1994. **68**(7): p. 4262-4273.

22. DeCaprio, J., A., et al., *SV40 large tumor antigen forms a specific complex with the product of the retinoblastoma susceptibility gene.* Cell, 1988. **54**(2): p. 275-283.

23. Dyson, N., et al., *The human papilloma virus-16 E7 oncoprotein is able to bind to the retinoblastoma gene product.* Science, 1989. **243**(4893): p. 934-937.

24. Egan, C., S. Bayley, T., and P. Branton, E., *Binding of the Rb1 protein to E1A products is required for adenovirus transformation.* Oncogene, 1989. **4**(3): p. 383-388.

25. Epstein, M., A., B. Achong, G., and Y. Barr, M. , *Virus particles in cultured lymphoblasts from Burkitt's lymphoma.* Lancet, 1964. **1**: p. 702-703.

26. zur Hausen, H., *Viruses in human cancers.* Science, 1991. **254**(5035): p. 1176-1173.

27. Bosch, F., X., et al., *The causal relation between human papillomavirus and cervical cancer.* Journal of Clinical Pathology, 2002. **55**: p. 244-265.

28. Beasley, R., P., *Hepatitis B Virus: The Major Etiology of Hepatocellular Carcinoma.* Cancer, 1988. **61**(10): p. 1942-1956.

29. Dunn, G., P., L. Old, J., and R. Schreiber, D., *The three Es of cancer immunoediting.* Annual review of Immunology, 2004. **22**: p. 329-60.

30. Kim, R., M. Emi, and K. Tanabe, *Cancer immunosuppression and autoimmune disease: beyond immunosuppressive networks for tumour immunity.* Immunology, 2006. **119**(2): p. 254-264.

31. Thomas, M., A., et al., *Immunosuppression Enhances Oncolytic Adenovirus Replication and Antitumor Efficacy in the Syrian Hamster Model.* Molecular Therapy, 2008. **16**(10): p. 1665-1673.

32. Bluming, A.Z., *Regression of Burkitt's Lymphoma in Association with Measles Infection.* The Lancet, 1971. **298**(7715): p. 105-106.

33. Kelly, E. and S.J. Russell, *History of Oncolytic Viruses: Genesis to Genetic Engineering.* Molecular Therapy, 2007. **15**(4): p. 651-659.

34. Smith, R.R., et al., *Studies on the use of viruses in the treatment of carcinoma of the cervix.* Cancer, 1956. **9**: p. 1211-1218.

35. Wheelock, E., F. and J. Dingle, H., *Observations on the Repeated Administration of Viruses to a Patient with Acute Leukemia — A Preliminary Report.* New England Journal of Medicine, 1964. **271**: p. 645-651.

36. Dörig, R., E., et al., *The human CD46 molecule is a receptor for measles virus (Edmonston strain).* Cell, 1993. **75**(2): p. 295–305.

37. Niehans, G., A., et al., *Human carcinomas variably express the complement inhibitory proteins CD46 (membrane cofactor protein), CD55 (decay-accelerating*

factor), and CD59 (protectin). The American Journal of Pathology, 1996. **149**(1): p. 129-142.

38. Anderson, B.D., et al., *High CD46 receptor density determines preferential killing of tumor cells by oncolytic measles virus.* Cancer research, 2004. **64**(14): p. 4919-26.

39. Nakai, R., et al., *Overexpression of Necl-5 correlates with unfavorable prognosis in patients with lung adenocarcinoma.* Cancer Science, 2010. **101**(5): p. 1326-1330.

40. Skelding, K., A. , R. Barry, D. , and D. Shafren, R., *Systemic targeting of metastatic human breast tumor xenografts by Coxsackievirus A21.* Breast Cancer Research Treatment, 2009. **113**(1): p. 21-30.

41. Stojdl, D., F., et al., *Exploiting tumor-specific defects in the interferon pathway with a previously unknown oncolytic virus.* Nature medicine, 2000. **6**(7): p. 821-825.

42. Mansour, M., P. Palese, and D. Zamarin, *Oncolytic Specificity of Newcastle Disease Virus Is Mediated by Selectivity for Apoptosis-Resistant Cells.* Journal of Virology, 2011. **85**(12): p. 6015-6023.

43. Fiola, C., et al., *Tumor selective replication of Newcastle disease virus: association with defects of tumor cells in antiviral defence.* International Journal of Cancer, 2006. **119**(2): p. 328-338.

44. Coffey, M., C., et al., *Reovirus Therapy of Tumors with Activated Ras Pathway.* Science, 1998. **282**(5392): p. 1332-1334.

45. Farassati, F., A. Yang, D., and P. Lee, W., *Oncogenes in Ras signalling pathway dictate host-cell permissiveness to herpes simplex virus 1.* Nature Cell Biology, 2001. **3**(8): p. 745-750.

46. Wang, G., et al., *Infection of human cancer cells with myxoma virus requires Akt activation via interaction with a viral ankyrin-repeat host range factor* Proceedings of the National Academy of Sciences of the United States of America, 2006. **103**(12): p. 4640-4645.

47. Altomare, D., A. and J. Testa, R., *Perturbations of the AKT signaling pathway in human cancer.* Oncogene, 2005. **24**: p. 7455-7464.

48. Bischoff, J., R., et al., *An adenovirus mutant that replicates selectively in p53-deficient human tumor cells.* Science, 1996. **274**(5286): p. 373-376.

49. Petitjean, A., et al., *Impact of mutant p53 functional properties on TP53 mutation patterns and tumor phenotype: lessons from recent developments in the IARC TP53 database.* Human Mutations, 2007. **28**(6): p. 622-629.

50. Heise, C., et al., *ONYX-015, an E1B gene-attenuated adenovirus, causes tumor-specific cytolysis and antitumoral efficacy that can be augmented by standard chemotherapeutic agents.* Nature Medicine, 1997. **3**: p. 639-645.

51. Rothmann, T., et al., *Replication of ONYX-015, a Potential Anticancer Adenovirus, Is Independent of p53 Status in Tumor Cells.* Journal of virology, 1998. **72**(12): p. 9470–9478.

52. O'Shea, C.C., et al., *Late viral RNA export, rather than p53 inactivation, determines ONYX-015 tumour selectivity.* Cancer Cell, 2004. **6**: p. 611-623.

53. Ganly, I., et al., *A Phase I Study of Onyx-015, an E1B Attenuated Adenovirus, Administered Intratumorally to Patients with Recurrent Head and Neck Cancer* Clinical Cancer Research, 2000. **6**: p. 798-806.

54. Ko, D., L. Hawkins, and D.-C. Yu, *Development of transcriptionally regulated oncolytic adenoviruses.* Oncogene, 2005. **24**: p. 7763-7774.

55. DeWeese, T., L., et al., *A phase I trial of CV706, a replication-competent, PSA selective oncolytic adenovirus, for the treatment of locally recurrent prostate cancer following radiation therapy.* Cancer Research, 2001. **61**(20): p. 7464-7472.

56. Rodriguez, R., et al., *Prostate attenuated replication competent adenovirus (ARCA) CN706: a selective cytotoxic for prostate-specific antigen-positive prostate cancer cells.* Cancer Research, 1997. **57**(13): p. 2559-2563.

57. Small, E.J., et al., *A phase I trial of intravenous CG7870, a replication-selective, prostate-specific antigen-targeted oncolytic adenovirus, for the treatment of hormone-refractory, metastatic prostate cancer.* Molecular therapy: The Journal of the American Society of Gene Therapy, 2006. **14**(1): p. 107-17.

58. Yu, D., C., et al., *The addition of adenovirus type 5 region E3 enables calydon virus 787 to eliminate distant prostate tumor xenografts.* Cancer Research, 1999. **59**(17): p. 4200-4203.

59. Chen, C., H. and R. Chen, J., *Prevalence of telomerase activity in human cancer.* Journal of the Formosan Medical Association, 2011. **110**(5): p. 275-289.

60. Kirkpatrick, K., L., et al., *hTERT mRNA expression correlates with telomerase activity in human breast cancer.* European Journal of Surgical Oncology, 2003. **29**(4): p. 231-236.

61. Kawashima, T., et al., *Telomerase-specific replication-selective virotherapy for human cancer.* Clinical Cancer Research, 2004. **10**(1Pt1): p. 285-292.

62. Duarte, S., et al., *Suicide gene therapy in cancer: Where do we stand now?* Cancer Letters, 2012. **324**: p. 160-170.

63. Dmitriev, I., et al., *A Phase I Clinical Trial of Ad5.SSTR/TK.RGD, a Novel Infectivity-Enhanced Bicistronic Adenovirus, in Patients with Recurrent Gynecologic Cancer.* Clinical Cancer Research, 2012. **18**(12): p. 3440-3451.

64. Freytag, S., O., et al., *Phase I study of replication-competent adenovirus-mediated double suicide gene therapy for the treatment of locally recurrent prostate cancer.* Cancer research, 2002. **62**: p. 4968-4976.

65. Freytag, S.O., et al., *Phase I study of replication-competent adenovirus-mediated double-suicide gene therapy in combination with conventional-dose three-dimensional conformal radiation therapy for the treatment of newly diagnosed, intermediate- to high-risk prostate cancer.* Cancer research, 2003. **63**(21): p. 7497-506.

66. Lichty, B., D., et al., *Going viral with cancer immunotherapy.* Nature Reviews Cancer, 2014. **14**(8): p. 559-567.

67. Liu, B., L., et al., *ICP34.5 deleted herpes simplex virus with enhanced oncolytic, immune stimulating, and anti-tumour properties.* Gene Therapy, 2003. **10**: p. 292-303.

68. Senzer, N., N., et al., *Phase II Clinical Trial of a Granulocyte-Macrophage Colony-Stimulating Factor–Encoding, Second-Generation Oncolytic Herpesvirus in Patients With Unresectable Metastatic Melanoma.* Journal of Clinical Oncology, 2009. **27**(34): p. 5763-5771.

69. Kuhn, I., et al., *Directed evolution generates a novel oncolytic virus for the treatment of colon cancer.* PloS one, 2008. **3**(6): p. 2409.

70. Yan, W., et al., *Developing Novel Oncolytic Adenoviruses through Bioselection.* Journal of Virology, 2003. **77**(4): p. 2640-2650.

71. Uil, T., G., et al., *Directed adenovirus evolution using engineered mutator viral polymerases.* Nucleic Acids Research, 2011. **39**(5): p. e30.

72. Russell, S.J., K.-W. Peng, and J.C. Bell, *Oncolytic Virotherapy.* Nature biotechnology, 2012. **30**(7): p. 1-13.

73. Sheridan, C., *Amgen announces oncolytic virus shrinks tumors.* Nature Biotechnology, 2013. **31**: p. 471-472.

74. Kirn, D., *Clinical research results with dl1520 (Onyx-015), a replication-selective adenovirus for the treatment of cancer: what have we learned?* Gene therapy, 2001. **8**(2): p. 89-98.

75. Nemunaitis, J., et al., *Phase II trial of intratumoral administration of ONYX-015, a replication-selective adenovirus, in patients with refractory head and neck cancer.* Journal of Clinical Oncology, 2001. **19**(2): p. 289-298.

76. Nemunaitis, J., et al., *Selective replication and oncolysis in p53 mutant tumors with Onyx-015, an E1B-55kD gene-deleted adenovirus, in patients with head and neck cancer: a phase II trial.* Cancer Research, 2000. **60**(22): p. 6359-6366.

77. Khuri, F., R., et al., *A controlled trial of intratumoral ONYX-015, a selectively-replicating adenovirus, in combination with cisplatin and 5-fluorouracil in patients with recurrent head and neck cancer.* Nature medicine, 2000. **6**: p. 879-885.

78. Xia, Z., J., et al., *Phase III randomized clinical trial of intratumoral injection of E1B gene-deleted adenovirus (H101) combined with cisplatin-based chemotherapy in treating squamous cell cancer of head and neck or esophagus.* 2004. **23**(12): p. 1666-1670.

79. Lui, T.-C., E. Galanis, and D. Kirn, *Clinical trial results with oncolytic virotherapy: a century of promise, a decade of progress.* Nature Reviews. Clinical practice., 2007. **4**(2): p. 101-117.

80. Breitbach, C., J., et al., *Intravenous delivery of a multi-mechanistic cancer-targeted oncolytic poxvirus in humans.* Nature, 2011. **477**(7362): p. 99-102.

81. Guedan, S., et al., *Hyaluronidase expression by an oncolytic adenovirus enhances its intratumoral spread and suppresses tumor growth.* Molecular Therapy, 2010. **18**(7): p. 1275-1283.

82. Seregin, S., S. and A. Amalfitano, *Overcoming pre-existing adenovirus immunity by genetic engineering of adenovirus-based vectors.* Expert Opinion in Biological Therapy, 2009. **9**(12): p. 1521-1531.

83. Vogels, R., et al., *Replication-Deficient Human Adenovirus Type 35 Vectors for Gene Transfer and Vaccination: Efficient Human Cell Infection and Bypass of Preexising Adenovirus Immunity.* Journal of Virology, 2003. **77**(15): p. 8263-8271.

84. Rowe, W.P., et al., *Isolation of a Cytopathogenic Agent from Human Adenoids Undergoing Spontaneous Degeneration in Tissue Culture.* Experimental Biology and Medicine, 1953. **84**(3): p. 570-573.

85. Rosen, L., *A Hemagglutination-Inhibition Technique for Typing Adenoviruses.* American Journal of Epidemiology, 1960. **71**(1): p. 120-128.

86. Harwood, L.M.J. and P.H. Gallimore, *A Study of the Oncogenicity of Adenovirus Type 2 Transformed Rat Embryo Cells.* International Journal of Cancer, 1975. **16**: p. 498-508.

87. Green, M., et al., *Thirty-One Human Adenovirus Serotypes (Ad1 - Ad31) Form Five Groups (A - E) Based upon DNA Genome Homologies.* Virology, 1979. **93**: p. 481 - 492.

88. Vellinga, J., S. Van der Heijdt, and R.C. Hoeben, *The adenovirus capsid: major progress in minor proteins.* Journal of General Virology, 2005. **86**(6): p. 1581-1588.

89. Colby, W., W. and T. Shenk, *Adenovirus type 5 virions can be assembled in vivo in the absence of detectable polypeptide IX.* Journal of Virology, 1981. **39**(3): p. 977-980.

90. Crawford-Miksza, L. and D. Schnurr, P., *Analysis of 15 adenovirus hexon proteins reveals the location and structure of seven hypervariable regions containing serotype-specific residues.* Journal of Virology, 1996. **70**(3): p. 1836-1844.

91. Russell, W.C., *Adenoviruses: update on structure and function.* The Journal of General Virology, 2009. **90**: p. 1-20.

92. Nicklin, S.A., et al., *The influence of adenovirus fiber structure and function on vector development for gene therapy.* Molecular therapy: The Journal of the American Society of Gene Therapy, 2005. **12**(3): p. 384-93.

93. Wu, E., et al., *Flexibility of the adenovirus fiber is required for efficient receptor interaction.* Journal of Virology, 2003. **77**(13): p. 7225-7235.

94. Zhang, Y. and J.M. Bergelson, *Adenovirus Receptors.* Journal of Virology, 2005. **79**(19): p. 12125-12131.

95. Rux, J. and R.M. Burnett, *Adenovirus Structure.* Human gene therapy, 2004. **15**: p. 1167-1176.

96. Tomko, R., P. , R. Xu, and L. Philipson, *HCAR and MCAR: The human and mouse cellular receptors for subgroup C adenoviruses and group B coxsackieviruses.* Proceedings of the National Academy of Sciences of the United States of America, 1997. **94**: p. 3352-3356.

97. Roelvink, P.W., et al., *The Coxsackievirus-Adenovirus Receptor Protein Can Function as a Cellular Attachment Protein for Adenovirus Serotypes from Subgroups A, C, D, E, and F.* Journal of Virology, 1998. **72**(10): p. 7909-7915.

98. Howitt, J., et al., *Structural Basis for Variation in Adenovirus Affinity for the Cellular Coxsackievirus and Adenovirus Receptor.* The Journal of Biological Chemistry, 2003. **278**(28): p. 26208-26215.

99. Walters, R., W., et al., *Basolateral localization of fiber receptors limits adenovirus infection from the apical surface of airway epithelia.* Journal of Biological Chemistry, 1999. **274**(15): p. 10219-10226.

100. Coyne, C., B. and J. Bergelson, M., *CAR: a virus receptor within the tight junction.* Advanced Drug Delivery Reviews, 2005. **57**(6): p. 869-882.

101. Sachs, M., D., et al., *Integrin alpha(v) and coxsackie adenovirus receptor expression in clinical bladder cancer.* Urology, 2002. **60**(3): p. 531-536.

102. Gaggar, A., D.M. Shayakhmetov, and A. Lieber, *CD46 is a cellular receptor for group B adenoviruses.* Nature medicine, 2003. **9**(11): p. 1408-12.

103. Wang, H., et al., *Desmoglein 2 is a receptor for adenovirus serotypes 3, 7, 11 and 14.* Nature Medicine, 2010. **17**(1): p. 96-105.

104. Wickman, T.J., et al., *Integrins alpha v beta 3 and alpha v beta 5 promote adenovirus internalization but not virus attachment.* Cell, 1993. **73**: p. 309-319.

105. Meier, O. and U.F. Greber, *Adenovirus endocytosis.* The Journal of Gene Medicine, 2004. **6**: p. S152-63.

106. Wang, K., et al., *Adenovirus internalization and infection require dynamin.* Journal of Virology, 1998. **72**(4): p. 3455-3458.

107. Wiethoff, C.M., et al., *Adenovirus Protein VI Mediates Membrane Disruption following Capsid Disassembly.* Journal of Virology, 2005. **79**(4): p. 1992-2000.

108. Bailey, C., J., R.G. Crystal, and P.L. Leopold, *Association of Adenovirus with the Microtubule Organizing Center.* Journal of Virology, 2003. **77**(24): p. 13275-13287.

109. Leopold, P.L. and R.G. Crystal, *Intracellular trafficking of adenovirus: Many means to many ends.* Advanced Drug Delivery Reviews, 2007. **59**: p. 810-821.

110. Miyazawa, N., R.G. Crystal, and P.L. Leopold, *Adenovirus Serotype 7 Retention in a Late Endosomal Compartment prior to Cytosol Escape Is Modulated by Fiber Protein.* Journal of Virology, 2001. **75**(3): p. 1387-1400.

111. Lee, T., W, R., G. Blair, E. , and D. Matthews, A., *Adenovirus core protein VII contains distinct sequences that mediate targeting to the nucleus and nucleolus, and colocalization with human chromosomes.* Journal of General Virology, 2003. **84**(12): p. 3423-3428.

112. Chakraborty, A., A. and W. Tansey, P., *Adenoviral E1A function through Myc.* Cancer Research, 2009. **69**(1): p. 6-9.

113. Dekker, J., et al., *Multimerization of the adenovirus DNA-binding protein is the driving force for ATP-independant DNA unwinding during strand displacement synthesis.* THE EMBO Journal, 1997. **16**(6): p. 1455-1463.

114. Berget, S.M., C. Moore, and P. Sharp, *Sliced segments at the 5' terminus of Ad2 late mRNA.* Proceedings of the National Academy of Sciences of the United States of America, 1977. **74**: p. 3171-3175.

115. Tollefson, A.E., et al., *The Adenovirus Death Protein (E3-11.6K) Is Required at Very Late Stages of Infection for Efficient Cell Lysis and Release of Adenovirus from Infected Cells.* Journal of VIirology, 1996. **70**(4): p. 2296-2306.

116. Mei, Y.-F., et al., *Comparative analysis of the genome organization of human adenovirus 11, a member of the human adenovirus species B, and the commonly used human adenovirus 5 vector, a member of species C.* Journal of General Virology, 2003. **84**(8): p. 2061-2071.

117. Miron, M., J., et al., *Nuclear localization of the adenovirus E4orf4 protein is mediated through an arginine-rich motif and correlates with cell death.* Oncogene, 2004. **23**(45): p. 7458-7468.

118. Müller, U., T. Kleinberger, and T. Shenk, *Adenovirus E4orf4 protein reduces phosphorylation of c-Fos and E1A proteins while simultaneously reducing the level of AP-1.* Journal of Virology, 1992. **66**(10): p. 5867–5878.

119. Medghalchi, S., R. Padmanabhan, and G. Ketner, *Early Region 4 Modulates Adenovirus DNA Replication by Two Genetically Separable Mechanisms.* Virology, 1997. **236**: p. 8-17.

120. Kanopka, A., et al., *Regulation of adenovirus alternative RNA splicing by dephosphorylation of SR proteins.* Nature, 1998. **393**: p. 185-187.

121. O'Shea, C., et al., *Adenoviral proteins mimic nutrient/growth signals to activate the mTOR pathway for viral replication.* The EMBO Journal, 2005. **24**: p. 1211-1221.

122. Bridge, E., et al., *Adenovirus early region 4 and viral DNA synthesis.* Virology, 1993. **193**(2): p. 794-801.

123. Fu, J., L. Li, and M. Bouvler, *Adenovirus E3-19K Proteins of Different Serotypes and Subgroups Have Similar, Yet Distinct, Immunomodulatory Functions toward Major Histocompatibility Class I Molecules.* The Journal of Biological Chemistry, 2011. **286**: p. 17631-17639.

124. Chotai, N., P. and K. Patel, T., *Documentation and Records: Harmonized GMP Requirements.* Journal of Young Pharmacists, 2011. **3**(2): p. 138-150.

125. Lusky, M., *Good manufacturing practice production of adenoviral vectors for clinical trials.* Human gene therapy, 2005. **16**(3): p. 281-91.

126. Working, P.K., A. Lin, and F. Borellini, *Meeting product development challenges in manufacturing clinical grade oncolytic adenoviruses.* Oncogene, 2005. **24**(52): p. 7792-801.

127. Fallaux, F.J., et al., *New helper cells and matched early region 1-deleted adenovirus vectors prevent generation of replication competent adenoviruses.* Human gene therapy, 2008. **9**(13): p. 1909-1917.

128. Graham, F.L. and J. Smiley, *Characteristics of a Human Cell Line Transformed by DNA from Human Adenovirus Type 5.* Journal of General Virology, 1977. **36**: p. 59-72.

129. Titus, K., et al., *Closed System Cell Culture Protocol Using HYPERStack Vessels with Gas Permeable Material Technology.* Journal of Visualised Experiments, 2010. **45**(e2499): p. 1-5.

130. Durrschmid, M., et al., *Scalable Inoculation Strategies for Microcarrier-Based Animal Cell Bioprocesses.* Biotechnology and Bioengineering, 2003. **83**(6): p. 681-686.

131. Lennaertz, A., et al., *Viral vector production in the integrity® iCELLis® single-use fixed-bed bioreactor, from bench-scale to industrial scale.* BMC Proceedings, 2013. **7**(Suppl 6): p. 59.

132. Bieback, K., S. Kinzebach, and M. Karagianni, *Translating Research into Clinical Scale Manufacturing of Mesenchymal Stromal Cells.* Stem Cells International, 2010. **193519**: p. 1-11.

133. Robinson, D., K. and L. Chu, *Industrial choices for protein production by large-scale cell culture.* Current opinion in biotechnology, 2001. **12**(2): p. 180-187.

134. Singh, V., *Disposable bioreactor for cell culture using wave-induced agitation.* Cytotechnology, 1999. **30**(1-3): p. 149-158.

135. Varley, J. and J. Birch, *Reactor design for large scale suspension animal cell culture.* Cytotechnology, 1999. **29**(3): p. 177-205.

136. Liu, X., et al., *Effects of Calcium Ion on Adenovirus Production with High Densities of HEK293 Cells.* Biotechnology and Bioprocess Engineering, 2010. **15**: p. 414-420.

137. Nadeau, I., et al., *Low-protein medium affects the 293SF central metabolism during growth and infection with adenovirus.* Biotechnology and Bioengineering, 2002. **77**(1): p. 91-104.

138. Henry, O., M. Perrier, and A. Kamen, *Metabolic flux analysis of HEK-293 cells in perfusion cultures for the production of adenoviral vectors.* Metabolic engineering, 2005. **7**(5-6): p. 467-76.

139. Maizel, J.V., et al., *The Polypeptides of Adenovirus.* Virology, 1968. **36**: p. 115-125.

140. Dechecchi, M.C., et al., *Heparan sulfate glycosaminoglycans are involved in adenovirus type 5 and 2-host cell interactions.* Virology, 2000. **268**(2): p. 382-390.

141. Jonsson, M., I., et al., *Coagulation Factors IX and X Enhance Binding and Infection of Adenovirus Types 5 and 31 in Human Epithelial Cells.* Virology, 2009. **83**(8): p. 3816-3825.

142. Hong, S., S., et al., *Adenovirus type 5 fiber knob binds to MHC class I alpha2 domain at the surface of human epithelial and B lymphoblastoid cells.* EMBO, 1997. **16**(1997).

143. Chu, Y., et al., *Vascular cell adhesion molecule-1 augments adenovirus-mediated gene transfer.* Arteriosclerosis, thrombosis and vascular biology, 2001. **21**(2): p. 238-242.

144. Khare, R., et al., *Identification of Adenovirus Serotype 5 Hexon Regions That Interact with Scavenger Receptors.* Virology, 2012. **86**(4): p. 2293-2301.

145. Marttila, M., et al., *CD46 Is a Cellular Receptor for All Species B Adenoviruses except Types 3 and 7.* Journal of VIirology, 2005. **79**(22): p. 14429-14436.

146. Garrod, D. and M. Chidgey, *Desmosome structure, composition and function.* Biochimica et Biophysica Act, 2008. **1778**: p. 572 - 587.

147. Hall, K., M.E. Blair Zajdel, and G.E. Blair, *Unity and diversity in the human adenoviruses: exploiting alternative entry pathways for gene therapy.* Biochemistry Journal, 2010. **431**: p. 321-336.

148. Hardie, D.G., F.A. Ross, and S.A. Hawley, *AMPK: a nutrient and energy sensor that maintains energy homeostasis.* Molecular Cell Biology, 2012. **13**: p. 251-262.

149. Hawley, S.A., et al., *Characterization of the AMP-activated protein kinase kinase from rat liver and identification of threonine 172 as the major site at which it phosphorylates AMP-activated protein kinase.* Journal of Biological Chemistry, 1996. **271**(44): p. 27879-87.

150. Xiao, B., et al., *Structure of mammalian AMPK and its regulation by ADP.* Nature, 2011. **472**(7342): p. 230-233.

151. Woods, A., et al., *LKB1 Is the Upstream Kinase in the AMP-Activated Protein Kinase Cascade.* Current Biology, 2003. **13**(22): p. 2004-2008.

152. Davies, S.P., et al., *5'-AMP inhibits dephosphorylation, as well as promoting phosphorylation, of the AMP activated protein kinase. Studies using bacterially expressed human protein phosphatase-2C and native bovine protein phosphatase-2Ac* Federation of Euopean Biochemical Societies, 1995. **377**: p. 421-425.

153. Mankouri, J. and M. Harris, *Viruses and the fuel sensor: the emerging link between AMPK and virus replication.* Reviews in Medical Virology, 2011. **21**: p. 205-212.

154. Mankouri, J., et al., *Enhanced hepatitis C virus genome replication and lipid accumulation mediated by inhibition of AMP-activated protein kinase.* Proceedings of the National Academy of Sciences of the United States of America, 2010. **107**(25): p. 11549-11554.

155. Kudchodkar, S., B., et al., *AMPK-Mediated Inhibition of mTOR Kinase Is Circumvented during Immediate-Early Times of Human Cytomegalovirus Infection.* Journal of Virology, 2007. **81**(7).

156. Kumar, S., H. and A. Rangarajan, *Simian virus 40 small T antigen activates AMPK and triggers autophagy to protect cancer cells from nutrient deprivation.* Journal of VIirology, 2009. **83**: p. 8565-8574.

157. Ji WT, et al., *AMP-activated protein kinase (AMPK) facilitates avian reovirus to induce MKK3/6 and MAPK p38 signaling that is beneficial for virus replication.* The Journal of General Virology, 2009. **90**: p. 3002-3009.

158. Shimobayashi, M. and M. Hall, N., *Making new contacts: the mTOR network in metabolism and signalling crosstalk.* Nature Reviews Molecular Cell Biology, 2014. **15**(3): p. 155-162.

159. Hurley, R., L., et al., *The Ca2+/Calmodulin-dependent Protein Kinase Kinases Are AMP-activated Protein Kinase Kinases.* The Journal of Biological Chemistry, 2005. **280**: p. 29060-29066.

160. Schumacher, A., M., et al., *A calmodulin-regulated protein kinase linked to neuron survival is a substrate for the calmodulin-regulated death-associated protein kinase.* Biochemistry, 2004. **43**(25): p. 8116-8124.

161. Inoki, K., T. Zhu, and K.-L. Guan, *TSC2 mediates cellular energy response to control cell growth and survival.* Cell, 2003. **115**: p. 577-590.

162. Gwinn, D.M., et al., *AMPK Phosphorylation of Raptor Mediates a Metabolic Checkpoint.* Cell, 2008. **30**: p. 214-226.

163. Zhou, G., et al., *Role of AMP-activated protein kinase in mechanism of metformin action.* Journal of Clinical Investigation, 2001. **108**(8): p. 1167-1174.

164. Viollet, B., et al., *Cellular and molecular mechanisms of metformin: an overview.* Clinical Science, 2012. **122**: p. 253-270.

165. De Jong, P.J., et al., *The ATP Requirements of Adenovirus Type 5 DNA Replication and Cellular DNA Replication.* Virology, 1983. **124**: p. 45-58.

166. Flint, S., J. and R. Gonzalez, A., *Regulation of mRNA production by the adenoviral E1B 55-kDa and E4 Orf6 proteins.* Current Topics in Microbiology and Immunology, 2003. **272**: p. 287-330.

167. Gingras, A.C., *35 years later, mRNA caps still matter.* Nature Reviews Molecular Cell Biology, 2009. **10**(11): p. 735.

168. Schneider, R., L and I. Mohr, *Translation initiation and viral tricks.* Trends in Biochemical Sciences, 2003. **28**(3): p. 130-136.

169. Jackson, R., J., *The ATP requirement for initiation of eukaryotic translation varies according to the mRNA species.* European Journal of Biochemistry, 1991. **200**(2): p. 285-294.

170. Walsh, D. and I. Mohr, *Viral subversion of the host protein synthesis machinery.* Nature Reviews Microbiology, 2011. **9**: p. 860-875.

171. Gingras, A., C., et al., *Activation of the translational suppressor 4E-BP1 following infection with encephalomyocarditis virus and poliovirus.* Proceedings of the National Academy of Sciences of the United States of America, 1996. **93**: p. 5578–5583.

172. Saffran, H., A., S. Readm G, and J. Smiley, *Evidence for Translational Regulation by the Herpes Simplex Virus Virion Host Shutoff Protein.* Journal of Virology, 2010. **84**(12): p. 6041-6049.

173. Gingras, A.C. and N. Sonenberg, *Adenovirus infection inactivates the translational inhibitors 4E-BP1 and 4E-BP2.* Virology, 1997. **237**(1): p. 182-186.

174. Zhang, Y. and R. Schneider, L, *Adenovirus inhibition of cellular protein synthesis and the specific translation of late viral mRNAs.* Seminars in Virology, 1993. **4**(4): p. 229-236.

175. Zhang, Y., D. Feigenblum, and R. Schneider, L, *A late adenovirus factor induces eIF-4E dephosphorylation and inhibition of cell protein synthesis.* Virology, 1994. **68**(11): p. 7040-7050.

176. El-Mir, M., Y., et al., *Dimethylbiguanide inhibits cell respiration via an indirect effect targeted on the respiratory chain complex I.* The Journal of Biological Chemistry, 2000. **275**(1): p. 223-228.

177. *Metformin, Independent of AMPK, Inhibits mTORC1 in a Rag GTPase-Dependent Manner.* Cell metabolism, 2010. **11**(5): p. 390-401.

178. Haase, V., H., *The VHL/HIF oxygen-sensing pathway and its relevance to kidney disease.* Kidney International, 2006. **69**(8): p. 1302-1307.

179. Azar, R., et al., *Contribution of HIF-1 alpha in 4E-BP1 gene expression.* Molecular Cancer Research, 2013. **1**: p. 54-61.

180. Warburg, O., Posener K, and N. E., *Ueber den Stoffwechsel der Tumoren.* Journal of Biological Chemistry, 1924. **152**: p. 319–344.

181. Amann, T., et al., *GLUT1 expression is increased in hepatocellular carcinoma and promotes tumorigenesis.* 2009.

182. Suzuki, T., et al., *Enhanced expression of glucose transporter GLUT3 in tumorigenic HeLa cell hybrids associated with tumor suppressor dysfunction.* European Journal of Biochemistry, 1999. **262**: p. 534-540.

183. Juweid, M., E. and B. Cheson, D., *Positron-Emission Tomography and Assessment of Cancer Therapy.* New England Journal of Medicine, 2006. **354**(5): p. 496-507.

184. Bustamante, E., H. Morris, P., and P. Pedersen, L., *Energy metabolism of tumor cells. Requirement for a form of hexokinase with a propensity for mitochondrial binding.* Journal of Biological Chemistry, 1981. **256**(16): p. 8699-8704.

185. Bustamante, E. and P. Pedersen, L., *High aerobic glycolysis of rat hepatoma cells in culture: Role of mitochondrial hexokinase.* Proceedings of the National Academy of Sciences of the United States of America, 1977. **74**(9): p. 3735–3739.

186. Lunt, S., Y. and M. Vander Heiden, G., *Aerobic Glycolysis: Meeting the Metabolic Requirements of Cell Proliferation.* Annual Review of Cell and Developmental Biology, 2011. **27**(1): p. 441–464.

187. Vander Heiden, M., G., L. Cantley, C., and C. Thompson, B., *Understanding the Warburg Effect: The Metabolic Requirements of Cell Proliferation.* Science, 2009. **324**(5930): p. 1029-1033.

188. Rossignol, R., et al., *Energy substrate modulates mitochondrial structure and oxidative capacity in cancer* Cancer research, 2004. **64**: p. 985-993.

189. Michelakis, E., D., L. Webster, and J. Mackey, R., *Dichloroacetate (DCA) as a potential metabolic-targeting therapy for cancer.* British Journal of Cancer 2008. **99**: p. 989 – 994.

190. Ying, W., *NAD+/NADH and NADP+/NADPH in Cellular Functions and Cell Death: Regulation and Biological Consequences.* Antioxidants and Redox Signaling, 2008. **10**(2): p. 179-206.

191. Tsao, Y.-S., et al., *Development and improvement of a serum-free suspension process for the production of recombinant adenoviral vectors using HEK293 cells.* Cytotechnology, 2001. **37**: p. 189-198.

192. Mari, M., et al., *Mitochondrial Glutathione, a Key Survival Antioxidant.* Antioxidants and Redox Signaling, 2009. **11**(11): p. 2685-2700.

193. Kim, K., C., et al., *N-acetylcysteine Amide Augments the Therapeutic Effect of Neural Stem Cell-Based Antiglioma Oncolytic Virotherapy.* The American Society of Gene and Cell Therapy, 2013. **21**(11): p. 2063-2073.

194. Scott, G.M., V.M. Ratnamohan, and W.D. Rawlinson, *Improving permissive infection of human cytomegalovirus in cell culture.* Archives of Virology, 2000. **145**: p. 2431-2438.

195. Zhao, L., et al., *The role of microenvironment in aggregation of the 293-human embryonic Kidney cells.* Korean Journal of Chemical Engineering, 2007. **24**(5): p. 796-799.

196. Marroquin, L., D., et al., *Circumventing the Crabtree Effect: Replacing Media Glucose with Galactose Increases Suceptibility of HepG2 Cells to Mitochondrial Toxicants.* Toxicological Sciences, 2007. **97**(2): p. 539-547.

197. Yuk, I., H, Y., et al., *Perfusion cultures of human tumor cells: a scalable production platform for oncolytic adenoviral vectors.* Biotechnology and Bioengineering, 2004. **86**(6): p. 637-642.

198. Korenaga, M., et al., *Hepatitis C Virus Core Protein Inhibits Mitochondrial Electron Transport and Increases Reactive Oxygen Species (ROS) Production.* Journal of Biological Chemistry, 2005. **280**: p. 37481-37488.

199. Bonnet, S., et al., *A mitochondria-K+ channel axis is suppressed in cancer and its normalization promotes apoptosis and inhibits cancer growth.* Cancer cell, 2007. **11**(1): p. 37-51.

200. Stacpool, *A controlled clinical trial of dichloroacetate for treatment of lactate acidosis in adults.* The New England Journal of Medicine, 1992: p. 1564.

201. Michelakis, E., D., *Metabolic Modulation of Glioblastoma with Dichloroacetate.* Science Translational Medicine, 2010. **2**(31): p. 31-34.

202. Hamilton, A., J. and D. Baulcombe, C., *A species of small antisense RNA in posttranscriptional gene silencing in plants.* Science, 1999. **286**(5441): p. 950-952.

203. Elbashir, S., M., et al., *Duplexes of 21-nucleotide RNAs mediate RNA interference in cultured mammalian cells.* Nature, 2001. **411**: p. 494-498.

204. Wilson, R., C. and J. Doudna, A., *Molecular mechanisms of RNA interference.* Annual Reviews of Biophysics, 2013. **42**: p. 217-239.

205. Rao, D., D., et al., *siRNA vs. shRNA: Similarities and differences.* Advanced Drug Delivery Reviews, 2009. **61**(9): p. 746-759.

206. Warner, N., et al., *A Genome-Wide siRNA Screen Reveals Positive and Negative Regulators of the NOD2 and NF-κB Signaling Pathways.* Science, 2013. **6**.

207. Chung, N., et al., *Median Absolute Deviation to Improve Hit Selection for Genome-Scale RNAi Screens.* Journal of Biomolecular Screening, 2008. **13**(2): p. 149-158.

208. Brickley, D., R., et al., *Serum- and glucocorticoid-induced protein kinase 1 (SGK1) is regulated by store-operated Ca2+ entry and mediates cytoprotection against necrotic cell death.* Journal of Biological Chemistry, 2013. **288**(45): p. 32708-32719.

209. Hammonda, M., et al., *Design and synthesis of orally bioavailable serum and glucocorticoid-regulated kinase 1 (SGK1) inhibitors.* Bioorganic & Medicinal Chemistry Letters, 2009. **19**(15): p. 4441-4445.

210. IY, D. and J. GL., *MAGI-1 interacts with beta-catenin and is associated with cell-cell adhesion structures.* Biochemical and Biophysical Research Communications, 2000. **270**(3): p. 903-909.

211. Glaunsinger, B., A., et al., *Interactions of the PDZ-protein MAGI-1 with adenovirus E4-ORF1 and high-risk papillomavirus E6 oncoproteins.* Oncogene, 2000. **19**(46): p. 5270-5280.

212. Latorre, I., J., et al., *Viral oncoprotein-induced mislocalization of select PDZ proteins disrupts tight junctions and causes polarity defects in epithelial cells.* Journal of Cell Science, 2005. **118**(Pt18): p. 4283-4293.

213. Yang, K.-M., et al., *DRAK2 Participates in a Negative Feedback Loop to Control TGF-β/Smads Signaling by Binding to Type I TGF-β Receptor.* Cell Reports, 2012. **2**(5).

214. Doherty, G., A., et al., *Regulation of the apoptosis-inducing kinase DRAK2 by cyclooxygenase-2 in colorectal cancer.* British Journal of Cancer, 2009. **101**(3): p. 483-491.

215. Kuwahara, H., et al., *The apoptosis-inducing protein kinase DRAK2 is inhibited in a calcium-dependent manner by the calcium-binding protein CHP*. Journal of Biochemistry, 2003. **134**(2): p. 245-250.

216. Knippschilda, U., et al., *The casein kinase 1 family: participation in multiple cellular processes in eukaryotes.* Cellular Signalling, 2005. **17**(6): p. 675-689.

217. Behrend, L., et al., *Interaction of casein kinase 1 delta (CK1delta) with post-Golgi structures, microtubules and the spindle apparatus.* European Journal of Cell Biology, 2000. **79**(4): p. 240-251.

218. Cozza, G., et al., *Identification of novel protein kinase CK1 delta (CK1delta) inhibitors through structure-based virtual screening.* Bioorganic & Medicinal Chemistry Letters, 2008. **18**(20): p. 5672-5675.

219. Potter, L., R. and T. Hunter, *Guanylyl Cyclase-linked Natriuretic Peptide Receptors: Structure and Regulation.* The Journal of Biological Chemistry, 2001. **276**: p. 6057-6060.

220. J, D., et al., *Development of a selective peptide antagonist for the human natriuretic peptide receptor-B.* Peptides, 2005. **26**(3): p. 517-524.

221. Simarro, M., et al., *Fas-activated serine/threonine phosphoprotein (FAST) is a regulator of alternative splicing.* Proceedings of the National Academy of Sciences of the United States of America, 2007. **104**(27): p. 11370-11375.

222. Li, W., et al., *FAST is a survival protein that senses mitochondrial stress and modulates TIA-1-regulated changes in protein expression.* Molecular and Cellular Biology, 2004. **24**(24): p. 10718-10732.

223. Timmins, J., M., et al., *Calcium/calmodulin-dependent protein kinase II links ER stress with Fas and mitochondrial apoptosis pathways.* The Journal of Clinical Investigation, 2009. **119**(10): p. 2925-2941.

224. Diekmann, D., et al., *Bcr encodes a GTPase-activating protein for p21rac.* Nature, 1991. **351**(6325): p. 400-402.

225. Yoo, H., J., et al., *DAPk1 inhibits NF-κB activation through TNF-α and INF-γ-induced apoptosis.* Cell Signalling, 2012. **24**(7): p. 1471-1477.

226. de Diego, I., et al., *Molecular Basis of the Death-Associated Protein Kinase–Calcium/Calmodulin Regulator Complex.* Science Signaling, 2010. **3**(106): p. 6.

227. Okamoto, M., et al., *Identification of death-associated protein kinases inhibitors using structure-based virtual screening.* Journal of Medicinal Chemistry, 2009. **52**(22): p. 7323-7327.

228. Shaw, G., et al., *Preferential transformation of human neuronal cells by human adenoviruses and the origin of HEK 293 cells.* Federation of American Societies for Experimental Biology, 2002. **16**(8): p. 869-871.

229. Loffing, J., S. Flores, Y., and O. Staub, *SGK Kinases and their Role in Epithelial Transport.* Annual Review of Physiology, 2006. **68**: p. 461-490.

230. Shohat, G., et al., *The Pro-apoptotic Function of Death-associated Protein Kinase Is Controlled by a Unique Inhibitory Autophosphorylation-based Mechanism.* Journal of Biological Chemistry, 2001. **276**: p. 47460-47467.

231. Gozuacik, D., et al., *DAP-kinase is a mediator of endoplasmic reticulum stress-induced caspase activation and autophagic cell death.* Cell Death and Differentiation, 2008. **15**(1875-1886).

232. Di, Y., L.W. Seymour, and K. Fisher, *Activity of a group B oncolytic adenovirus (ColoAd1) in whole human blood.* Gene therapy, 2014. **21**(4): p. 440-443.

233. Ahi, Y.S., D.S. Bangari, and S.K. Mittal, *Adenoviral vector immunity: its implications and circumvention strategies.* Current Gene Therapy, 2011. **11**(4): p. 307-320.

234. Yamada, K., et al., *Adenovirus vector production using low-multiplicity infection of 293 cells.* Cytotechnology, 2009. **59**(3): p. 153-160.

235. Stone, D., et al., *Development and Assessment of Human Adenovirus Type 11 as a Gene Transfer Vector.* Journal of Virology, 2005. **79**(8): p. 5090-5104.

236. Liu, J., et al., *In Vitro Characterization of Human Adenovirus Type 55 in Comparison with Its Parental Adenoviruses, Types 11 and 14.* PloS one, 2014.

237. Weiss, K., et al., *Influence of process conditions on measles virus stability.* American Journal of Biochemistry and Biotechnology, 2013. **9**(3): p. 243-254.

238. Trinh, H.V., et al., *Avidity binding of human adenovirus serotypes 3 and 7 to the membrane cofactor CD46 triggers infection.* Journal of Virology, 2012. **86**(3): p. 1623-1637.

239. Lu, Z., Z., et al., *Penton-dodecahedral particles trigger opening of intercellular junctions and facilitate viral spread during adenovirus serotype 3 infection of epithelial cells.* PLOS Pathogens, 2013. **9**(10): p. e1003718.

240. Kovesdi, I. and S. Hedley, J., *Adenoviral producer cells.* Viruses, 2010. **2**(8): p. 1681-1703.

241. Seshidhar Reddy, P., et al., *Development of adenovirus serotype 35 as a gene transfer vector.* Virology, 2003. **311**(2): p. 384-393.

242. Gaio, W., P. Robbins, D., and A. Gambotto, *Human adenovirus type 35: nucleotide sequence and vector development.* Gene therapy, 2003: p. 1941-1949.

243. Wides, R., J., et al., *Adenovirus origin of DNA replication: sequence requirements for replication in vitro.* Molecular and Cellular Biology, 1987. **7**(2): p. 864-874.

244. Sablina, A., A. and W. Hahn, C., *SV40 small T antigen and PP2A phosphatase in cell transformation.* Journal of VIirology, 2008. **27**: p. 137-146.

245. Anand, S., K., et al., *Effect of bovine adenovirus 3 on mitochondria.* Veterinary Research, 2014. **45**(45): p. 1-8.

246. Anand, S.K. and S.K. Tikoo, *Viruses as Modulators of Mitochondrial Functions.* Advances in Virology, 2013. **2013**: p. 17.

247. Zorov, D., B., M. Juhaszova, and S. Sollott, J., *Mitochondrial reactive oxygen species (ROS) and ROS-induced ROS release.* Physiological Reviews, 2014. **94**(3): p. 909-950.

248. Rizzuto, R., et al., *Mitochondria as sensors and regulators of calcium signalling.* Nature Reviews Molecular Cell Biology, 2012. **13**: p. 566-578.

249. Rattan, R., et al., *5-Aminoimidazole-4-carboxamide-1-beta-D-ribofuranoside inhibits cancer cell proliferation in vitro and in vivo via AMP-activated protein kinase.* Journal of Biological Chemistry, 2005. **280**(47): p. 39582-39593.

250. Hadad, S., M., et al., *Effects of metformin on breast cancer cell proliferation, the AMPK pathway and the cell cycle.* Clinical Translational Oncology, 2014. **16**(8): p. 746-752.

251. Zhang, P., et al., *Association of metformin use with cancer incidence and mortality: a meta-analysis.* Cancer epidemiology, 2013. **37**(3): p. 207-218.

252. Fulda, S., *Alternative Cell Death Pathways and Cell Metabolism.* International Journal of Cell Biology, 2013.

253. Martins, I., et al., *Molecular mechanisms of ATP secretion during immunogenic cell death.* Cell Death and Differentiation, 2014. **21**(7): p. 79-91.

254. Afifi, R., et al., *Selection of apoptosis-deficient adenovirus E4orf4 mutants in Saccharomyces cerevisiae.* Journal of VIirology, 2001. **75**(9): p. 4444-4447.

255. Branton, P., E. and D. Roopchand, E., *The role of adenovirus E4orf4 protein in viral replication and cell killing.* Oncogene, 2001. **20**(54): p. 7855-7865.

256. Horowitz, B., et al., *Structure and Modeling-Based Identification of the Adenovirus E4orf4 Binding Site in the Protein Phosphatase 2A B55alpha Subunit.* J. Biol. Chem, 2013. **288**: p. 13718-13727.

257. Miron, M.-J.l., *Localization and Importance of the Adenovirus E4orf4 Protein during Lytic Infection.* Journal of Virology, 2009. **83**(4): p. 1689.

258. Wu, Y., et al., *Activation of Protein Phosphatase 2A by Palmitate Inhibits AMP-activated Protein Kinase.* The Journal of Biological Chemistry, 2007. **282**(13): p. 9777–9788.

259. Shtrichman, R., et al., *Induction of apoptosis by adenovirus E4orf4 protein is specific to transformed cells and requires an interaction with protein phosphatase 2A.* Proceedings of the National Academy of Sciences of the United States of America, 1999. **96**(18): p. 10080-10085.

260. Seshacharyulu, P., et al., *Phosphatase: PP2A structural importance, regulation and its aberrant expression in cancer.* Cancer Letters, 2013. **335**(1): p. 9-18.

261. Mannava, S., et al., *PP2A-B56α controls oncogene-induced senescence in normal and tumor human melanocytic cells.* Oncogene, 2012. **31**(12): p. 1484-1492.

262. Curtis, C., S. Shah, P., and S.-F. Chin, *The genomic and transcriptomic architecture of 2,000 breast tumours reveals novel subgroups.* Nature, 2012. **486**: p. 346-352.

263. Roberts, K., G., et al., *Essential requirement for PP2A inhibition by the oncogenic receptor c-KIT suggests PP2A reactivation as a strategy to treat c-KIT+ cancers.* Cancer Research, 2010. **70**(10): p. 5438-5447.

264. Dier, U., et al., *Bioenergetic Analysis of Ovarian Cancer Cell Lines: Profiling of Histological Subtypes and identification of a Mitochondria-Defective Cell Line.* PloS one, 2014. **9**(5): p. e98479.

265. Bittner, C., X., et al., *High resolution measurement of the glycolytic rate.* Frontiers in Neuroenergetics, 2010. **15**(2): p. 26.

266. Hsu, P., P. and D. Sabatini, M., *Cancer Cell Metabolism: Warburg and Beyond.* Cell, 2008. **134**(5): p. 703-707.

267. Grill, J., et al., *The Organotypic Multicellular Spheroid Is a Relevant Three-Dimensional Model to Study Adenovirus Replication and Penetration in Human Tumors in Vitro.* Gene Therapy, 2002. **6**(5): p. 609-614.

268. Shukla, A., A. and J. Thömmes, *Recent advances in large-scale production of monoclonal antibodies and related proteins.* Trends in Biotechnology, 2010. **28**(5): p. 253-261.

269. Whitfield, R.J., et al., *Rapid high-performance liquid chromatographic analysis of adenovirus type 5 particles with a prototype anion-exchange analytical monolith column.* Journal of Chromatography A, 2009. **1216**(13): p. 2725-9.

270. Bauzon, M., et al., *In vitro analysis of cidofovir and genetically engineered TK expression as potential approaches for the intervention of ColoAd1-based treatment of cancer.* Gene therapy, 2009. **16**(9): p. 1169-1174.